LA-UR-21-21323
Approved for public release; distribution is unlimited.

Title: Black Holes: Connecting Theory and Simulation to Observation

Author(s): Kinch, Brooks Evan

Intended for: visiting talk

Issued: 2021-02-11

Black Holes:
Connecting Theory and Simulation to Observation

Brooks E. Kinch
Los Alamos National Laboratory, Metropolis Fellow, CCS-2

Lawrence Livermore National Laboratory

2/17/2021

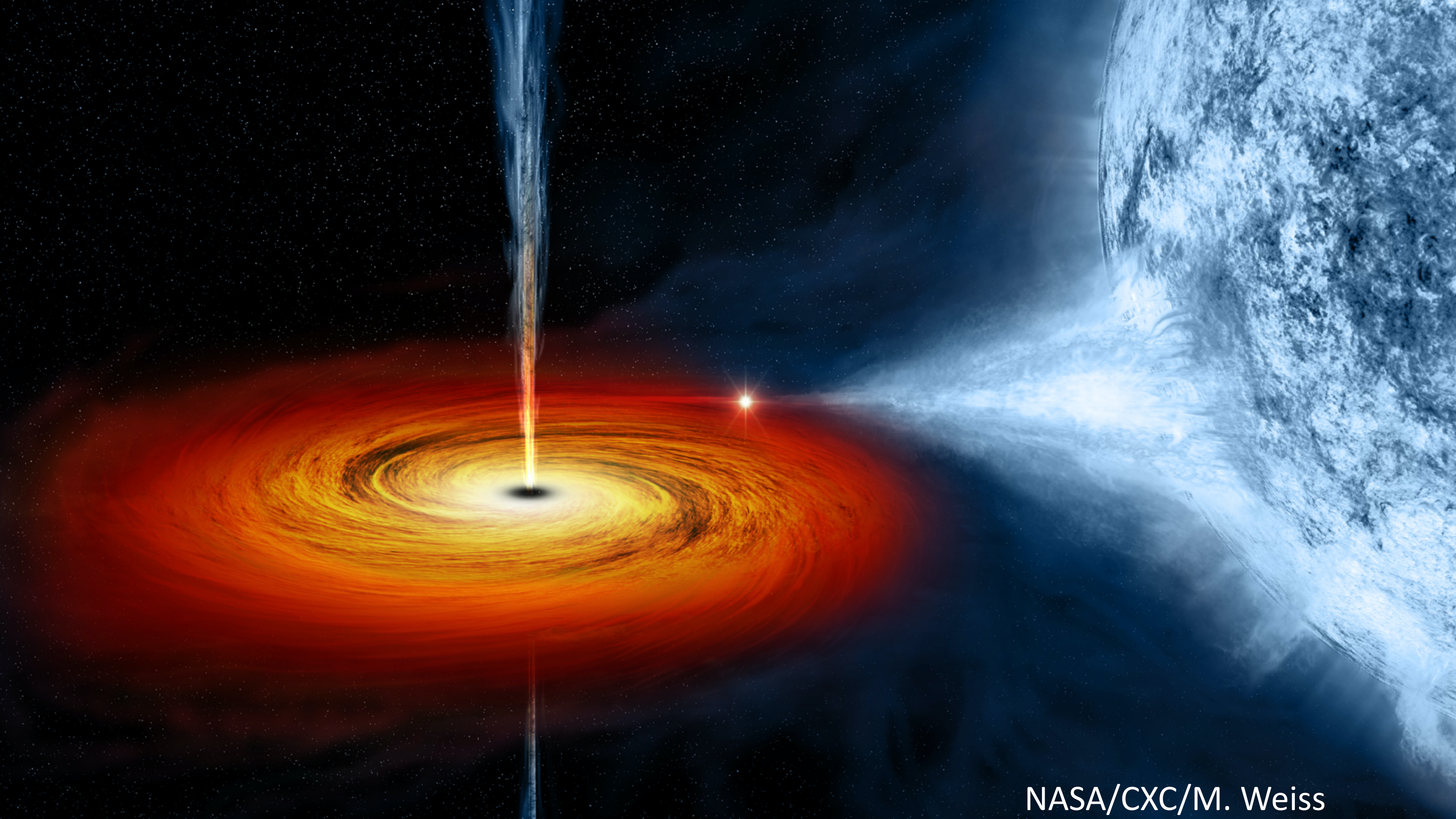

NASA/CXC/M. Weiss

Agenda:

- Review the relevant basics of black holes and black hole astrophysics.
- Discuss the underlying principles and methodology behind simulating infalling plasma, along with recent advances.
- Show how we generate synthetic X-ray spectra starting from simulation data.
- Connect these X-ray spectra to real observations.

- What are the current challenges facing this technique, and how might they be resolved?

black hole basics

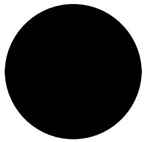

Black holes are characterized entirely by only two parameters: mass and dimensionless “spin.”

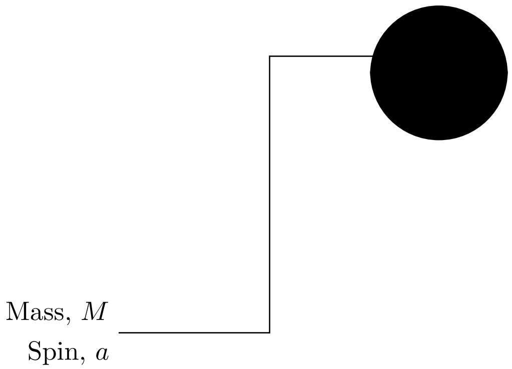

black hole basics

Black holes are characterized entirely by only two parameters: mass and dimensionless "spin."

$$-1 < a = \frac{J}{GM^2/c} < +1$$

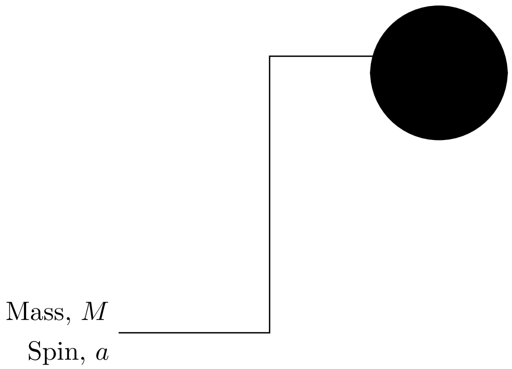

The central black hole mass sets the *length* and *time* scales for the whole system.

$$r_g = \frac{GM}{c^2} = \left(\frac{M}{M_\odot}\right) \cdot 1.5 \times 10^5 \text{ cm}$$

$$t_g = r_g/c = \left(\frac{M}{M_\odot}\right) \cdot 4.9 \times 10^{-6} \text{ s}$$

$$G = c = 1 \rightarrow r_g = t_g = 1M$$

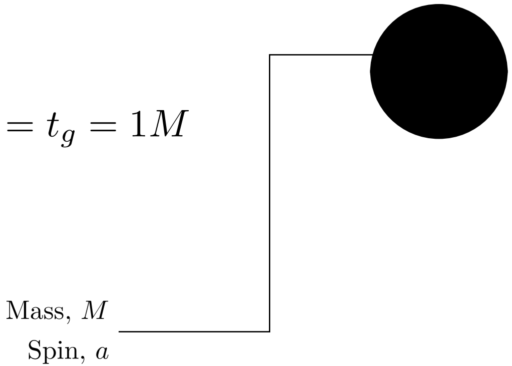

black hole basics

The central black hole mass sets the *length* and *time* scales for the whole system.

$$r_g = \frac{GM}{c^2} = \left(\frac{M}{M_\odot}\right) \cdot 1.5 \times 10^5 \text{ cm}$$

$$t_g = r_g/c = \left(\frac{M}{M_\odot}\right) \cdot 4.9 \times 10^{-6} \text{ s}$$

$$G = c = 1 \rightarrow r_g = t_g = 1M$$

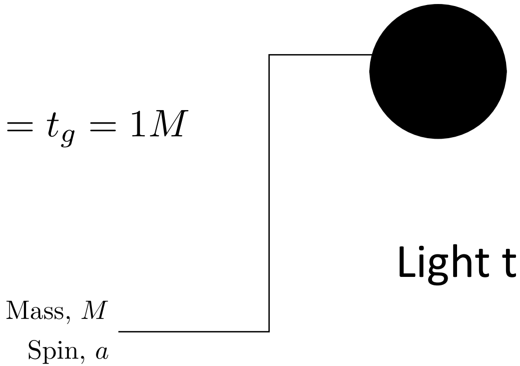

Light travels 1M (distance) in 1M (time).

black hole basics

The radius of the event horizon decreases with increasing spin.

$$r_h/M = 1 + \sqrt{1 - a^2}$$

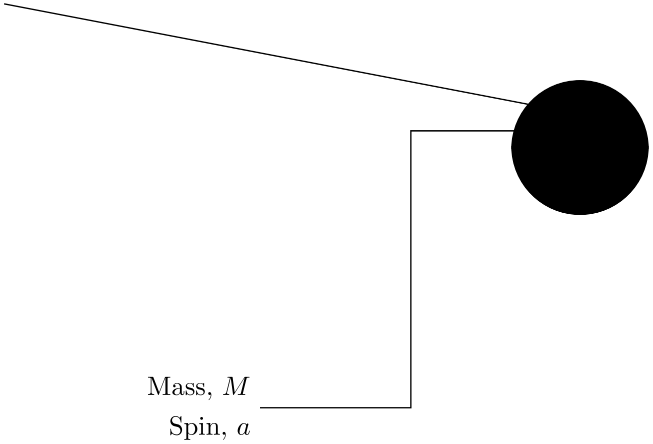

Inflowing matter loses energy by radiation but conserves angular momentum.

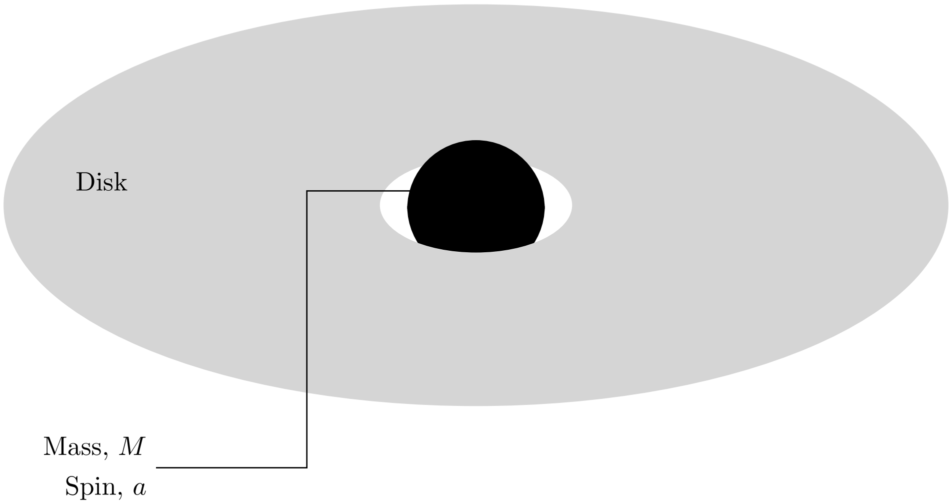

Inflowing matter loses energy by radiation
but conserves angular momentum.

Result: a geometrically thin, optically thick, slowly spiraling inward accretion disk.

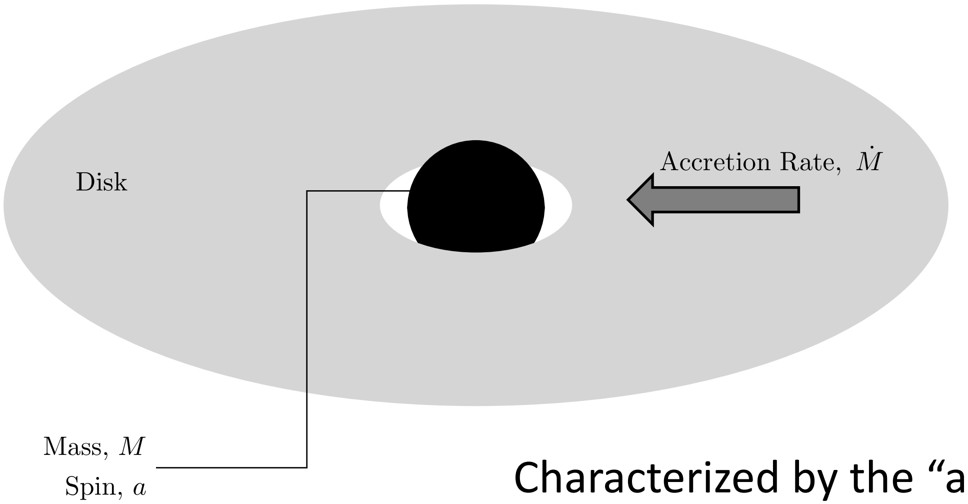

Characterized by the “accretion rate”:
inward mass flow rate per unit time.

The black hole mass sets the characteristic "Eddington" *luminosity* and *accretion rate*.

$$L_{\mathrm{Edd}} = \frac{4\pi G M m_p c}{\sigma_T} = \left(\frac{M}{M_\odot}\right) \cdot 1.3 \times 10^{38}\ \mathrm{erg\ s^{-1}} = \eta \dot{M}_{\mathrm{Edd}} c^2$$

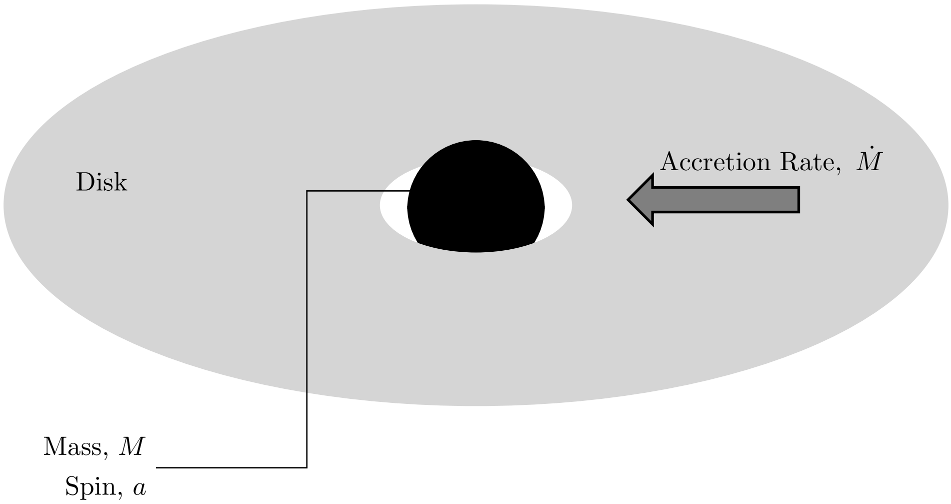

The black hole mass sets the characteristic "Eddington" *luminosity* and *accretion rate*.

$$L_{\rm Edd} = \frac{4\pi G M m_p c}{\sigma_T} = \left(\frac{M}{M_\odot}\right) \cdot 1.3 \times 10^{38}\ \mathrm{erg\ s^{-1}} = \eta \dot{M}_{\rm Edd} c^2$$

$$\eta \simeq 0.1$$

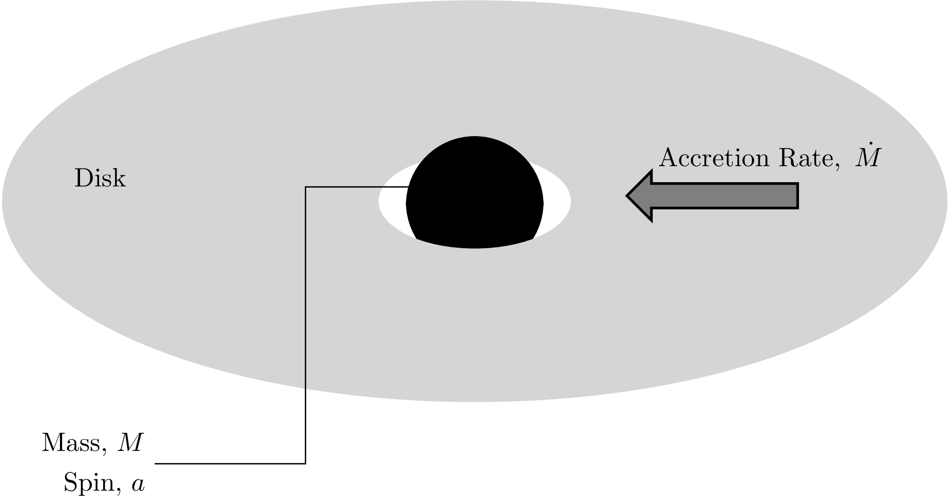

The black hole mass sets the characteristic "Eddington" *luminosity* and *accretion rate*.

$$L_{\mathrm{Edd}} = \frac{4\pi G M m_p c}{\sigma_T} = \left(\frac{M}{M_\odot}\right) \cdot 1.3 \times 10^{38} \ \mathrm{erg\ s^{-1}} = \eta \dot{M}_{\mathrm{Edd}} c^2$$

$$\eta \simeq 0.1$$

$$\dot{m} = \frac{\dot{M}}{\dot{M}_{\mathrm{Edd}}}$$

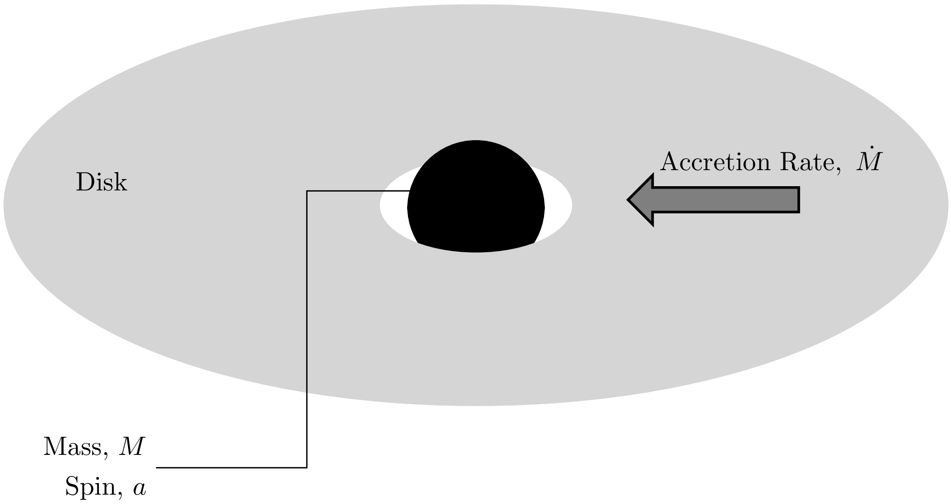

GR (unlike Newtonian gravity) constrains the existence of circular orbits.

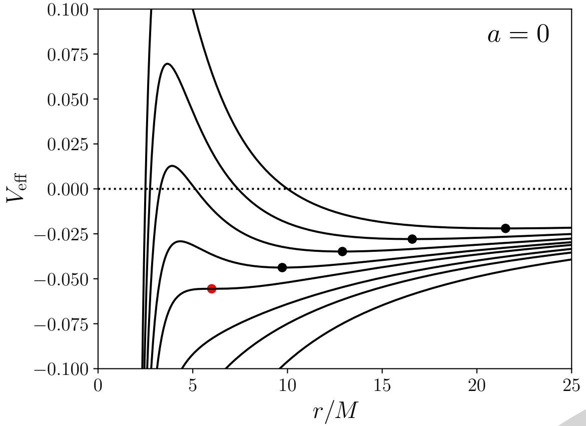

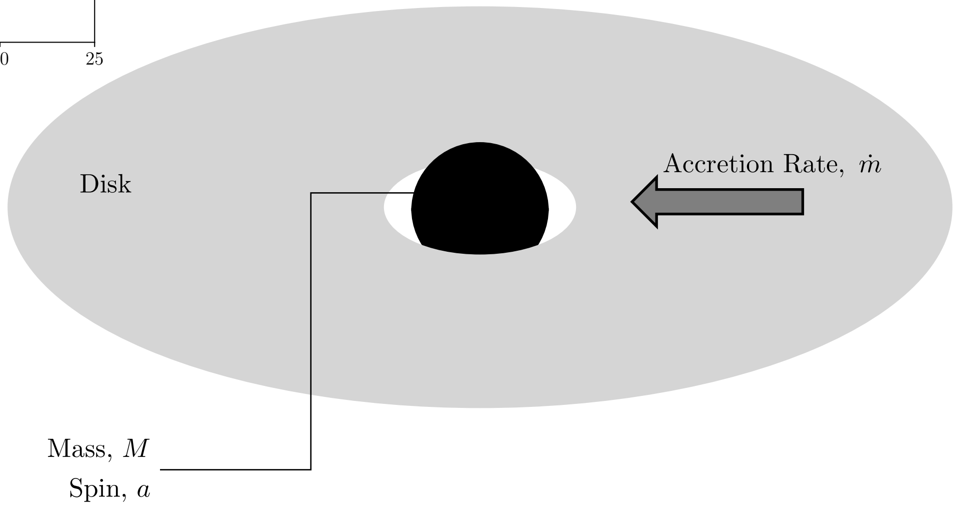

GR (unlike Newtonian gravity) constrains the existence of circular orbits.

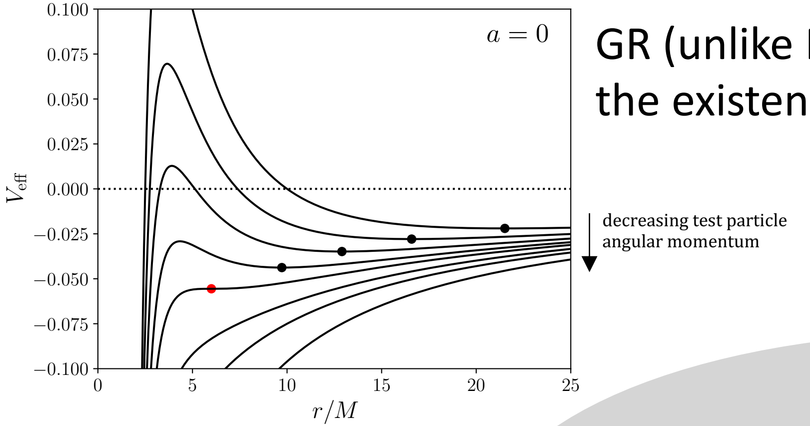

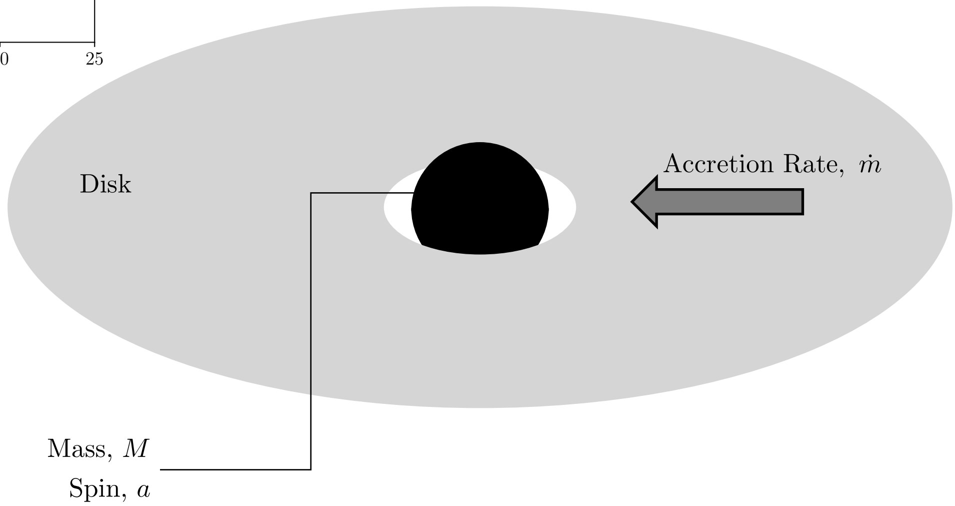

GR (unlike Newtonian gravity) constrains the existence of circular orbits.

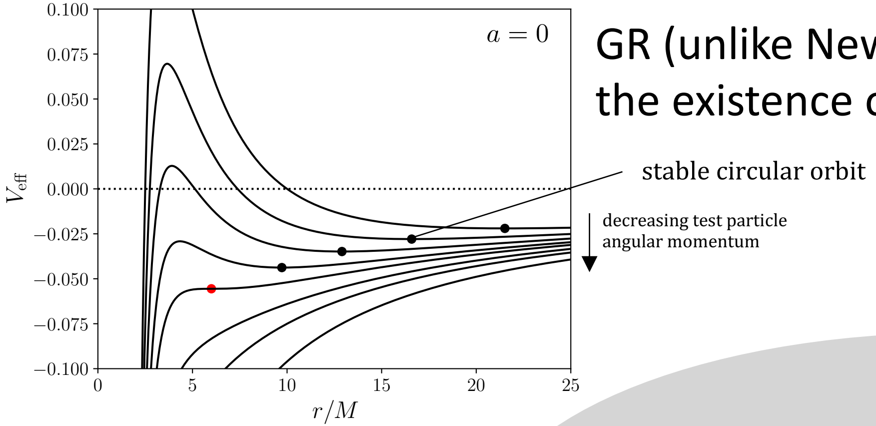

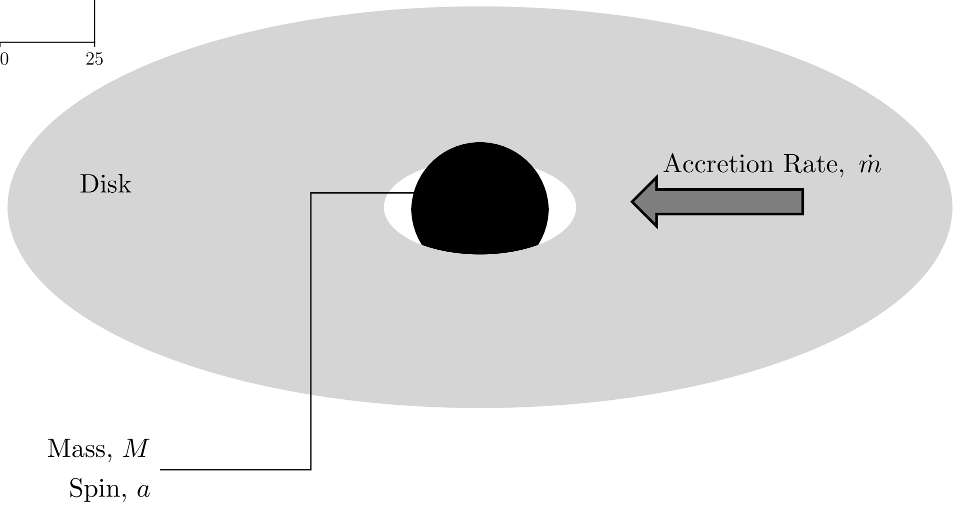

GR (unlike Newtonian gravity) constrains the existence of circular orbits.

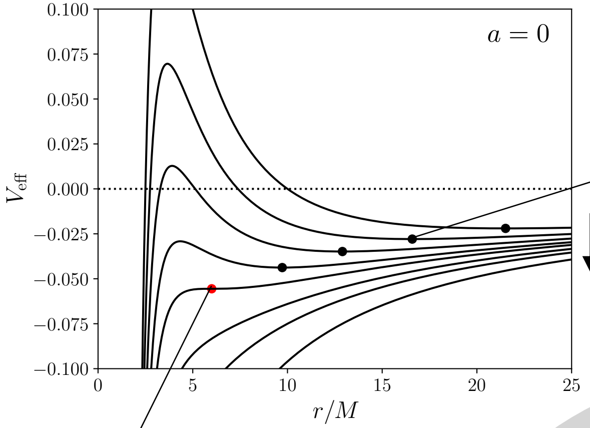

stable circular orbit

decreasing test particle angular momentum

radius of “marginal stability” or “innermost stable circular orbit (ISCO)”

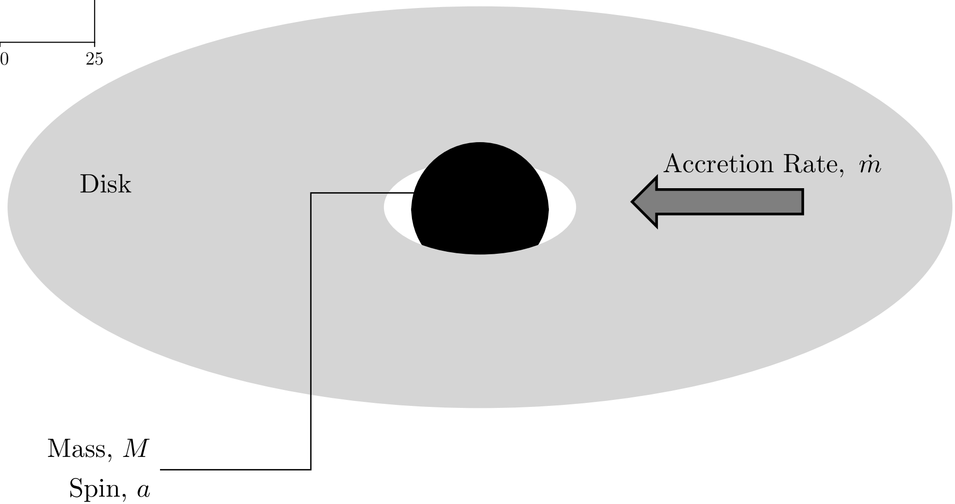

GR (unlike Newtonian gravity) constrains the existence of circular orbits.

black hole basics

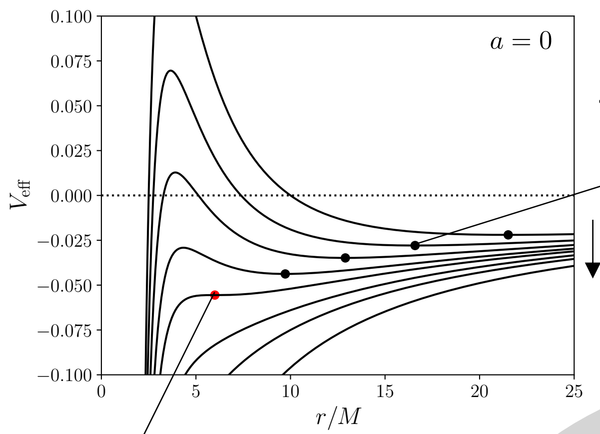

stable circular orbit

decreasing test particle angular momentum

radius of “marginal stability” or “innermost stable circular orbit (ISCO)”

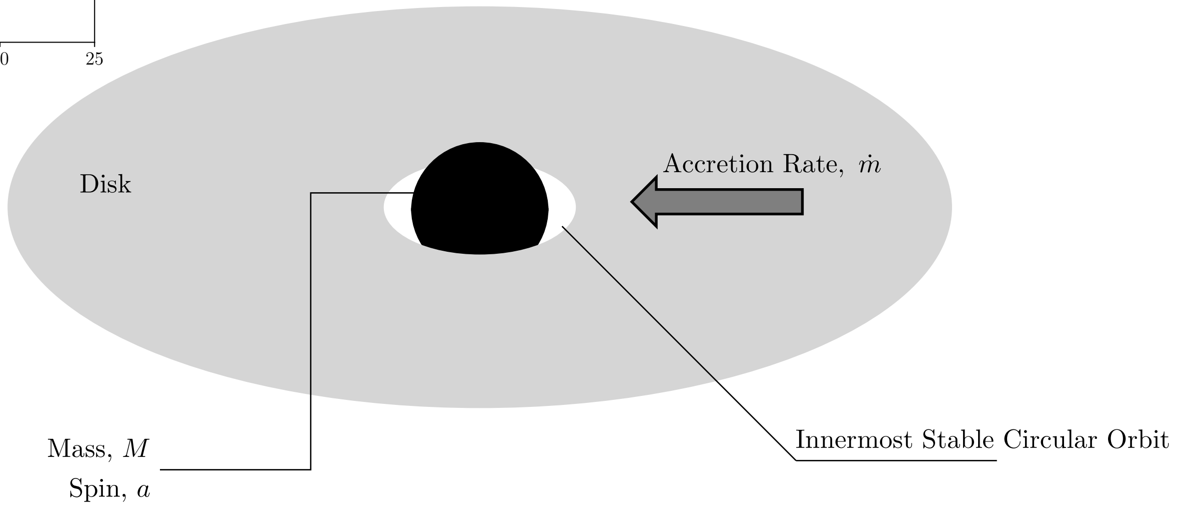

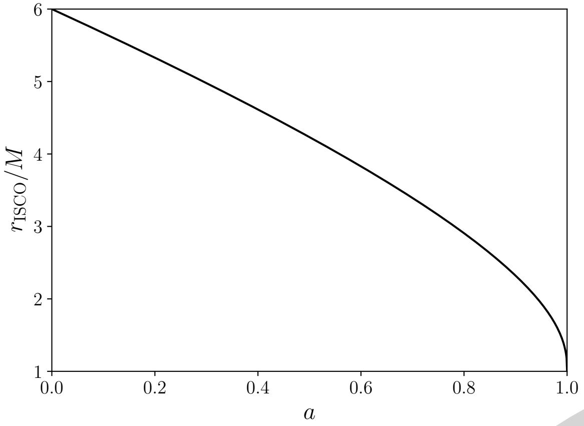

ISCO radius (like event horizon radius) decreases with increasing spin.

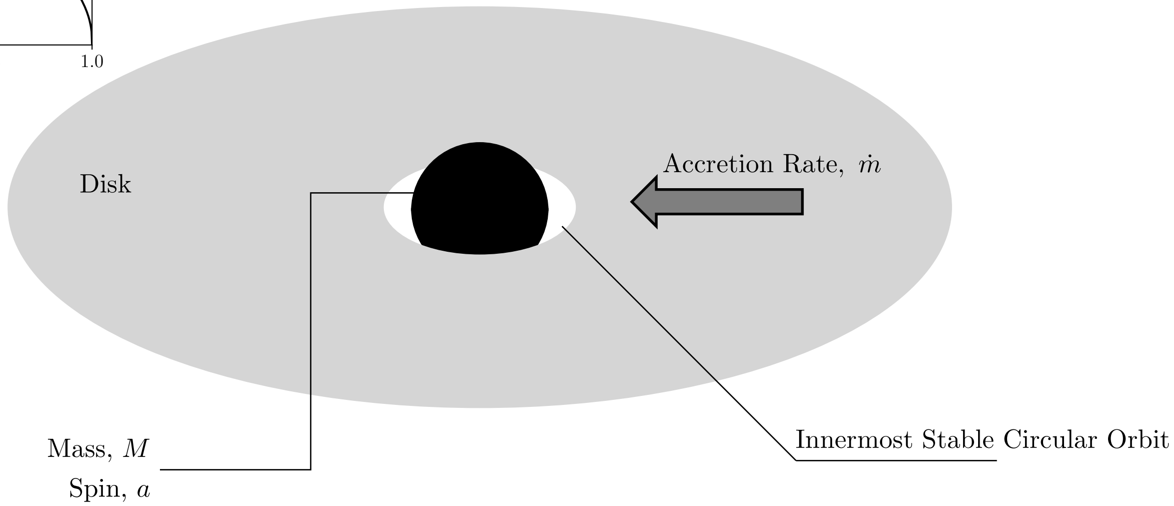

Above and below the dense cool disk lies
the magnetically-supported, hot, diffuse *corona*.

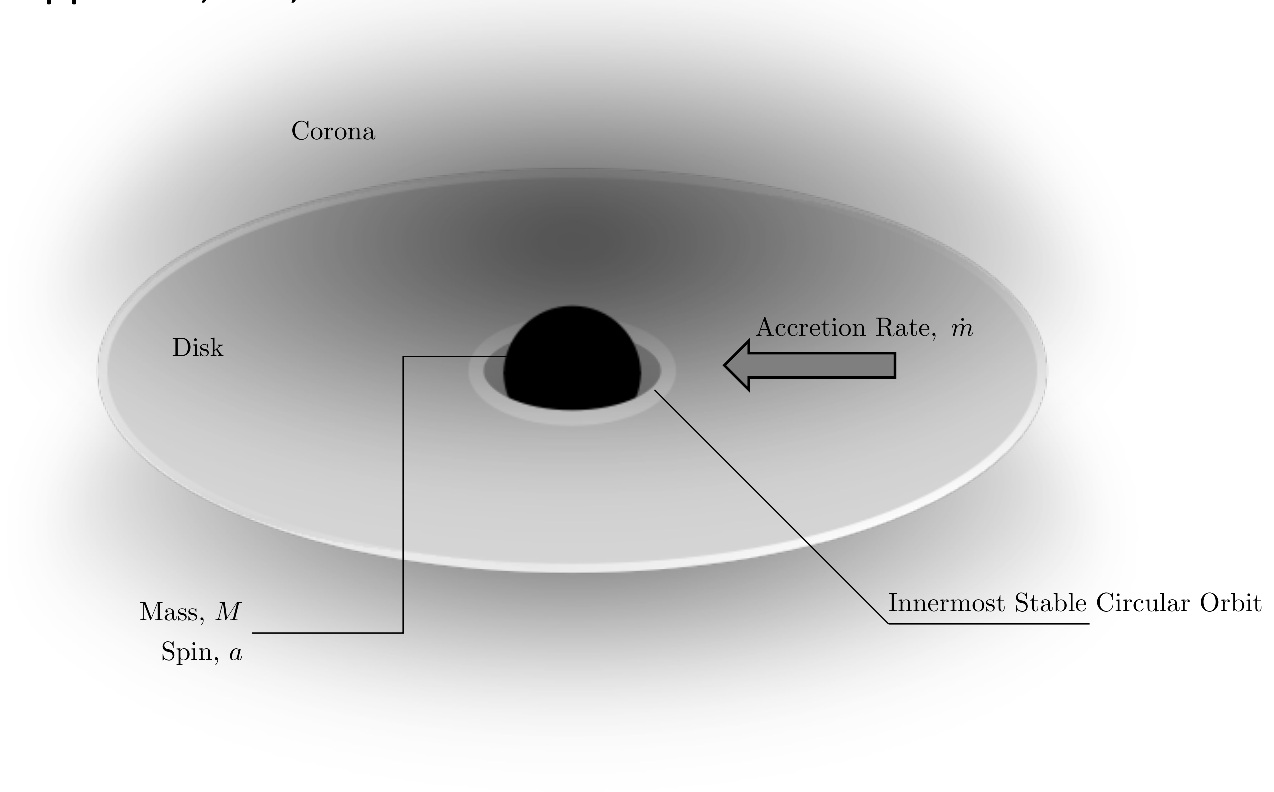

And in many systems, a relativistic *jet* launches perpendicular to the disk.

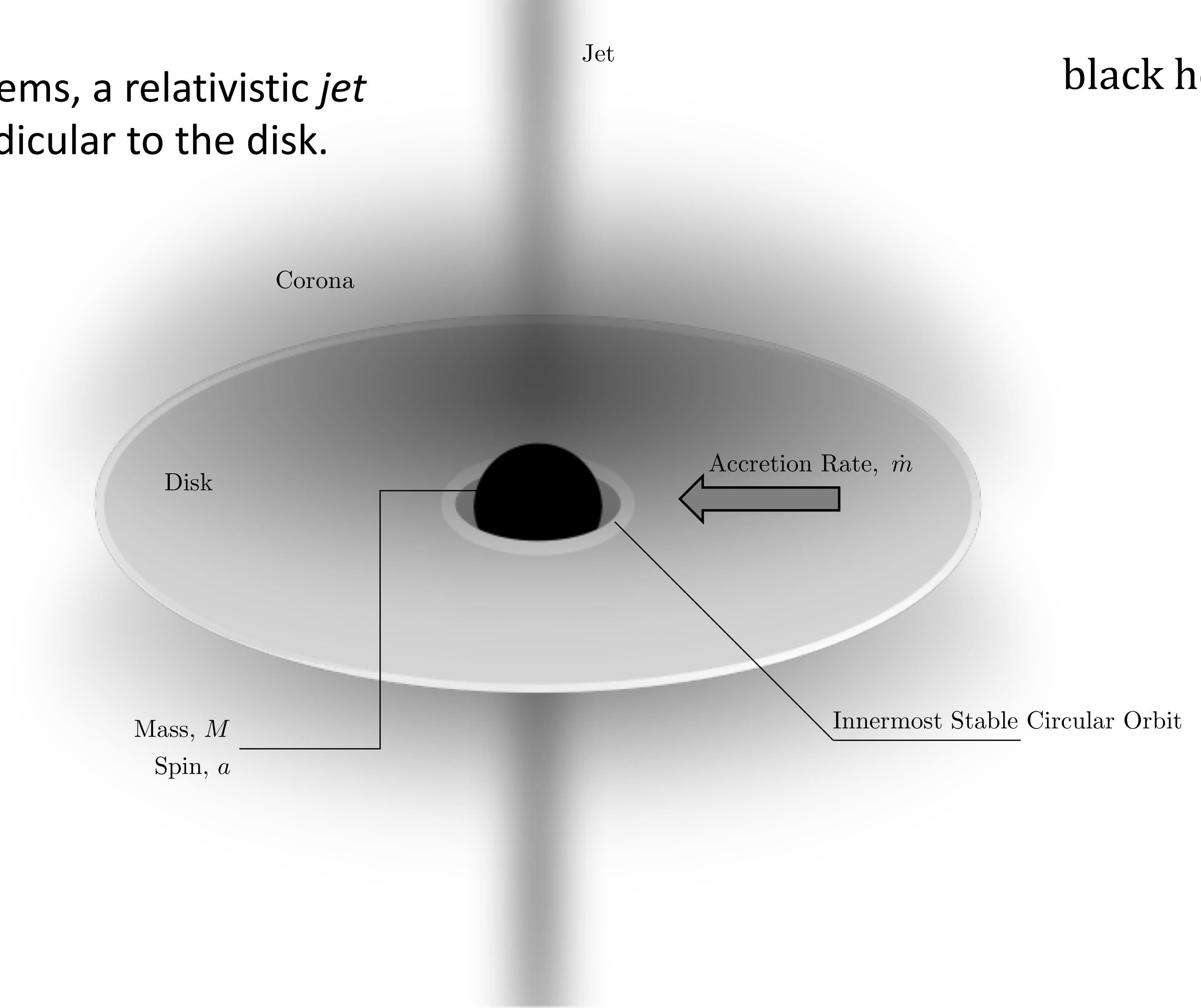

black hole basics

Observation is characterized by the *inclination angle:*
0° is a “face-on” disk, 90° is an “edge-on” disk.

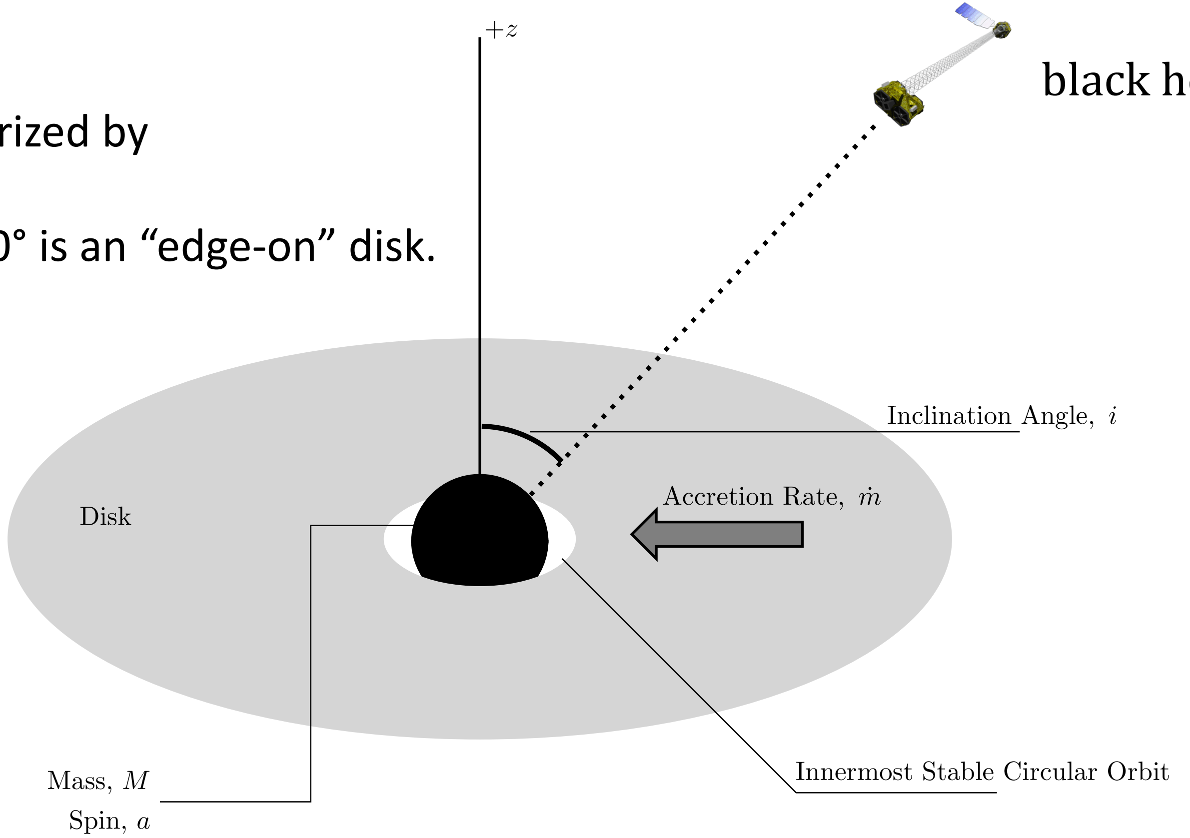

What does this X-ray telescope see?

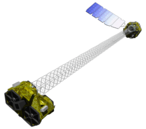

black hole basics

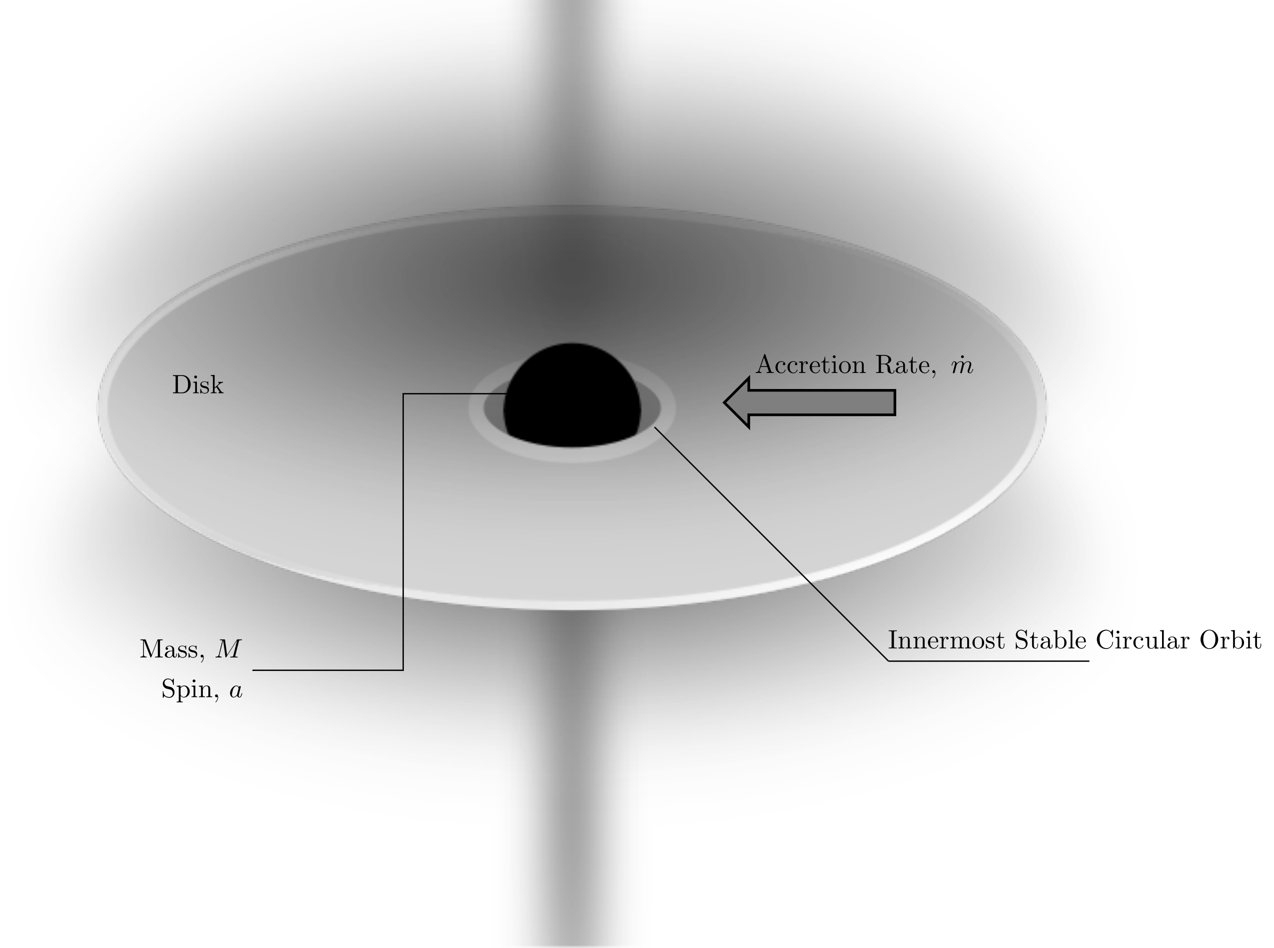

What does this X-ray telescope see?

The complex interactions between:

- thermal radiation from the disk
- Compton upscattering in the corona
- Compton downscattering in the disk
- reflection/“reprocessing” by the disk
- atomic processes (fluorescence)
- SR (boosting) and GR (redshifting) effects

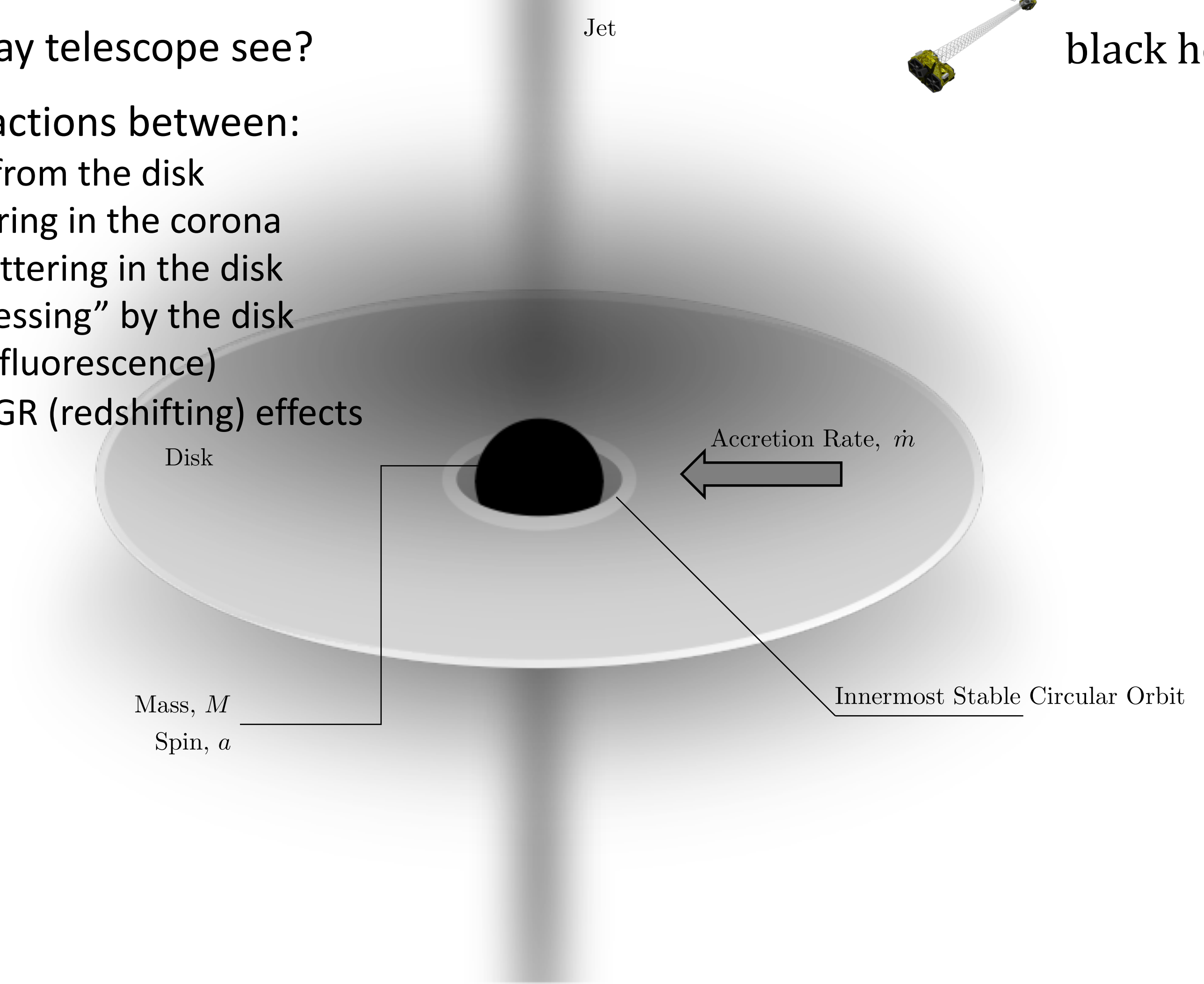

What does this X-ray telescope see?

The complex interactions between:

- thermal radiation from the disk
- Compton upscattering in the corona
- Compton downscattering in the disk
- reflection/“reprocessing” by the disk
- atomic processes (fluorescence)
- SR (boosting) and GR (redshifting) effects

All folded into one (point source) spectrum!

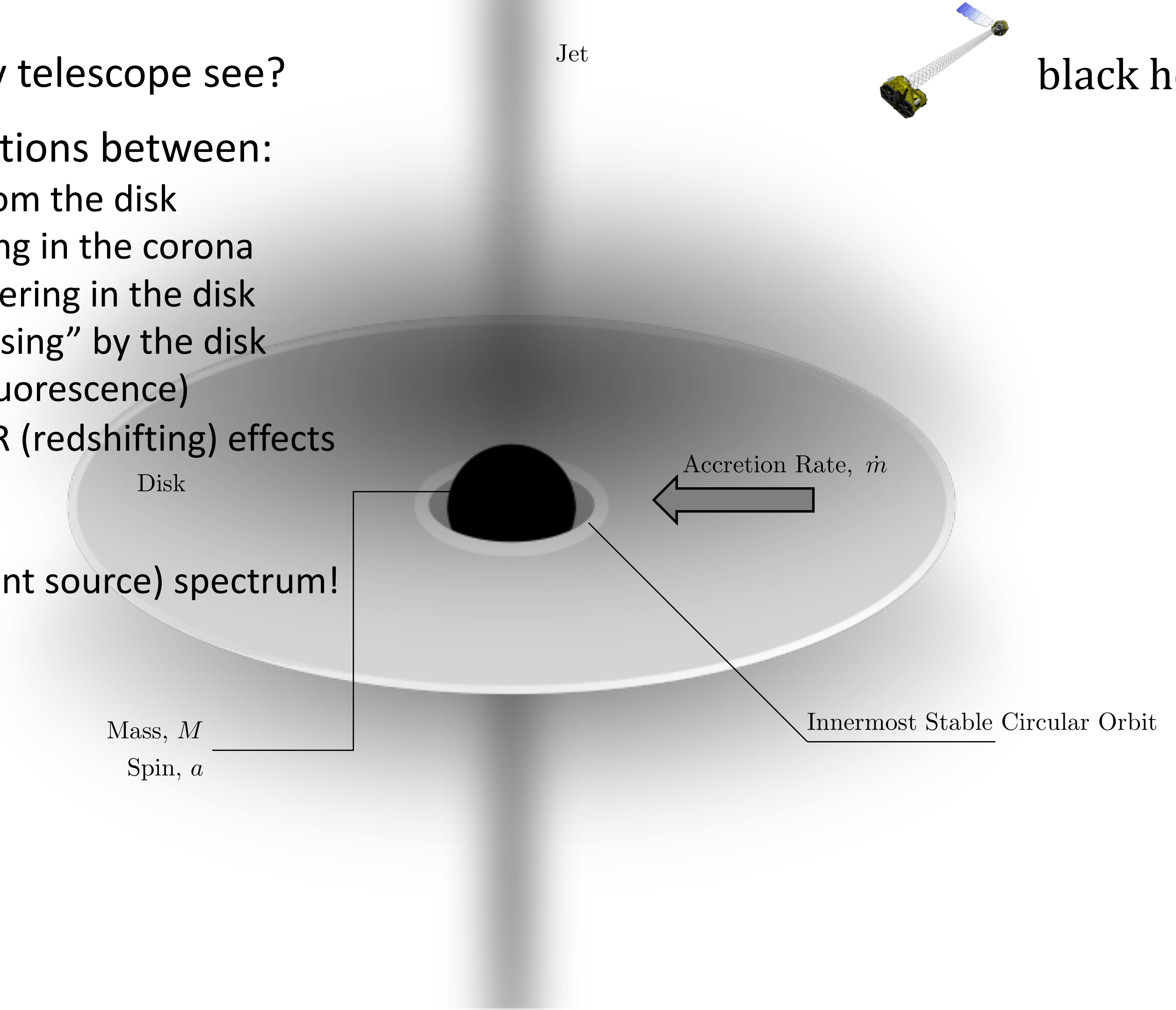

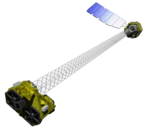

What does this X-ray telescope see?

The complex interactions between:

- thermal radiation from the disk
- Compton upscattering in the corona
- Compton downscattering in the disk
- reflection/“reprocessing” by the disk
- atomic processes (fluorescence)
- SR (boosting) and GR (redshifting) effects

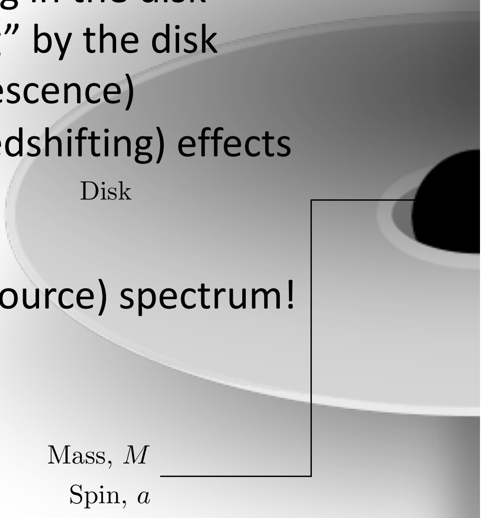

All folded into one (point source) spectrum!

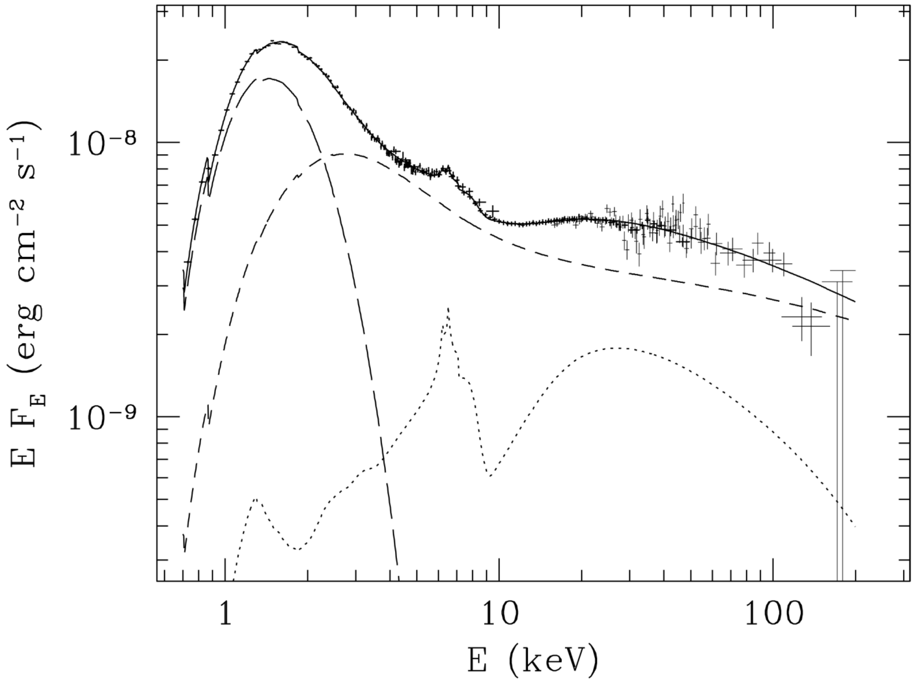

ASCA+RXTE spectra of Cyg X-1

(Gierliński & Zdziarski, 1999)

In order to model this spectrum…

We must first understand the nature of the accretion flow.

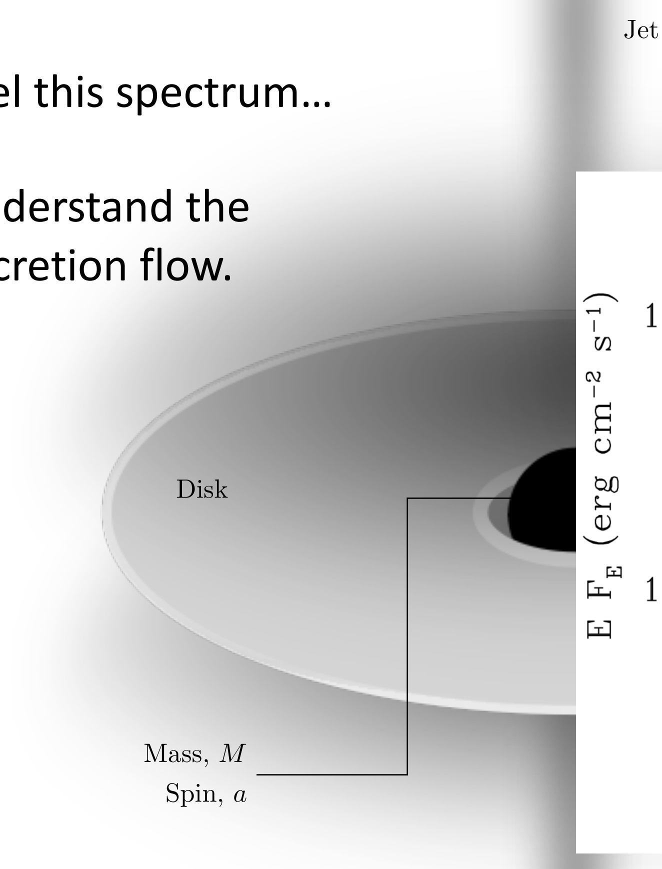

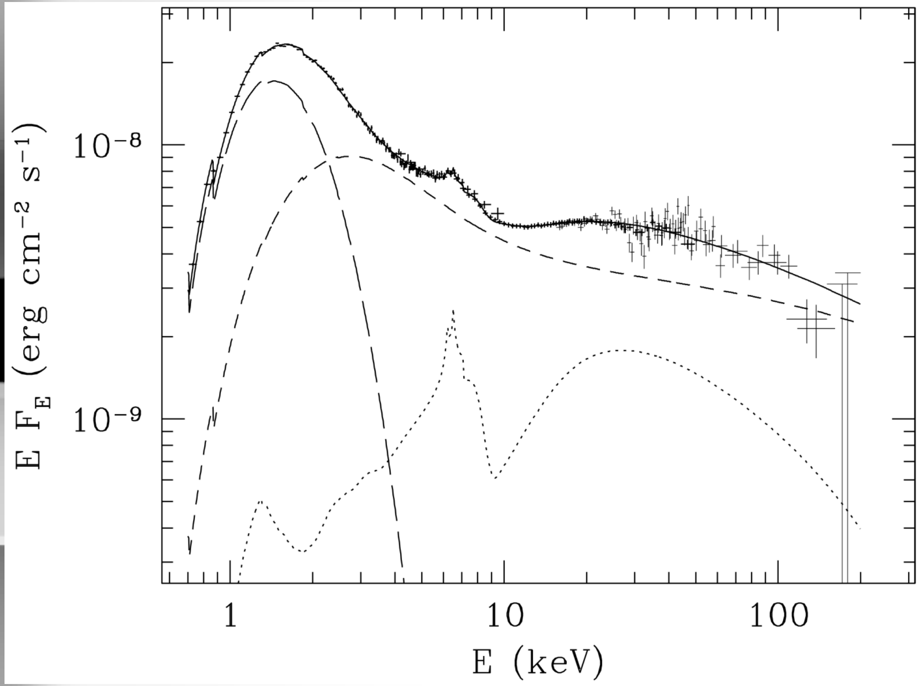

ASCA+RXTE spectra of Cyg X-1
(Gierliński & Zdziarski, 1999)

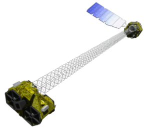

General Relativistic Magnetohydrodynamics (GRMHD)

$$\frac{1}{\sqrt{-g}}\partial_\mu\left(\sqrt{-g}\rho u^\mu\right) = 0$$ conservation of mass

$$\partial_t\left(\sqrt{-g}T^t{}_\nu\right) = -\partial_i\left(\sqrt{-g}T^i{}_\nu\right) + \sqrt{-g}T^\kappa{}_\lambda\Gamma^\lambda{}_{\nu\kappa}$$ conservation of energy-momentum (4 equations)

$$T^{\mu\nu}_{\mathrm{MHD}} = \left(\rho + u + p + b^2\right)u^\mu u^\nu + \left(p + \frac{b^2}{2}\right)g^{\mu\nu} - b^\mu b^\nu$$ <u>ideal</u> MHD tensor (zero fluid rest frame E field)

$$\partial_t\left(\sqrt{-g}B^i\right) = \partial_j\left[\sqrt{-g}\left(b^j u^i - b^i u^j\right)\right]$$ <u>ideal</u> MHD induction equation (Faraday's law + Ohm's law)

$$\frac{1}{\sqrt{-g}}\partial_i\left(\sqrt{-g}B^i\right) = 0$$ no magnetic monopoles constraint

$$p = (\Gamma - 1)u$$ ideal gas equation of state (for closure)

adiabatic index

General Relativistic Magnetohydrodynamics (GRMHD)

$$\frac{1}{\sqrt{-g}}\partial_\mu\left(\sqrt{-g}\rho u^\mu\right) = 0$$

$$\partial_t\left(\sqrt{-g}T^t{}_\nu\right) = -\partial_i\left(\sqrt{-g}T^i{}_\nu\right) + \sqrt{-g}T^\kappa{}_\lambda\Gamma^\lambda{}_{\nu\kappa}$$

$$T^{\mu\nu}_{\mathrm{MHD}} = \left(\rho + u + p + b^2\right)u^\mu u^\nu + \left(p + \frac{b^2}{2}\right)g^{\mu\nu} - b^\mu b^\nu$$

$$\partial_t\left(\sqrt{-g}B^i\right) = \partial_j\left[\sqrt{-g}\left(b^j u^i - b^i u^j\right)\right]$$

$$\frac{1}{\sqrt{-g}}\partial_i\left(\sqrt{-g}B^i\right) = 0$$

$$p = (\Gamma - 1)u$$

The HARM method:

A conservative, shock-capturing scheme which maintains a divergence-free magnetic field (Gammie, McKinney, & Tóth, 2003).

General Relativistic Magnetohydrodynamics (GRMHD)

$$\frac{1}{\sqrt{-g}}\partial_\mu\left(\sqrt{-g}\rho u^\mu\right)=0$$

$$\partial_t\left(\sqrt{-g}T^t{}_\nu\right)=-\partial_i\left(\sqrt{-g}T^i{}_\nu\right)+\sqrt{-g}T^\kappa{}_\lambda\Gamma^\lambda{}_{\nu\kappa}$$

$$T^{\mu\nu}_{\mathrm{MHD}}=\left(\rho+u+p+b^2\right)u^\mu u^\nu+\left(p+\frac{b^2}{2}\right)g^{\mu\nu}-b^\mu b^\nu$$

$$\partial_t\left(\sqrt{-g}B^i\right)=\partial_j\left[\sqrt{-g}\left(b^j u^i-b^i u^j\right)\right]$$

$$\frac{1}{\sqrt{-g}}\partial_i\left(\sqrt{-g}B^i\right)=0$$

$$p=(\Gamma-1)u$$

The `HARM` method:

1. Define a vector of conserved variables:

$$\mathbf{U}\equiv\sqrt{-g}\left(\rho u^t, T^t{}_t, T^t{}_i, B^i\right)$$

2. Define a vector of "primitive" variables:

$$\mathbf{P}\equiv\left(\rho, u, v^i, B^i\right)$$

3. Re-cast equations into flux-conservative form:

$$\partial_t\mathbf{U}\left(\mathbf{P}\right)=-\partial_i\mathbf{F}^i\left(\mathbf{P}\right)+\mathbf{S}\left(\mathbf{P}\right)$$

4. Update conserved variables (explicitly integrate above equation over one time step)

5. Recover primitives from conserved variables via multidimensional Newton-Raphson.

$$\mathbf{P}_{t+\Delta t}=g\left(\mathbf{U}_{t+\Delta t}\right)$$

General Relativistic Magnetohydrodynamics (GRMHD)

$$\frac{1}{\sqrt{-g}}\partial_\mu\left(\sqrt{-g}\rho u^\mu\right) = 0$$

total energy is conserved

$$\boxed{\partial_t\left(\sqrt{-g}T^t{}_\nu\right) = -\partial_i\left(\sqrt{-g}T^i{}_\nu\right) + \sqrt{-g}T^\kappa{}_\lambda\Gamma^\lambda{}_{\nu\kappa}}$$

$$T^{\mu\nu}_{\mathrm{MHD}} = \left(\rho + u + p + b^2\right)u^\mu u^\nu + \left(p + \frac{b^2}{2}\right)g^{\mu\nu} - b^\mu b^\nu$$

$$\partial_t\left(\sqrt{-g}B^i\right) = \partial_j\left[\sqrt{-g}\left(b^j u^i - b^i u^j\right)\right]$$

$$\frac{1}{\sqrt{-g}}\partial_i\left(\sqrt{-g}B^i\right) = 0$$

$$p = (\Gamma - 1)u$$

The HARM method:

1. Define a vector of conserved variables:
$$\mathbf{U} \equiv \sqrt{-g}\left(\rho u^t, T^t{}_t, T^t{}_i, B^i\right)$$
2. Define a vector of "primitive" variables:
$$\mathbf{P} \equiv \left(\rho, u, v^i, B^i\right)$$
3. Re-cast equations into flux-conservative form:
$$\partial_t\mathbf{U}\left(\mathbf{P}\right) = -\partial_i\mathbf{F}^i\left(\mathbf{P}\right) + \mathbf{S}\left(\mathbf{P}\right)$$
4. Update conserved variables (explicitly integrate above equation over one time step)
5. Recover primitives from conserved variables via multidimensional Newton-Raphson.
$$\mathbf{P}_{t+\Delta t} = g\left(\mathbf{U}_{t+\Delta t}\right)$$

Inflowing matter loses energy by radiation
but conserves angular momentum.

Result: a geometrically thin, optically thick, slowly spiraling inward accretion disk.

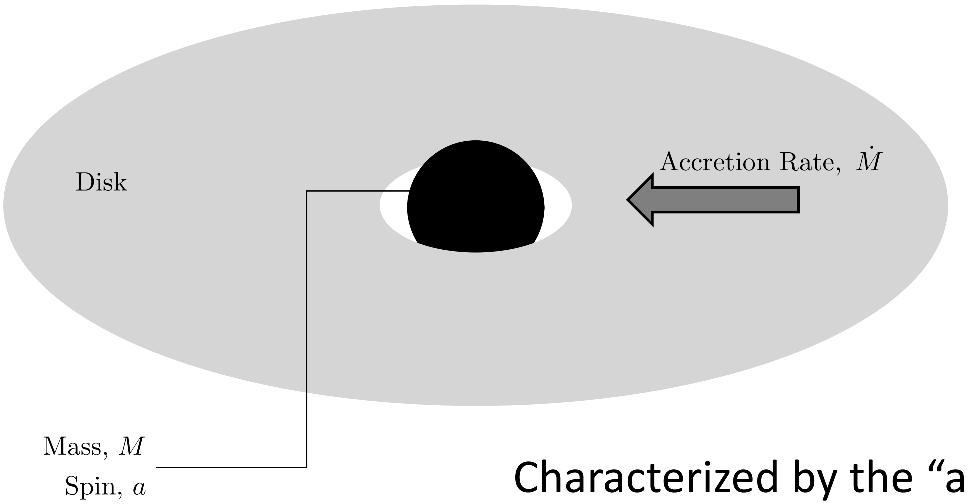

Characterized by the "accretion rate":
inward mass flow rate per unit time.

General Relativistic Magnetohydrodynamics (GRMHD)

$$\frac{1}{\sqrt{-g}}\partial_\mu\left(\sqrt{-g}\rho u^\mu\right)=0$$

total energy is conserved

$$\boxed{\partial_t\left(\sqrt{-g}T^t{}_\nu\right)=-\partial_i\left(\sqrt{-g}T^i{}_\nu\right)+\sqrt{-g}T^\kappa{}_\lambda\Gamma^\lambda{}_{\nu\kappa}}$$

$$T^{\mu\nu}_{\mathrm{MHD}}=\left(\rho+u+p+b^2\right)u^\mu u^\nu+\left(p+\frac{b^2}{2}\right)g^{\mu\nu}-b^\mu b^\nu$$

$$\partial_t\left(\sqrt{-g}B^i\right)=\partial_j\left[\sqrt{-g}\left(b^j u^i-b^i u^j\right)\right]$$

$$\frac{1}{\sqrt{-g}}\partial_i\left(\sqrt{-g}B^i\right)=0$$

$$p=(\Gamma-1)u$$

The `HARM` method:

1. Define a vector of conserved variables:
   $$\mathbf{U}\equiv\sqrt{-g}\left(\rho u^t,T^t{}_t,T^t{}_i,B^i\right)$$
2. Define a vector of "primitive" variables:
   $$\mathbf{P}\equiv\left(\rho,u,v^i,B^i\right)$$
3. Re-cast equations into flux-conservative form:
   $$\partial_t\mathbf{U}\left(\mathbf{P}\right)=-\partial_i\mathbf{F}^i\left(\mathbf{P}\right)+\mathbf{S}\left(\mathbf{P}\right)$$
4. Update conserved variables (explicitly integrate above equation over one time step)
5. Recover primitives from conserved variables via multidimensional Newton-Raphson.

To model moderately-accreting systems of interest (XRBs or AGN), we require GR**R**MHD (+ radiation)… or some means by which to mimic radiative losses.

General Relativistic Magnetohydrodynamics (GRMHD)

`HARM3D` (Noble, Krolik & Hawley 2009):

A 3D extension to the (original, 2D) `HARM` code,

including an energy *sink* term in the stress-energy conservation equations.

General Relativistic Magnetohydrodynamics (GRMHD)

`HARM3D` (Noble, Krolik & Hawley 2009):

A 3D extension to the (original, 2D) `HARM` code,
including an energy *sink* term in the stress-energy conservation equations.

Gas is cooled over an orbital time scale to achieve a target temperature, itself chosen to achieve a target *aspect ratio* – that of a geometrically thin disk.

$$T_{\text{target}} = \frac{\pi}{2} \frac{R_z(r)}{r} \underbrace{\left[\frac{H(r)}{r} \right]^2}_{\text{“aspect ratio”}}$$

General Relativistic Magnetohydrodynamics (GRMHD)

`HARM3D` (Noble, Krolik & Hawley 2009):

A 3D extension to the (original, 2D) `HARM` code,
including an energy *sink* term in the stress-energy conservation equations.

Gas is cooled over an orbital time scale to achieve a target temperature, itself chosen to achieve a target *aspect ratio* – that of a geometrically thin disk.

$$T_{\text{target}} = \frac{\pi}{2} \frac{R_z(r)}{r} \underbrace{\left[\frac{H(r)}{r}\right]^2}_{\text{“aspect ratio”}}$$

$$\mathcal{L}_{\text{TT}} = \underbrace{s\Omega\rho\epsilon\left[Y - 1 + |Y - 1|\right]^q}_{\text{“Cool gravitationally bound gas to target-T over one orbital period.”}}$$

target-temperature
cooling function

General Relativistic Magnetohydrodynamics (GRMHD)

HARM3D (Noble, Krolik & Hawley 2009):

A 3D extension to the (original, 2D) HARM code,
including an energy *sink* term in the stress-energy conservation equations.

Gas is cooled over an orbital time scale to achieve a target temperature, itself chosen to achieve a target *aspect ratio* – that of a geometrically thin disk.

$$T_{\text{target}} = \frac{\pi}{2}\frac{R_z(r)}{r}\left[\frac{H(r)}{r}\right]^2$$

“aspect ratio”

$$\mathcal{L}_{\text{TT}} = \underbrace{s\Omega\rho\epsilon\left[Y - 1 + |Y-1|\right]^q}_{\text{“Cool gravitationally bound gas to target-T over one orbital period.”}}$$

target-temperature cooling function

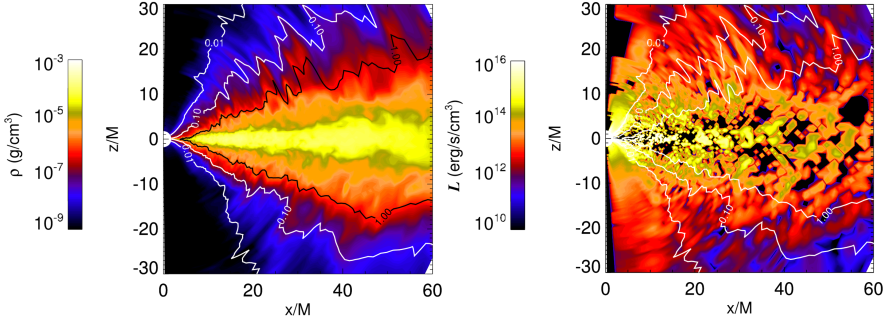

“ThinHR” simulation series:

- Achieves a thin disk in inflow equilibrium.
- Naturally produces an extended corona.
- Resolves the magneto-rotational instability.

Two microphysical improvements to `HARM3D`:

(Kinch, Noble, Schnittman, & Krolik 2020)

Inverse Compton Coronal Cooling Function

Two microphysical improvements to HARM3D:

(Kinch, Noble, Schnittman, & Krolik 2020)

Inverse Compton Coronal Cooling Function

- The cool, dense disk radiates (relatively) low energy thermal photons known as “seed photons.”

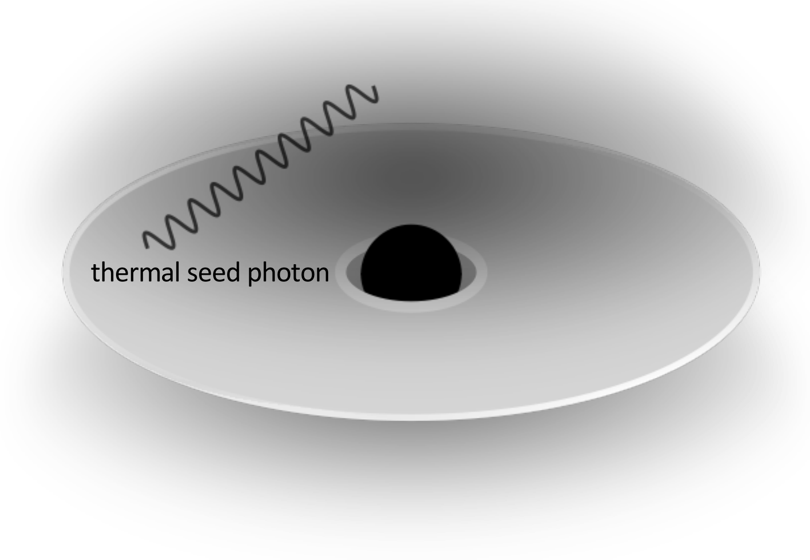

Two microphysical improvements to `HARM3D`:

(Kinch, Noble, Schnittman, & Krolik 2020)

Inverse Compton Coronal Cooling Function

- The cool, dense disk radiates (relatively) low energy thermal photons known as “seed photons.”
- These scatter off high energy electrons in the hot, diffuse corona, <u>*cooling*</u> the corona and *boosting* the photons.

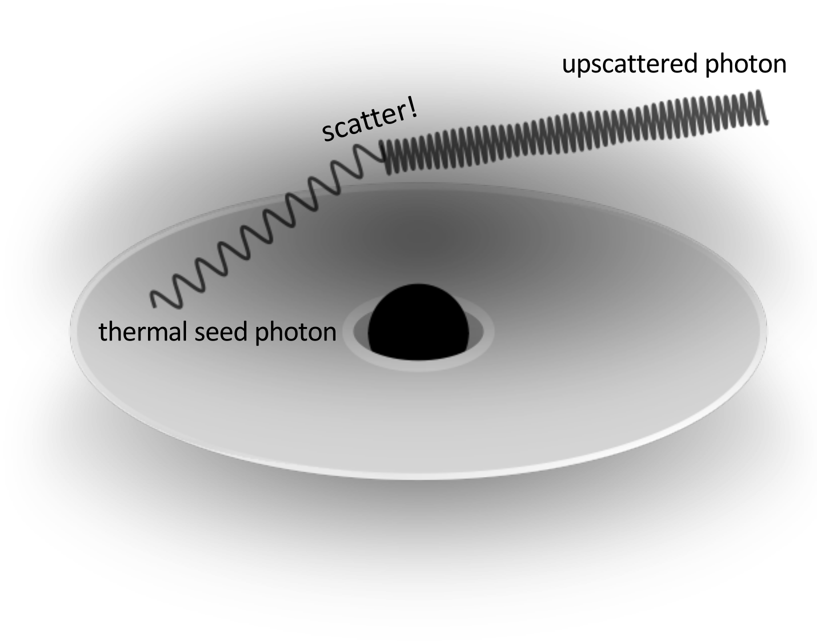

Two microphysical improvements to HARM3D:

(Kinch, Noble, Schnittman, & Krolik 2020)

Inverse Compton Coronal Cooling Function

- The cool, dense disk radiates (relatively) low energy thermal photons known as “seed photons.”
- These scatter off high energy electrons in the hot, diffuse corona, _cooling_ the corona and *boosting* the photons.

$$\mathcal{L}_{\rm IC} = \frac{4\sigma_T c\chi}{m_i}\rho u_{\rm rad}\Theta_e\left(1+4\Theta_e\right)$$

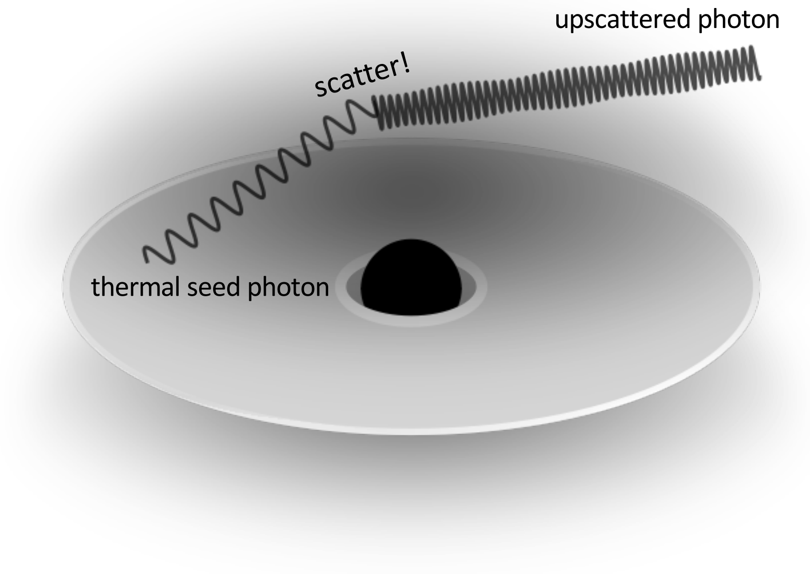

Two microphysical improvements to HARM3D:

(Kinch, Noble, Schnittman, & Krolik 2020)

Inverse Compton Coronal Cooling Function

- The cool, dense disk radiates (relatively) low energy thermal photons known as "seed photons."
- These scatter off high energy electrons in the hot, diffuse corona, <u>*cooling*</u> the corona and *boosting* the photons.

$$\mathcal{L}_{\rm IC} = \frac{4\sigma_T c\chi}{m_i}\rho u_{\rm rad}\Theta_e\left(1+4\Theta_e\right)$$

The challenge: arrive at a reasonable approximation for the radiation energy density…

without resorting to full transport.

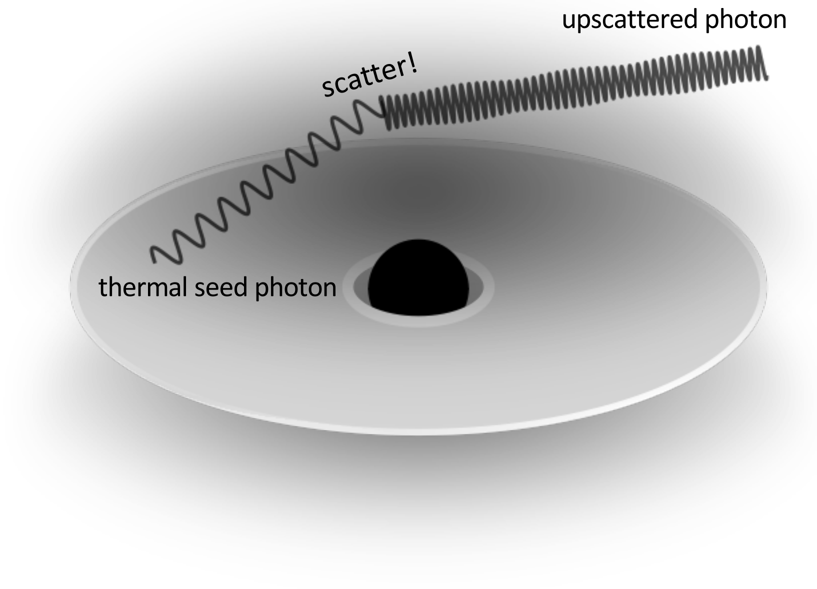

Two microphysical improvements to `HARM3D`:

(Kinch, Noble, Schnittman, & Krolik 2020)

Inverse Compton Coronal Cooling Function

$$\mathcal{L}_{\rm IC} = \frac{4\sigma_T c\chi}{m_i}\rho u_{\rm rad}\Theta_e\left(1+4\Theta_e\right)$$

As it turns out, if you assume:

1) The disk radiates a local blackbody,
2) The effects of SR and GR can be ignored,

and 3) Light travel time is instantaneous…

Two microphysical improvements to HARM3D:

(Kinch, Noble, Schnittman, & Krolik 2020)

Inverse Compton Coronal Cooling Function

$$\mathcal{L}_{\mathrm{IC}} = \frac{4\sigma_T c \chi}{m_i} \rho u_{\mathrm{rad}} \Theta_e \left(1 + 4\Theta_e\right)$$

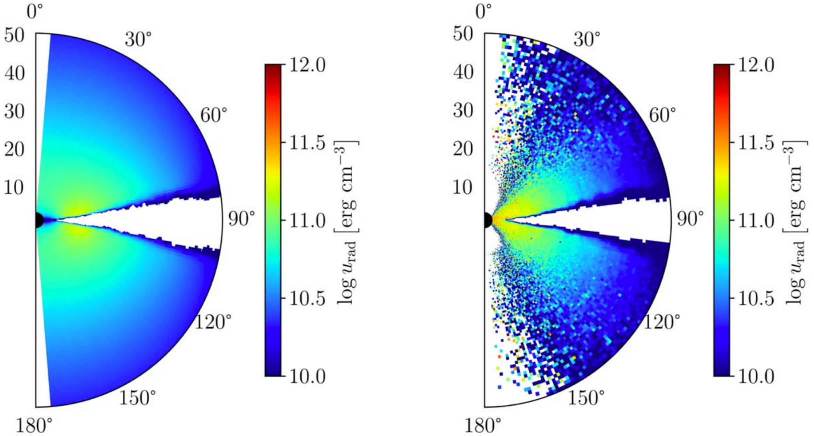

inline evaluation   ray-tracing

As it turns out, if you assume:

1) The disk radiates a local blackbody,

2) The effects of SR and GR can be ignored,

and 3) Light travel time is instantaneous…

You can get an expression which agrees reasonably well with detailed ray-tracing.

Two microphysical improvements to HARM3D:

(Kinch, Noble, Schnittman, & Krolik 2020)

Inverse Compton Coronal Cooling Function

$$\mathcal{L}_{\rm IC} = \frac{4\sigma_T c\chi}{m_i}\rho u_{\rm rad}\Theta_e\left(1+4\Theta_e\right)$$

As it turns out, if you assume:

1) The disk radiates a local blackbody,

2) The effects of SR and GR can be ignored,

and 3) Light travel time is instantaneous…

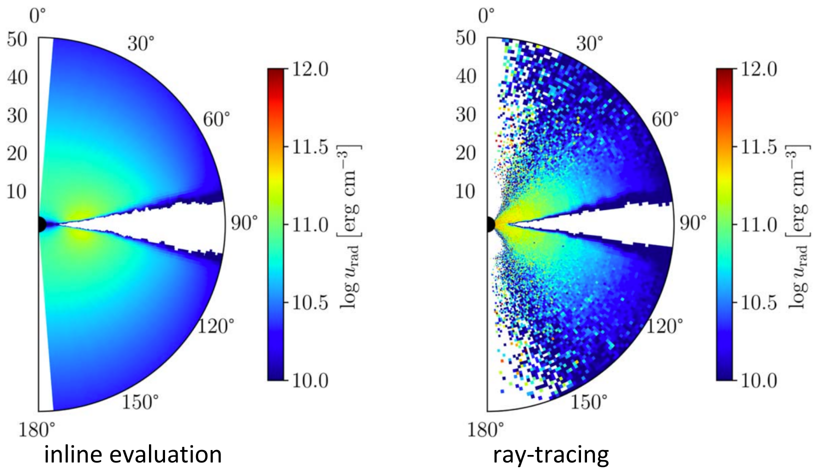

You can get an expression which agrees reasonably well with detailed ray-tracing.

Crucially important for modeling real black hole systems on human time scales.

Two microphysical improvements to `HARM3D`:

(Kinch, Noble, Schnittman, & Krolik 2020)

Two-Temperature Coronal Model

Turbulent energy eventually heats up the plasma *thermally* – how this heat is split between ions and electrons is a *difficult* plasma kinetics problem.

Two microphysical improvements to `HARM3D`:

(Kinch, Noble, Schnittman, & Krolik 2020)

Two-Temperature Coronal Model

Turbulent energy eventually heats up the plasma *thermally* – how this heat is split between ions and electrons is a *difficult* plasma kinetics problem.

But the *least radiatively efficient* scenario is that it's *all* dumped into the ions.

Two microphysical improvements to HARM3D:

(Kinch, Noble, Schnittman, & Krolik 2020)

Two-Temperature Coronal Model

Turbulent energy eventually heats up the plasma *thermally* – how this heat is split between ions and electrons is a *difficult* plasma kinetics problem.

But the *least radiatively efficient* scenario is that it's *all* dumped into the ions.

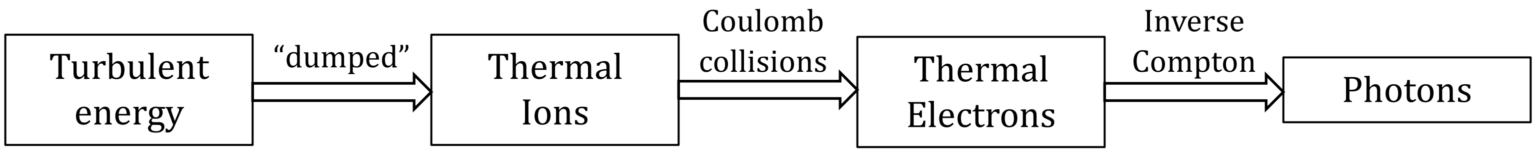

Two microphysical improvements to `HARM3D`:

(Kinch, Noble, Schnittman, & Krolik 2020)

Two-Temperature Coronal Model

Turbulent energy eventually heats up the plasma *thermally* – how this heat is split between ions and electrons is a *difficult* plasma kinetics problem.

But the *least radiatively efficient* scenario is that it's *all* dumped into the ions.

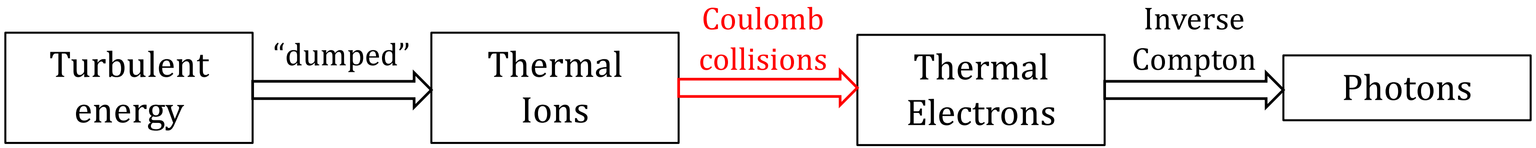

It turns out ion/electron *Coulomb heating* is the slowest rate by far.

Two microphysical improvements to HARM3D:

(Kinch, Noble, Schnittman, & Krolik 2020)

Two-Temperature Coronal Model

This allows us to replace cumbersome coupled rate equations with a

snap-to-equilibrium

lookup-table-accelerated

approximation to a 2T coronal plasma.

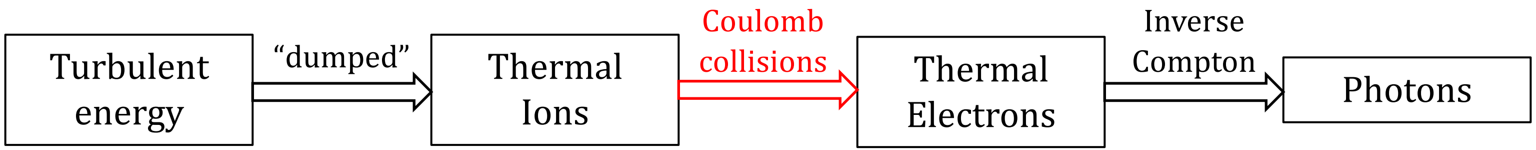

It turns out ion/electron *Coulomb heating* is the slowest rate by far.

Two microphysical improvements to HARM3D:

(Kinch, Noble, Schnittman, & Krolik 2020)

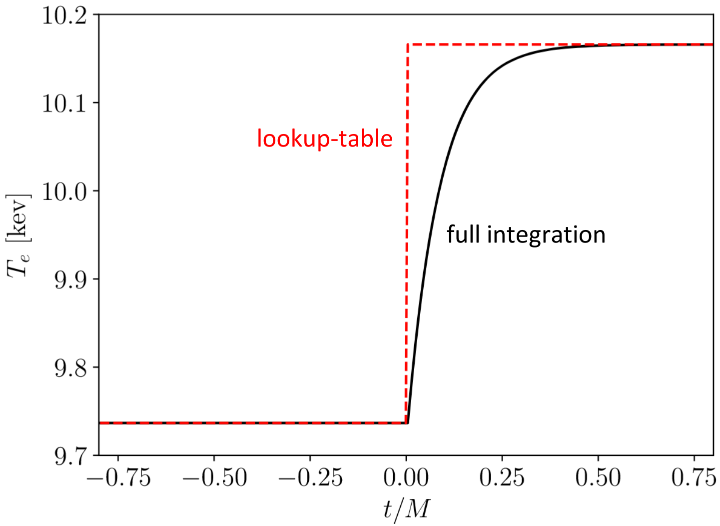

Two-Temperature Coronal Model

This allows us to replace cumbersome coupled rate equations with a

snap-to-equilibrium

lookup-table-accelerated

approximation to a 2T coronal plasma.

$$\frac{T_e}{T_i} = f\left(\frac{u}{\rho c^2}, \frac{u_{\rm rad}}{\rho c^2}, \frac{\langle\varepsilon\rangle}{m_e c^2}\right)$$

$$\langle\varepsilon\rangle = 4k_B T_C$$

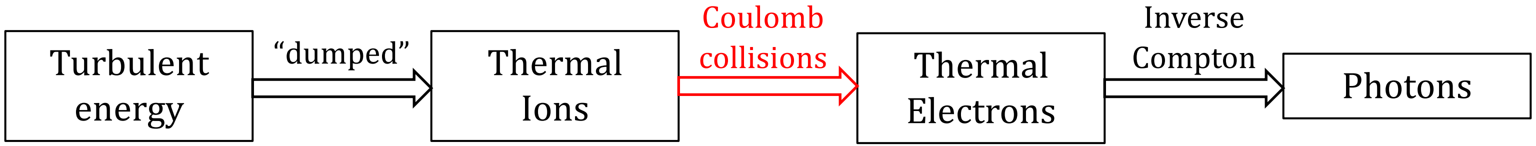

It turns out ion/electron *Coulomb heating* is the slowest rate by far.

General Relativistic Magnetohydrodynamics (GRMHD) – in review:

- HARM3D evolves a 3D, GRMHD environment around a black hole.

General Relativistic Magnetohydrodynamics (GRMHD) – in review:

- HARM3D evolves a 3D, GRMHD environment around a black hole.
- Using a target-temperature cooling function (in the disk), we can achieve an observationally-supported geometrically thin, optically thick, relatively cool disk.

General Relativistic Magnetohydrodynamics (GRMHD) – in review:

- HARM3D evolves a 3D, GRMHD environment around a black hole.
- Using a target-temperature cooling function (in the disk), we can achieve an observationally-supported geometrically thin, optically thick, relatively cool disk.
- Using an Inverse Compton cooling function (in the corona), we mimic the actual coronal cooling mechanism without the need for full transport.

General Relativistic Magnetohydrodynamics (GRMHD) – in review:

- HARM3D evolves a 3D, GRMHD environment around a black hole.
- Using a target-temperature cooling function (in the disk), we can achieve an observationally-supported geometrically thin, optically thick, relatively cool disk.
- Using an Inverse Compton cooling function (in the corona), we mimic the actual coronal cooling mechanism without the need for full transport.
- If we so choose, we can approximate a two-temperature plasma in the least radiatively efficient regime.

General Relativistic Magnetohydrodynamics (GRMHD) – in review:

- HARM3D evolves a 3D, GRMHD environment around a black hole.
- Using a target-temperature cooling function (in the disk), we can achieve an observationally-supported geometrically thin, optically thick, relatively cool disk.
- Using an Inverse Compton cooling function (in the corona), we mimic the actual coronal cooling mechanism without the need for full transport.
- If we so choose, we can approximate a two-temperature plasma in the least radiatively efficient regime.

- Thus we can simulate realistic black hole accretion flows.

General Relativistic Magnetohydrodynamics (GRMHD) – in review:

- HARM3D evolves a 3D, GRMHD environment around a black hole.
- Using a target-temperature cooling function (in the disk), we can achieve an observationally-supported geometrically thin, optically thick, relatively cool disk.
- Using an Inverse Compton cooling function (in the corona), we mimic the actual coronal cooling mechanism without the need for full transport.
- If we so choose, we can approximate a two-temperature plasma in the least radiatively efficient regime.

- Thus we can simulate realistic black hole accretion flows.

- The next step is to generate synthetic X-ray spectra from these simulations.

X-Ray Postprocessing – Overview

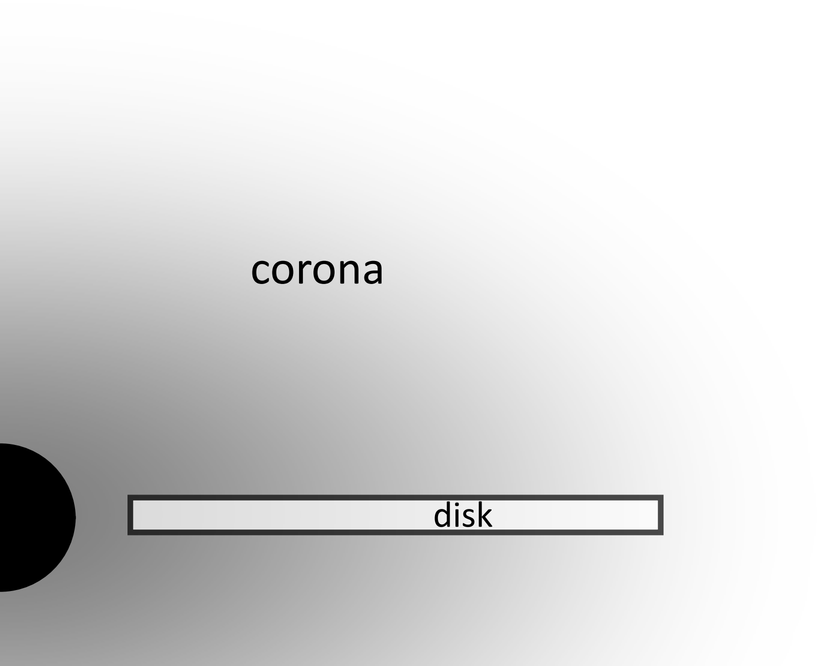

- Relatively cool, dense disk treated with deterministic, plane-parallel radiation transport code `PTRANSX`:
    - Feautrier method
    - coupled to photoionization code `XSTAR`
    - fully relativistic Compton using `compy`

X-Ray Postprocessing – Overview

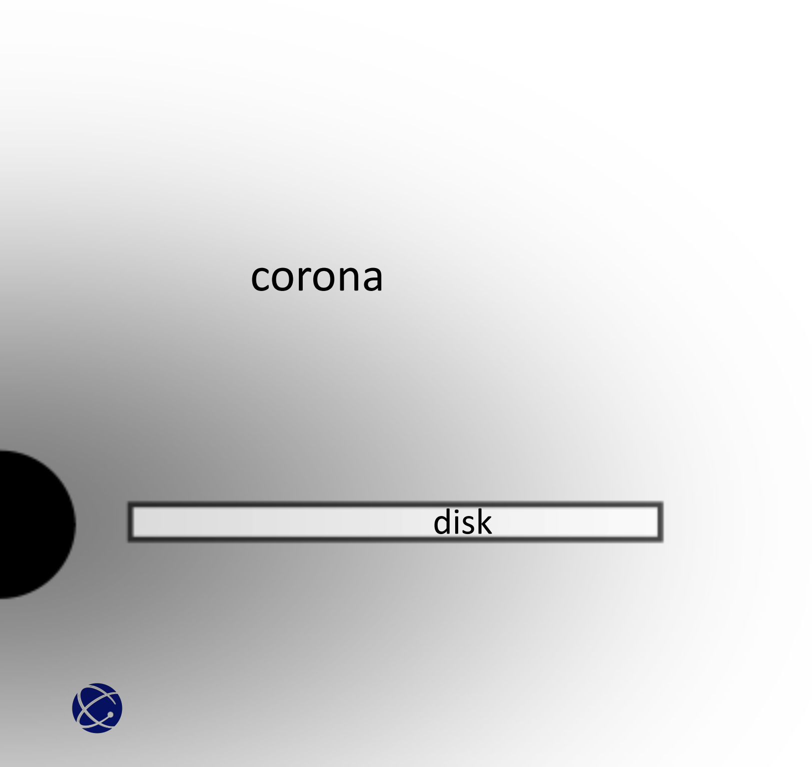

- Relatively cool, dense disk treated with deterministic, plane-parallel radiation transport code `PTRANSX`:
  - Feautrier method
  - coupled to photoionization code `XSTAR`
  - fully relativistic Compton using `compy`

- Hot, diffuse corona treated with Monte Carlo ray-tracing code `Pandurata`:
  - integrates geodesics (all SR and GR effects)
  - fully relativistic Compton using `compy`
  - generates distant observer spectrum

X-Ray Postprocessing – Overview

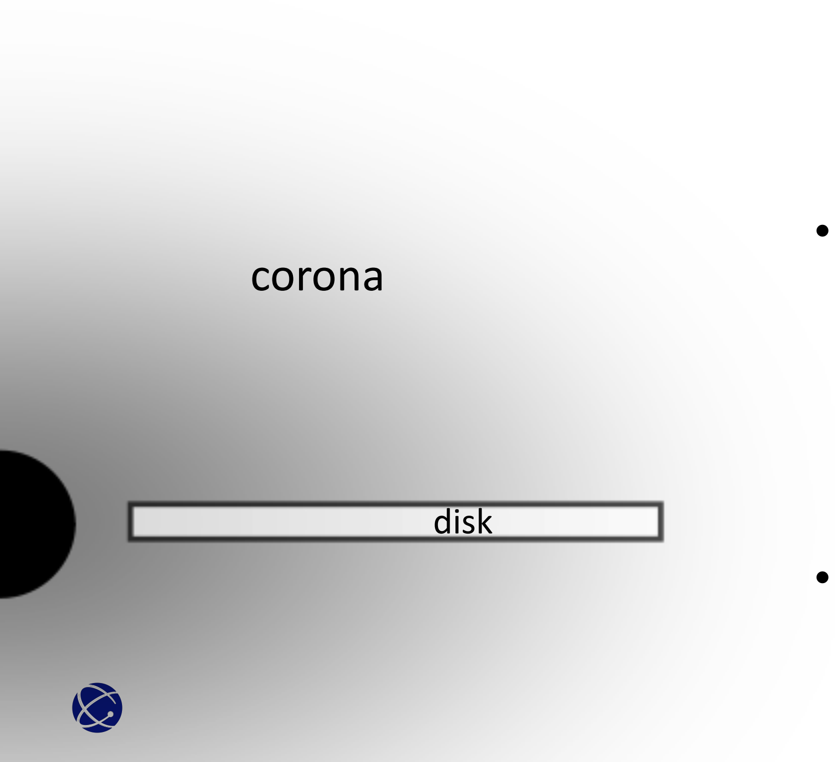

- Relatively cool, dense disk treated with deterministic, plane-parallel radiation transport code `PTRANSX`:
    - Feautrier method
    - coupled to photoionization code `XSTAR`
    - fully relativistic Compton using `compy`

- Hot, diffuse corona treated with Monte Carlo ray-tracing code `Pandurata`:
    - integrates geodesics (all SR and GR effects)
    - fully relativistic Compton using `compy`
    - generates distant observer spectrum

- Two codes handling two different regimes, interfaced to each other at disk/corona boundary.

X-Ray Postprocessing – Corona

1. Assume each plane-parallel slab of disk radiates a blackbody according to its vertically-integrated cooling rate.
2. Use `Pandurata` to transport photon packets to distant observers (emitter-to-observer ray-tracing).

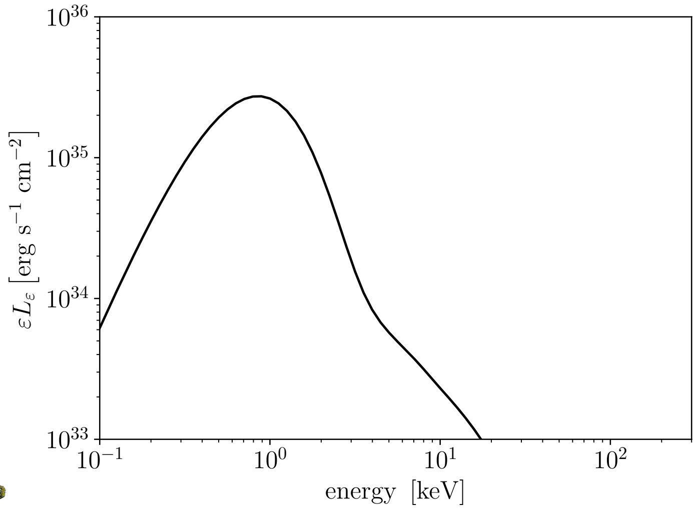

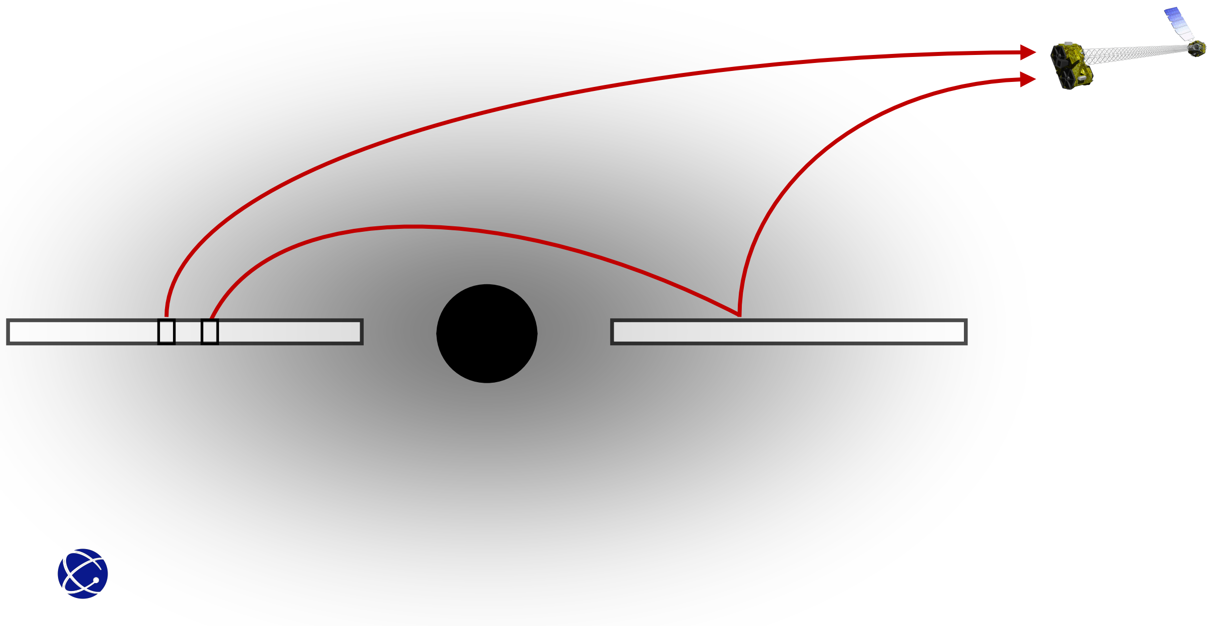

X-Ray Postprocessing – Corona

1. Assume each plane-parallel slab of disk radiates a blackbody according to its vertically-integrated cooling rate.
2. Use `Pandurata` to transport photon packets to distant observers (emitter-to-observer ray-tracing).
3. Convolve pre-scatter photon packet SED with interpolated `compy` table to get post-scatter SED.

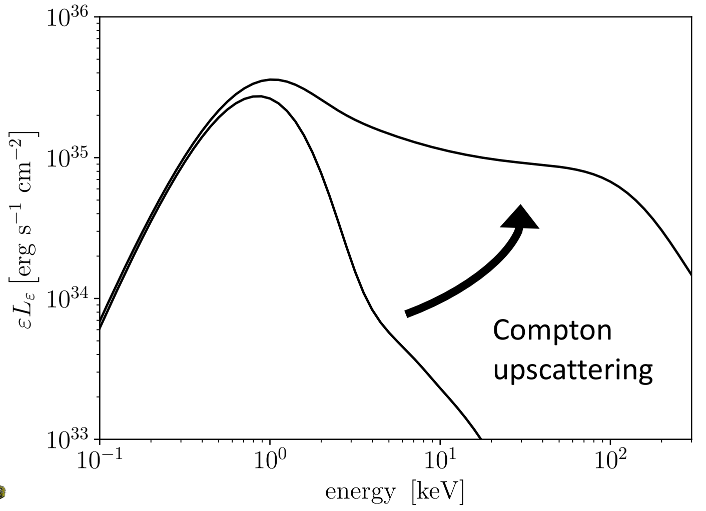

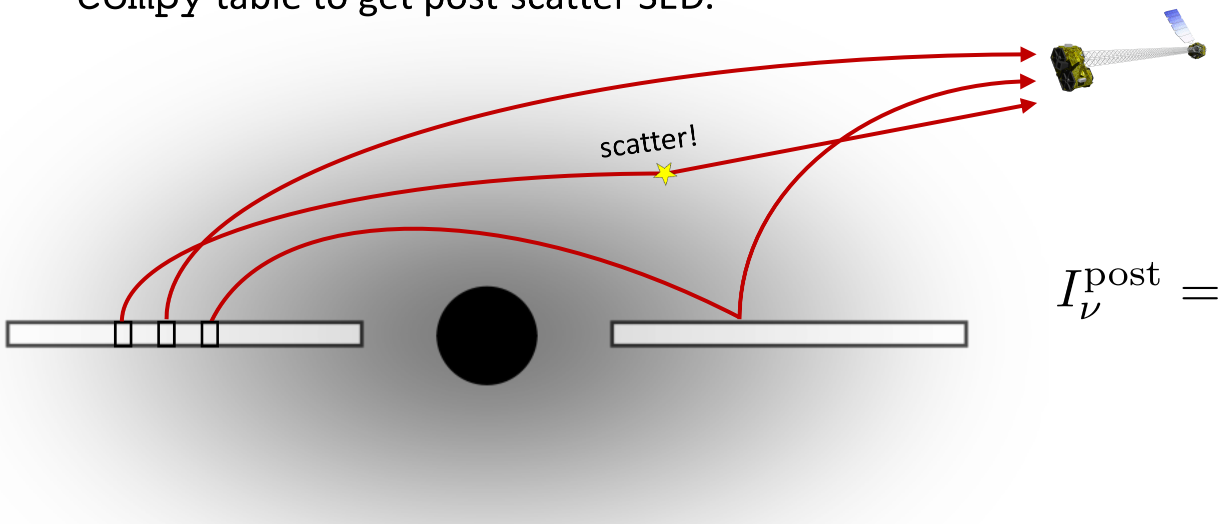

$$I_\nu^{\rm post} = \int_0^\infty I_{\nu'}^{\rm pre} \underbrace{R\left(T_e, \nu' \to \nu\right)} d\nu'$$

tabulated in advance by compy

X-Ray Postprocessing – Corona

1. Assume each plane-parallel slab of disk radiates a blackbody according to its vertically-integrated cooling rate.
2. Use `Pandurata` to transport photon packets to distant observers (emitter-to-observer ray-tracing).
3. Convolve pre-scatter photon packet SED with interpolated `compy` table to get post-scatter SED.

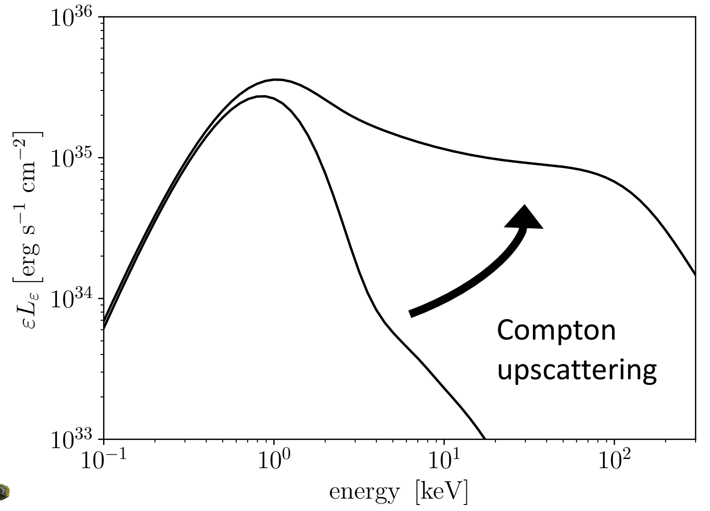

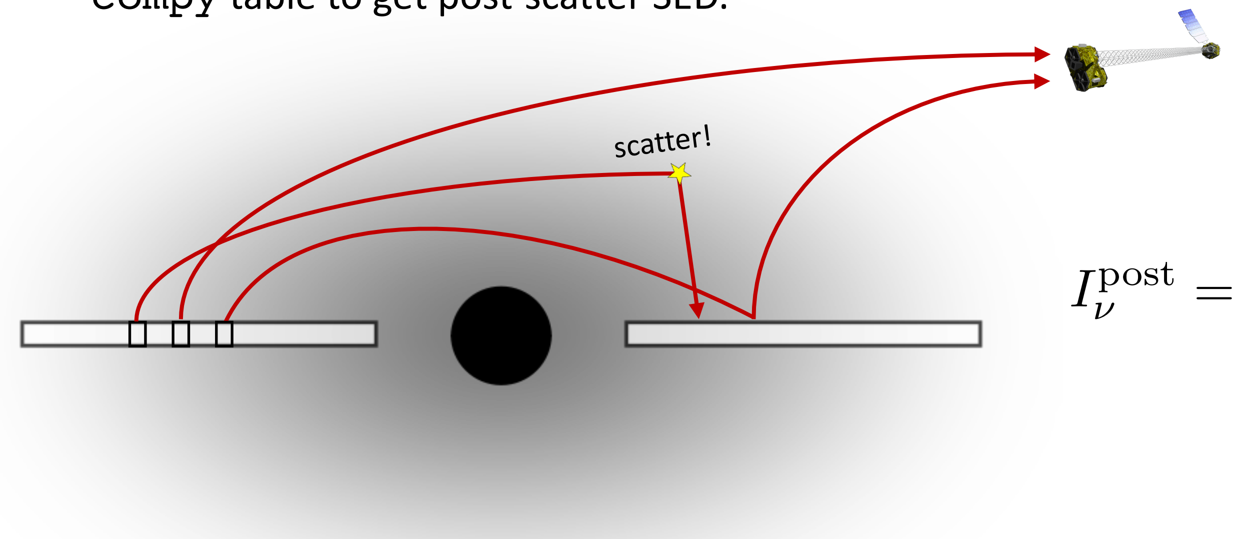

$$I_\nu^{\rm post} = \int_0^\infty I_{\nu'}^{\rm pre} \underbrace{R\left(T_e, \nu' \to \nu\right)}_{\text{tabulated in advance by compy}} d\nu'$$

X-Ray Postprocessing – Corona

4. Use Newton-Raphson iterations in every coronal *sector* to match `HARM3D`'s cooling rate with `Pandurata`'s electron temperature.

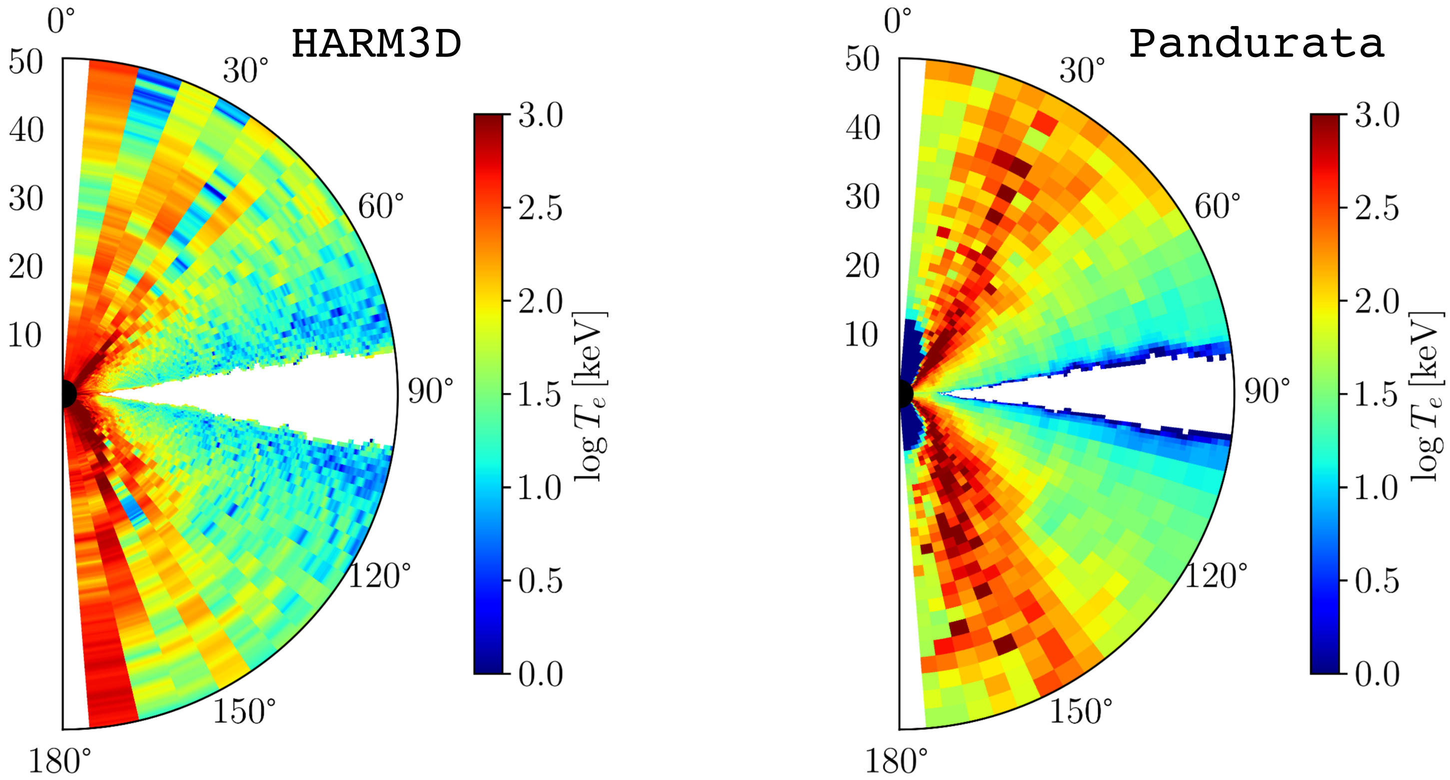

X-Ray Postprocessing – Corona + Disk

We still need a self-consistent treatment for:

- The seed photon spectrum (not simply a blackbody).
- How to transform a photon packet striking the disk surface.

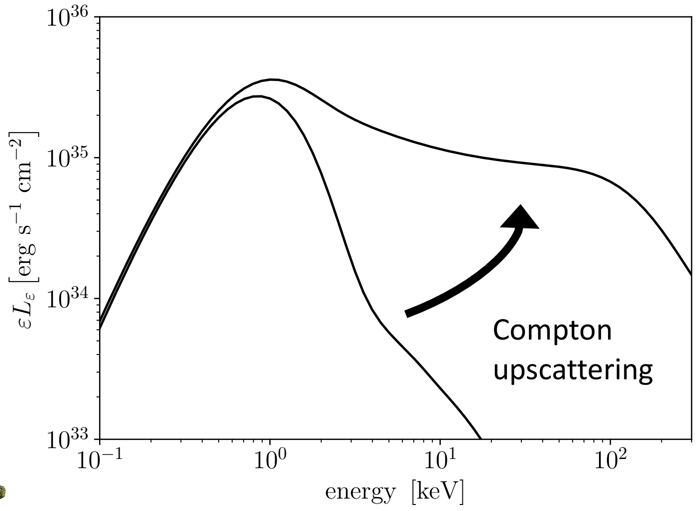

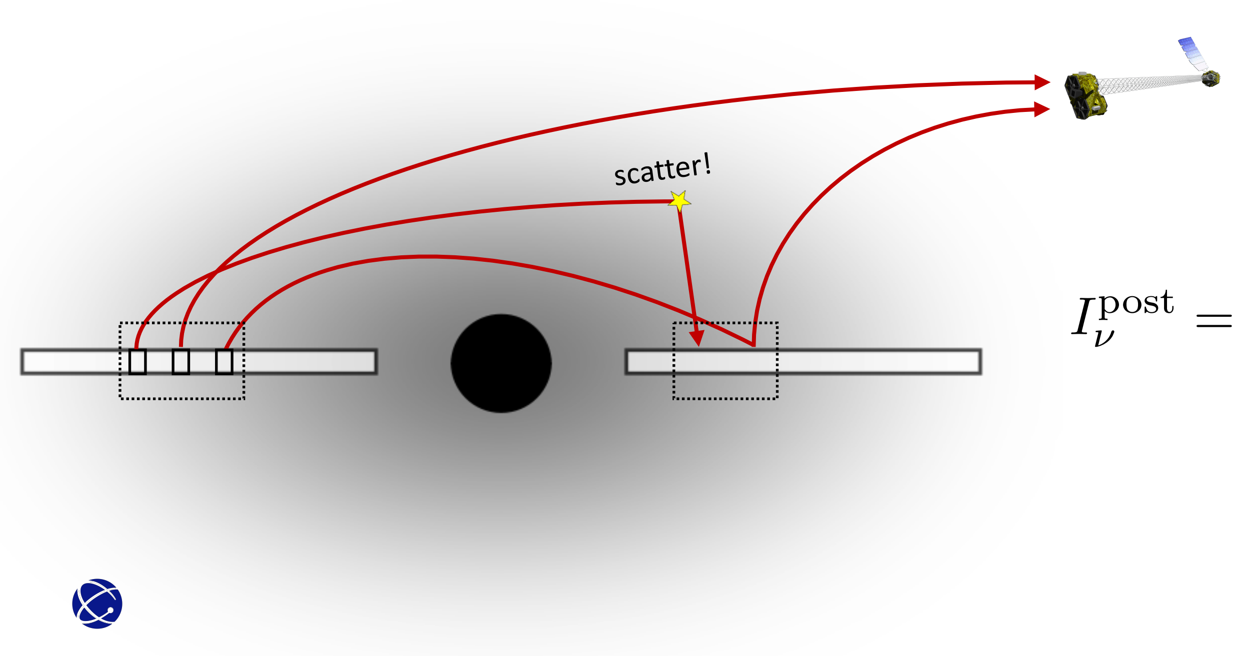

$$I_\nu^{\text{post}} = \int_0^\infty I_{\nu'}^{\text{pre}} \underbrace{R\left(T_e, \nu' \rightarrow \nu\right)}_{\text{tabulated in advance by compy}} d\nu'$$

X-Ray Postprocessing – Disk

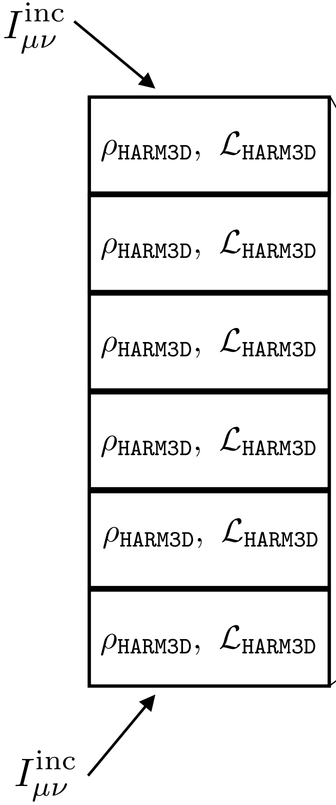

PTRANSX solves the plane-parallel time-independent transfer equation

$$\mu\frac{I_{\mu\nu}}{dz} = -\left[\alpha_\nu + \sigma_\nu\right] I_{\mu\nu} + j_\nu + \int_0^\infty \sigma_{\nu'} I_{\mu'\nu'} R\left(T_e, \{\mu', \nu'\} \to \{\mu, \nu\}\right) d\mu' d\nu'$$

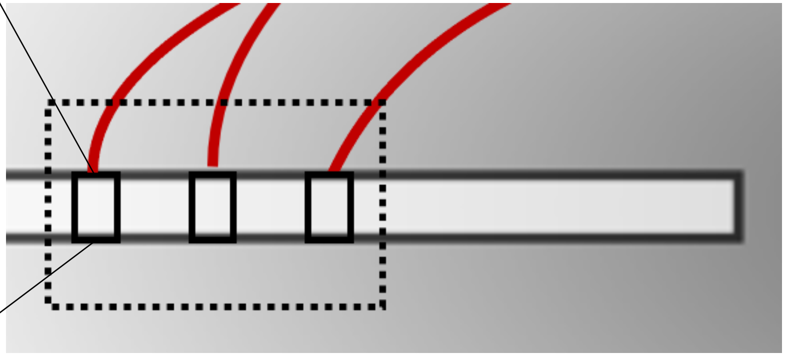

X-Ray Postprocessing – Disk

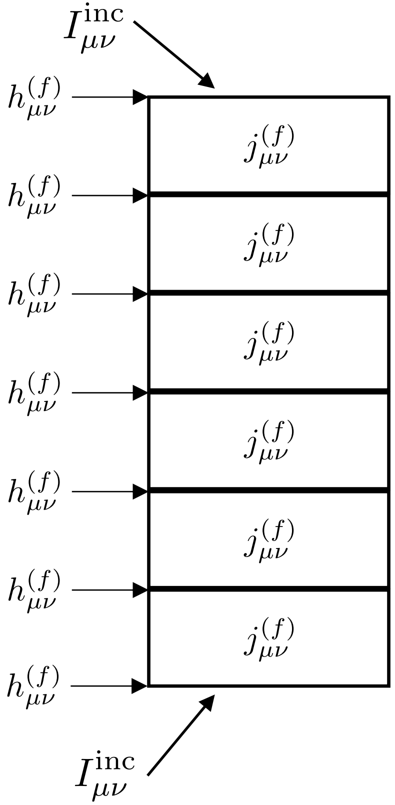

PTRANSX solves the plane-parallel time-independent transfer equation

$$\mu \frac{I_{\mu\nu}}{dz} = -\left[\alpha_\nu + \sigma_\nu\right] I_{\mu\nu} + j_\nu + \int_0^\infty \sigma_{\nu'} I_{\mu'\nu'} R\left(T_e, \{\mu', \nu'\} \to \{\mu, \nu\}\right) d\mu' d\nu'$$

via the Feautrier method – splitting the radiation field into symmetric and anti-symmetric averages:

$$j_{\mu\nu}^{(f)} = \frac{1}{2}\left(I_{\mu\nu}^{+} + I_{\mu\nu}^{-}\right) \qquad 0 \leq \mu \leq 1$$

$$h_{\mu\nu}^{(f)} = \frac{1}{2}\left(I_{\mu\nu}^{+} - I_{\mu\nu}^{-}\right)$$

Subject to *incident specific intensity* boundary conditions set by `Pandurata`.

X-Ray Postprocessing – Disk

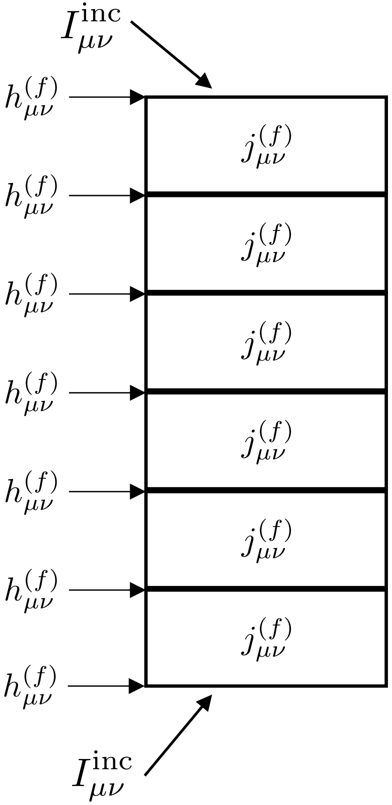

PTRANSX solves the plane-parallel time-independent transfer equation

$$\mu \frac{I_{\mu\nu}}{dz} = -\left[\alpha_\nu + \sigma_\nu\right] I_{\mu\nu} + j_\nu + \int_0^\infty \sigma_{\nu'} I_{\mu'\nu'} \underbrace{R\left(T_e, \{\mu', \nu'\} \to \{\mu, \nu\}\right)} d\mu' d\nu'$$

tabulated in advance by `compy`

X-Ray Postprocessing – Disk

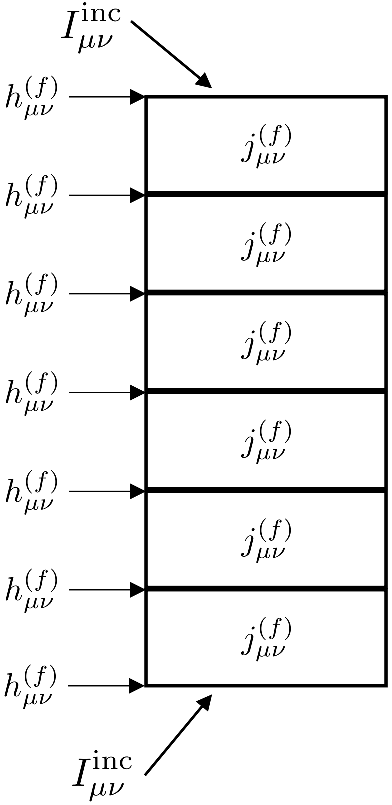

PTRANSX solves the plane-parallel time-independent transfer equation

$$\mu \frac{I_{\mu\nu}}{dz} = -\left[\alpha_\nu\left(T_e, J_\nu\right) + \sigma_\nu\left(T_e\right)\right] I_{\mu\nu} + j_\nu\left(T_e, J_\nu\right) + \int_0^\infty \sigma_{\nu'}\left(T_e\right) I_{\mu'\nu'} R\left(T_e, \{\mu', \nu'\} \to \{\mu, \nu\}\right) d\mu' d\nu'$$

absorption opacity includes:

free-free, bound-free photoionization edges

emissivity includes:

free-free, recombination continuum, line emission

X-Ray Postprocessing – Disk

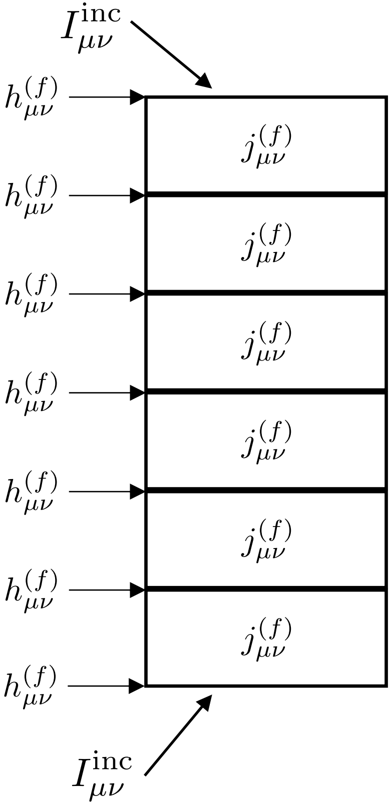

PTRANSX solves the plane-parallel time-independent transfer equation

$$\mu\frac{I_{\mu\nu}}{dz} = -\left[\alpha_\nu\left(T_e, J_\nu\right) + \sigma_\nu\left(T_e\right)\right] I_{\mu\nu} + j_\nu\left(T_e, J_\nu\right) + \int_0^\infty \sigma_{\nu'}\left(T_e\right) I_{\mu'\nu'} R\left(T_e, \{\mu', \nu'\} \to \{\mu, \nu\}\right) d\mu' d\nu'$$

absorption opacity includes:

free-free, bound-free photoionization edges

emissivity includes:

free-free, recombination continuum, line emission

We use the photoionization code XSTAR to determine the *photoionization equilibrium ionization balance* and corresponding absorption opacity and emissivity…

for a given temperature and radiation field (and density).

X-Ray Postprocessing – Disk

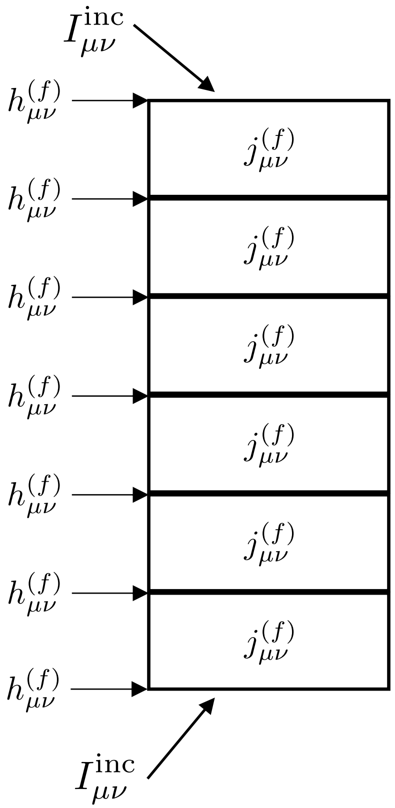

PTRANSX solves the plane-parallel time-independent transfer equation

$$\mu\frac{I_{\mu\nu}}{dz} = -\left[\alpha_\nu\left(T_e, J_\nu\right) + \sigma_\nu\left(T_e\right)\right] I_{\mu\nu} + j_\nu\left(T_e, J_\nu\right) + \int_0^\infty \sigma_{\nu'}\left(T_e\right) I_{\mu'\nu'} R\left(T_e, \{\mu', \nu'\} \rightarrow \{\mu, \nu\}\right) d\mu' d\nu'$$

1. Guess a radiation field and temperature structure – use `XSTAR` to determine PIE emissivity and opacity in every cell.

X-Ray Postprocessing – Disk

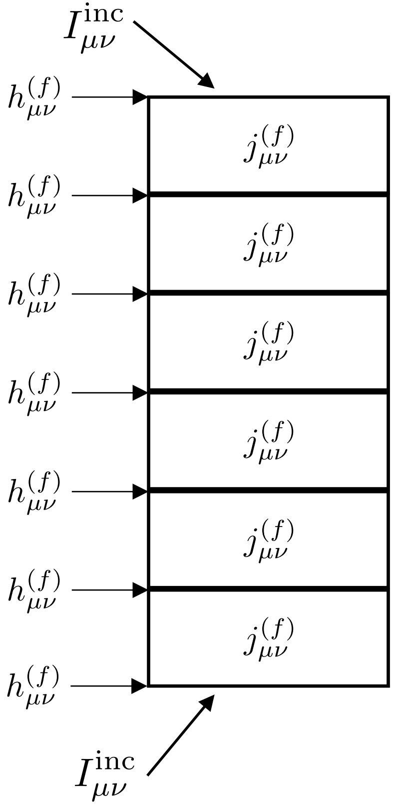

PTRANSX solves the plane-parallel time-independent transfer equation

$$\mu \frac{I_{\mu\nu}}{dz} = -\left[\alpha_\nu\left(T_e, J_\nu\right) + \sigma_\nu\left(T_e\right)\right] I_{\mu\nu} + j_\nu\left(T_e, J_\nu\right) + \int_0^\infty \sigma_{\nu'}\left(T_e\right) I_{\mu'\nu'} R\left(T_e, \{\mu', \nu'\} \rightarrow \{\mu, \nu\}\right) d\mu' d\nu'$$

$$4\pi \int_0^\infty \int_0^1 \left[h_{\mu\nu}^{(f),\mathrm{top}} - h_{\mu\nu}^{(f),\mathrm{bot}}\right] d\mu d\nu - \frac{\mathcal{L}_{\mathtt{HARM3D}}}{\Delta z} = 0$$

1. Guess a radiation field and temperature structure –
   use XSTAR to determine PIE emissivity and opacity in every cell.
2. *Holding the radiation field constant when calling XSTAR*, use multidimensional Newton-Raphson to solve for the temperature structure which satisfies energy conservation in every cell.

X-Ray Postprocessing – Disk

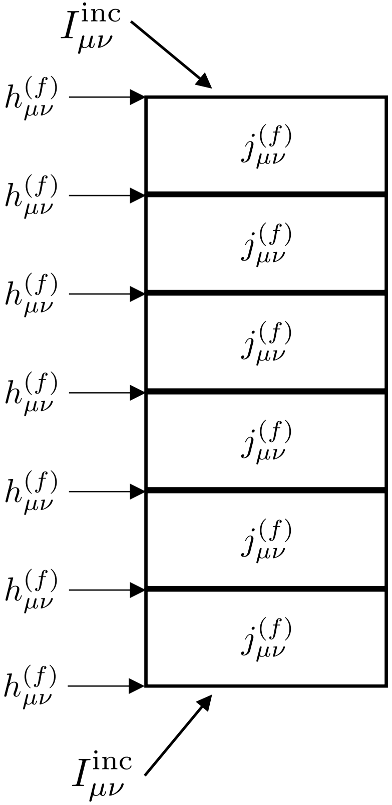

PTRANSX solves the plane-parallel time-independent transfer equation

$$\mu \frac{I_{\mu\nu}}{dz} = -\left[\alpha_\nu\left(T_e, J_\nu\right) + \sigma_\nu\left(T_e\right)\right] I_{\mu\nu} + j_\nu\left(T_e, J_\nu\right) + \int_0^\infty \sigma_{\nu'}\left(T_e\right) I_{\mu'\nu'} R\left(T_e, \{\mu', \nu'\} \to \{\mu, \nu\}\right) d\mu' d\nu'$$

$$4\pi \int_0^\infty \int_0^1 \left[h_{\mu\nu}^{(f),\mathrm{top}} - h_{\mu\nu}^{(f),\mathrm{bot}}\right] d\mu d\nu - \frac{\mathcal{L}_{\mathtt{HARM3D}}}{\Delta z} = 0$$

1. Guess a radiation field and temperature structure – use XSTAR to determine PIE emissivity and opacity in every cell.
2. *Holding the radiation field constant when calling XSTAR*, use multidimensional Newton-Raphson to solve for the temperature structure which satisfies energy conservation in every cell.
3. Update the radiation field used when calling XSTAR with this energy-conserving one.

X-Ray Postprocessing – Disk

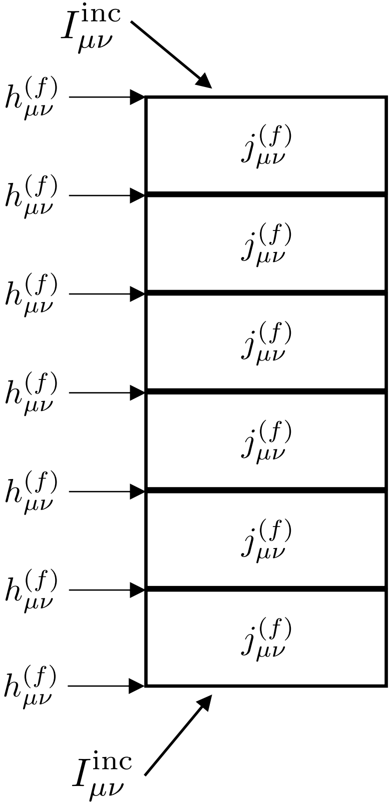

PTRANSX solves the plane-parallel time-independent transfer equation

$$\mu \frac{I_{\mu\nu}}{dz} = -\left[\alpha_\nu\left(T_e, J_\nu\right) + \sigma_\nu\left(T_e\right)\right] I_{\mu\nu} + j_\nu\left(T_e, J_\nu\right) + \int_0^\infty \sigma_{\nu'}\left(T_e\right) I_{\mu'\nu'} R\left(T_e, \{\mu', \nu'\} \rightarrow \{\mu, \nu\}\right) d\mu' d\nu'$$

$$4\pi \int_0^\infty \int_0^1 \left[h_{\mu\nu}^{(f),\mathrm{top}} - h_{\mu\nu}^{(f),\mathrm{bot}}\right] d\mu d\nu - \frac{\mathcal{L}_{\mathtt{HARM3D}}}{\Delta z} = 0$$

1. Guess a radiation field and temperature structure – use `XSTAR` to determine PIE emissivity and opacity in every cell.
2. *Holding the radiation field constant when calling `XSTAR`*, use multidimensional Newton-Raphson to solve for the temperature structure which satisfies energy conservation in every cell.
3. Update the radiation field used when calling `XSTAR` with this energy-conserving one.
4. Repeat steps 2 and 3 until the radiation field everywhere has converged.

X-Ray Postprocessing – Disk

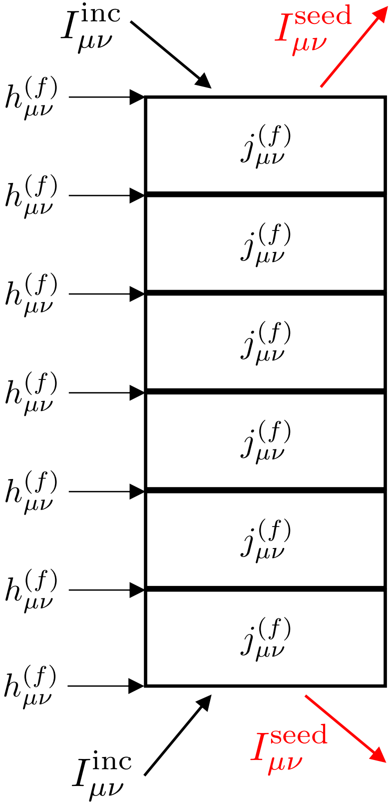

PTRANSX solves the plane-parallel time-independent transfer equation

$$\mu\frac{I_{\mu\nu}}{dz} = -\left[\alpha_\nu\left(T_e, J_\nu\right) + \sigma_\nu\left(T_e\right)\right] I_{\mu\nu} + j_\nu\left(T_e, J_\nu\right) + \int_0^\infty \sigma_{\nu'}\left(T_e\right) I_{\mu'\nu'} R\left(T_e, \{\mu', \nu'\} \rightarrow \{\mu, \nu\}\right) d\mu' d\nu'$$

$$4\pi \int_0^\infty \int_0^1 \left[h_{\mu\nu}^{(f),\rm top} - h_{\mu\nu}^{(f),\rm bot}\right] d\mu d\nu - \frac{\mathcal{L}_{\tt HARM3D}}{\Delta z} = 0$$

1. Guess a radiation field and temperature structure – use XSTAR to determine PIE emissivity and opacity in every cell.
2. *Holding the radiation field constant when calling XSTAR*, use multidimensional Newton-Raphson to solve for the temperature structure which satisfies energy conservation in every cell.
3. Update the radiation field used when calling XSTAR with this energy-conserving one.
4. Repeat steps 2 and 3 until the radiation field everywhere has converged.

5. Compute the *energy-conserving, photoionization equilibrium-consistent* outgoing seed photon spectrum.

X-Ray Postprocessing – Corona + Disk

We still need a self-consistent treatment for:

The seed photon spectrum (not simply a blackbody).

How to transform a photon packet striking the disk surface.

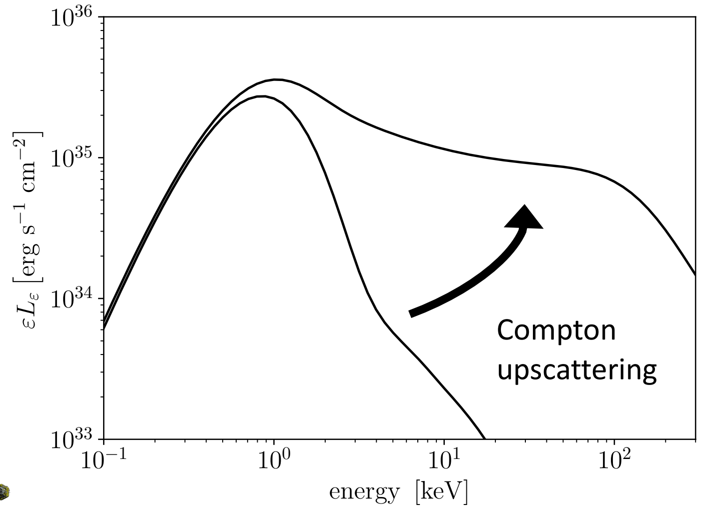

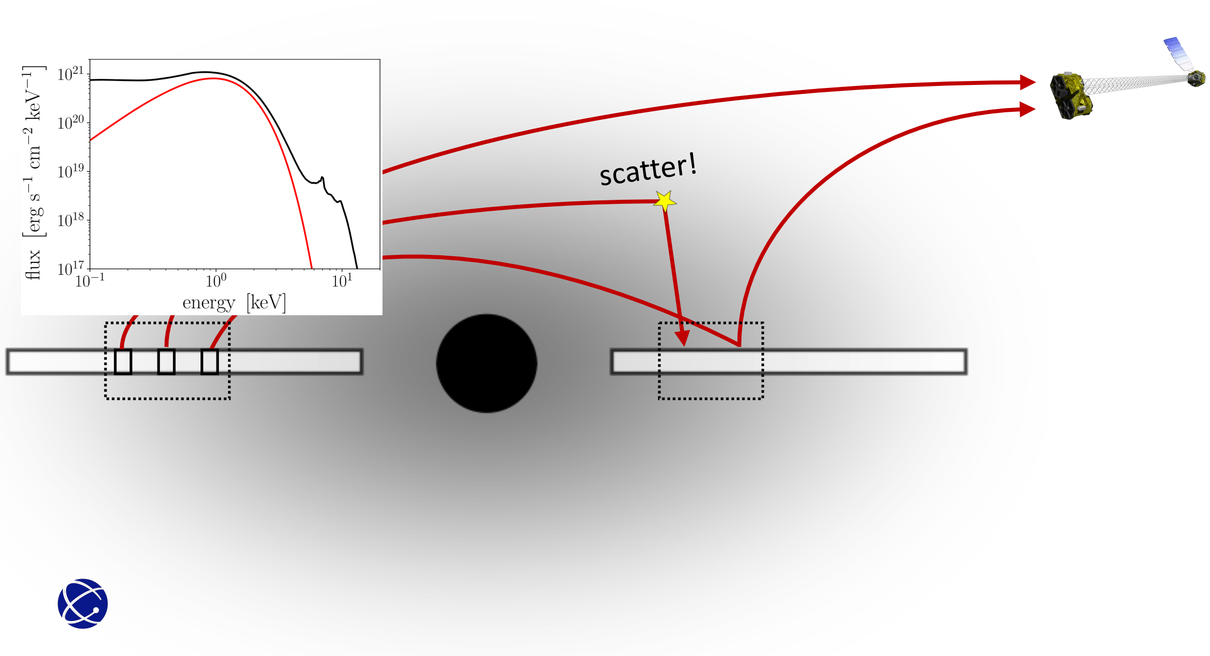

X-Ray Postprocessing – Corona + Disk

We still need a self-consistent treatment for:

The seed photon spectrum (not simply a blackbody).

How to transform a photon packet striking the disk surface.

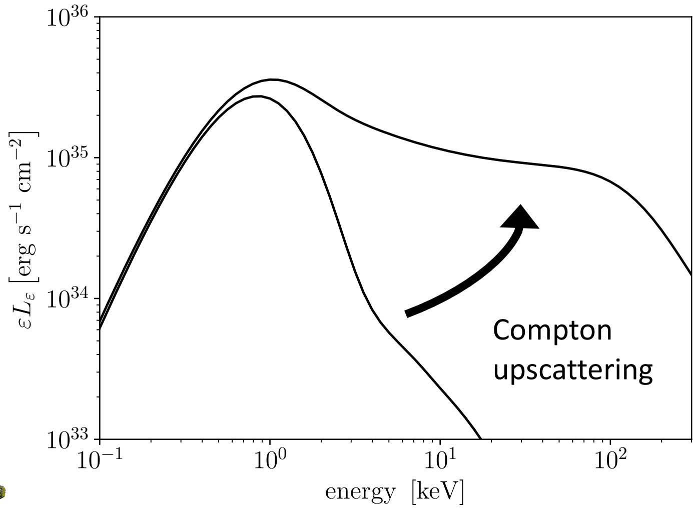

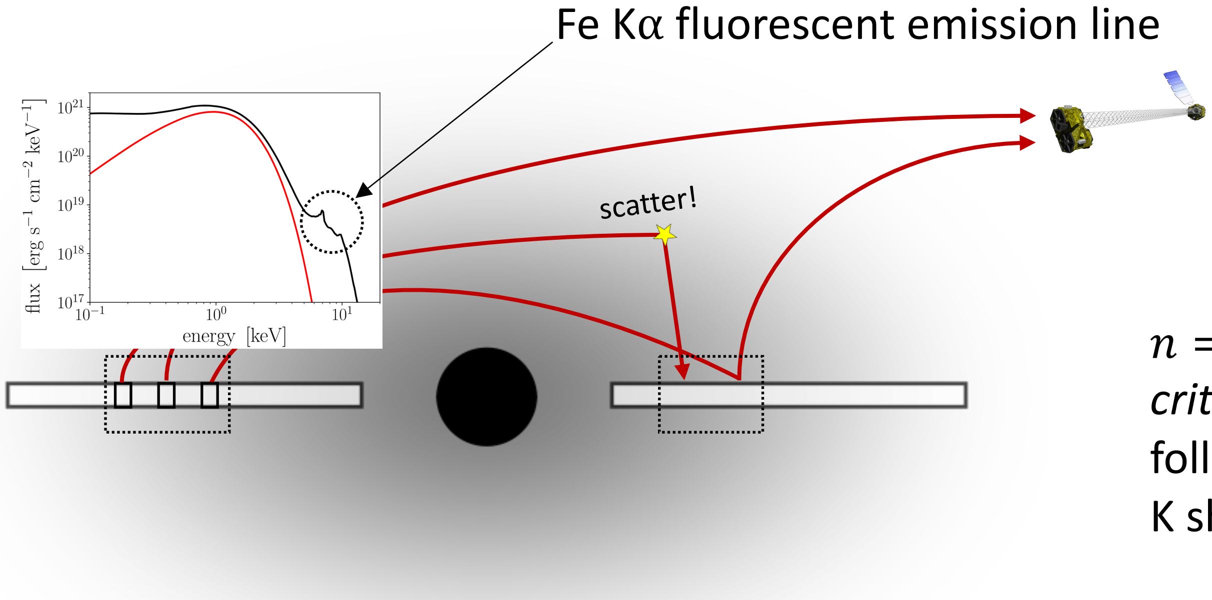

$n = 2 \rightarrow n = 1$ Fe transition: *critically important* X-ray diagnostic, follows from photo-ejection of K shell ($n = 1$) electron.

X-Ray Postprocessing – Disk

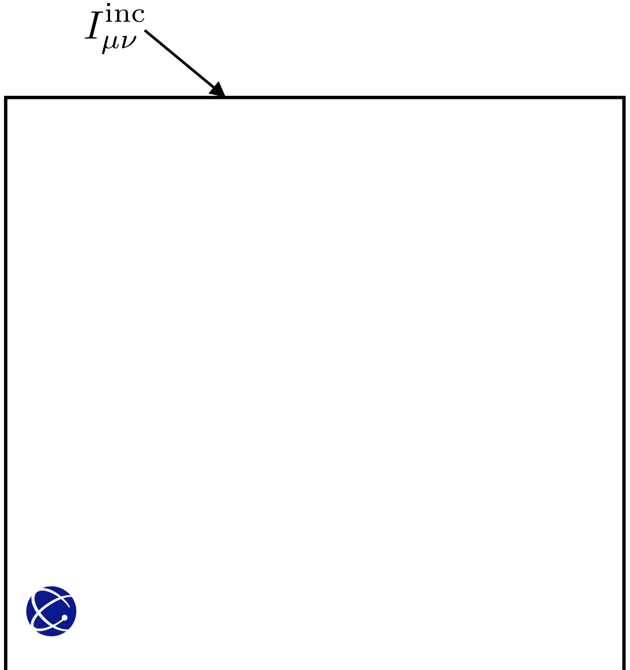

Auxiliary Monte Carlo code `response` –

1. Use `PTRANSX` output opacity and temperature structure for each plane-parallel slab.

X-Ray Postprocessing – Disk

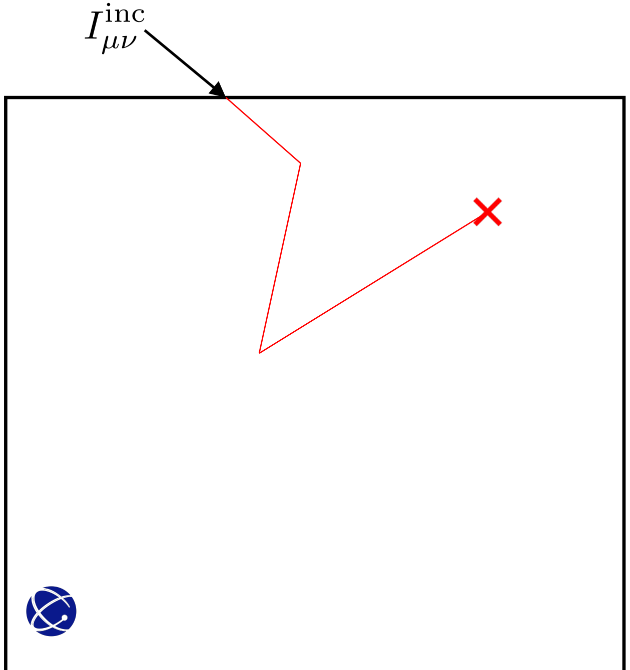

Auxiliary Monte Carlo code `response` –

1. Use `PTRANSX` output opacity and temperature structure for each plane-parallel slab.
2. Shoot photons in at each frequency grid-point and record the fraction that make it out (either side), i.e., the *albedo*.

X-Ray Postprocessing – Disk

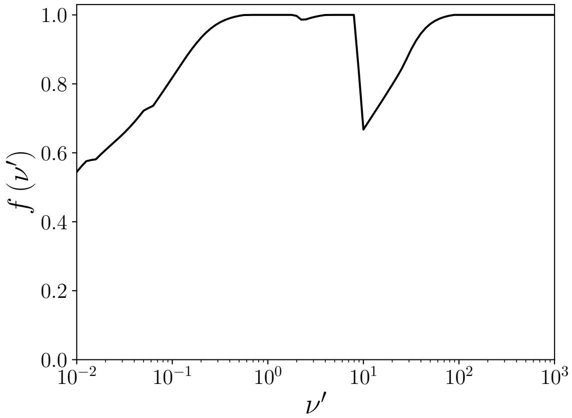

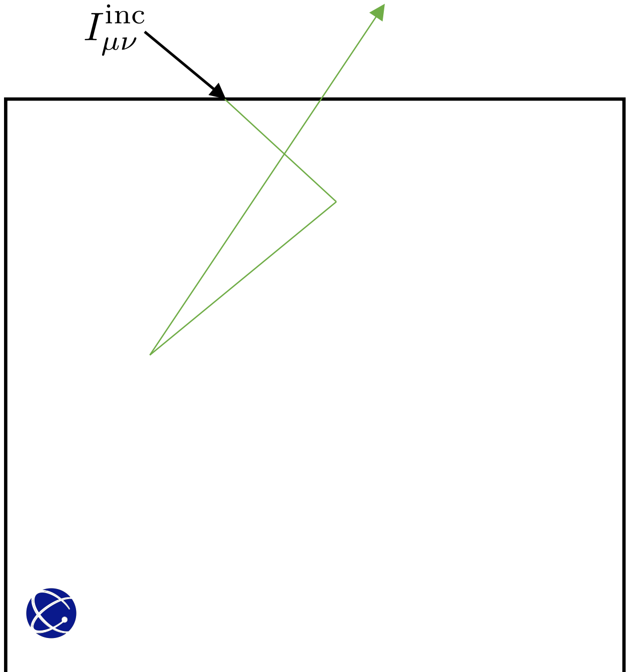

Auxiliary Monte Carlo code `response` –

1. Use `PTRANSX` output opacity and temperature structure for each plane-parallel slab.
2. Shoot photons in at each frequency grid-point and record the fraction that make it out (either side), i.e., the *albedo*.

X-Ray Postprocessing – Disk

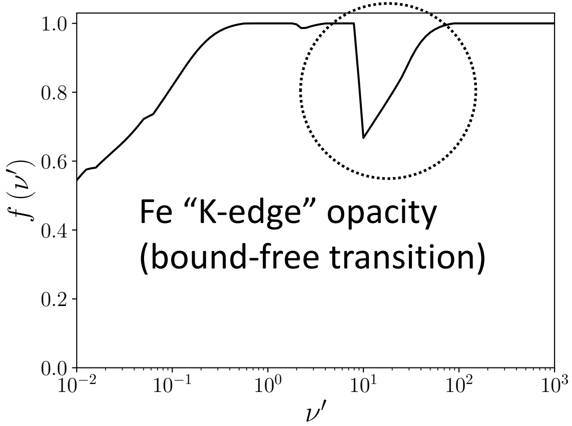

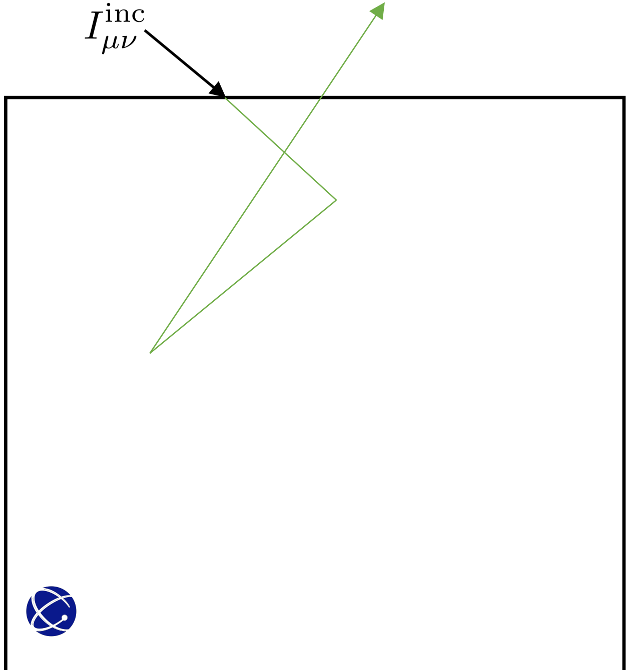

Auxiliary Monte Carlo code `response` –

1. Use `PTRANSX` output opacity and temperature structure for each plane-parallel slab.
2. Shoot photons in at each frequency grid-point and record the fraction that make it out (either side), i.e., the *albedo*.

X-Ray Postprocessing – Disk

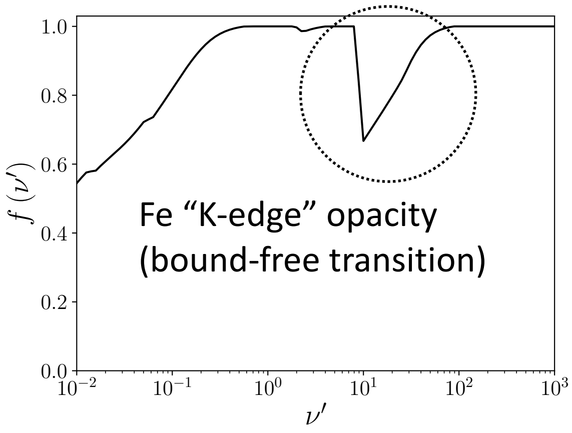

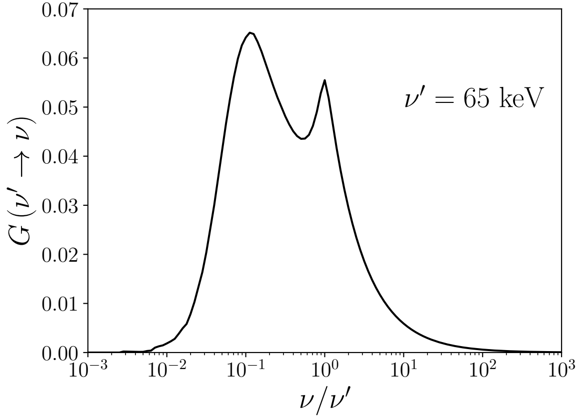

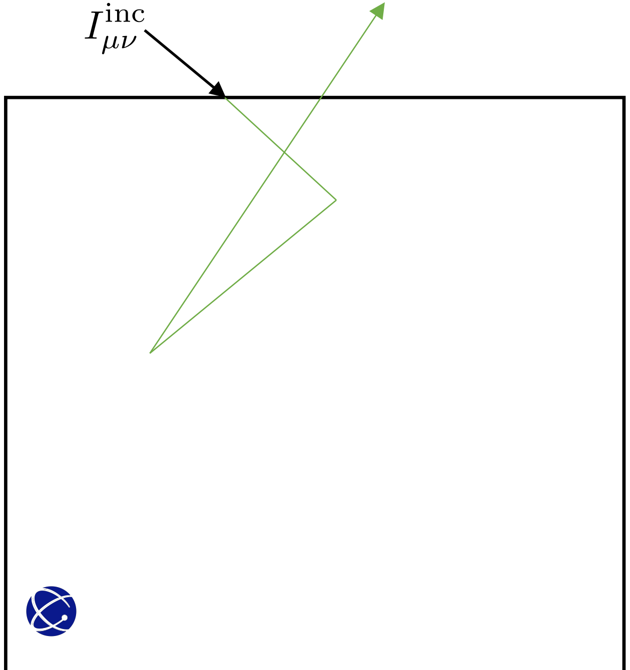

Auxiliary Monte Carlo code `response` –

1. Use `PTRANSX` output opacity and temperature structure for each plane-parallel slab.
2. Shoot photons in at each frequency grid-point and record the fraction that make it out (either side), i.e., the *albedo*.
3. Also record the distribution of outgoing frequencies for each incoming frequency (including transmission).

X-Ray Postprocessing – Disk

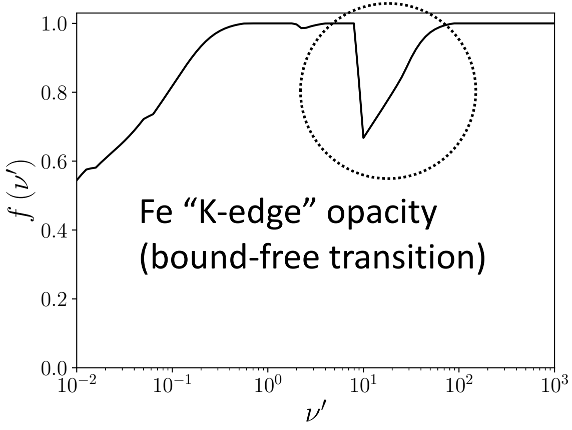

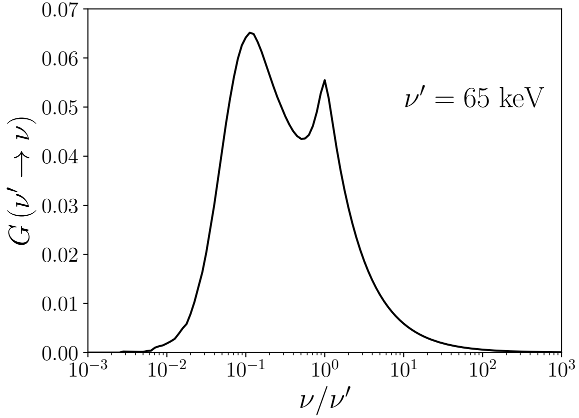

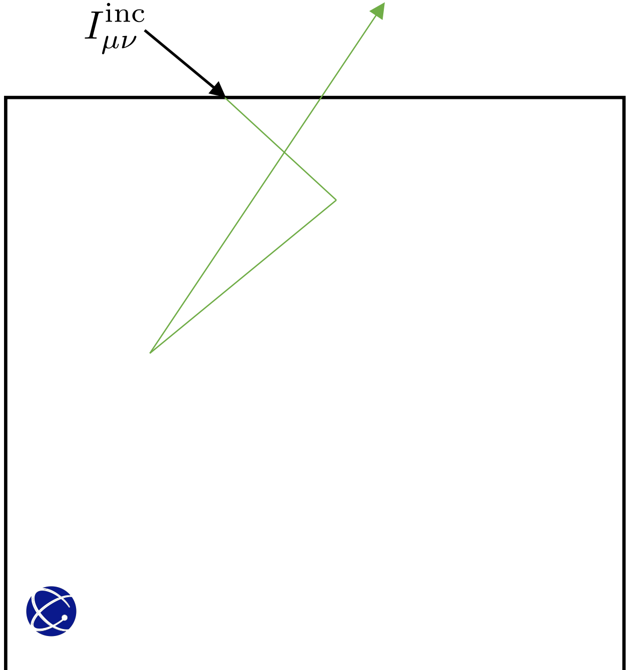

Auxiliary Monte Carlo code `response` –

1. Use `PTRANSX` output opacity and temperature structure for each plane-parallel slab.
2. Shoot photons in at each frequency grid-point and record the fraction that make it out (either side), i.e., the *albedo*.
3. Also record the distribution of outgoing frequencies for each incoming frequency (including transmission).
4. When a photon packet strikes the disk during `Pandurata` ray-tracing, *reduce* level by albedo and convolve with interpolated distribution:

$$I_\nu^{\mathrm{out}} = \int_0^\infty I_{\nu'}^{\mathrm{inc}} f(\nu')\, G(\nu' \to \nu)\, d\nu'$$

X-Ray Postprocessing – Corona + Disk

We still need a self-consistent treatment for:

The seed photon spectrum (not simply a blackbody).

How to transform a photon packet striking the disk surface.

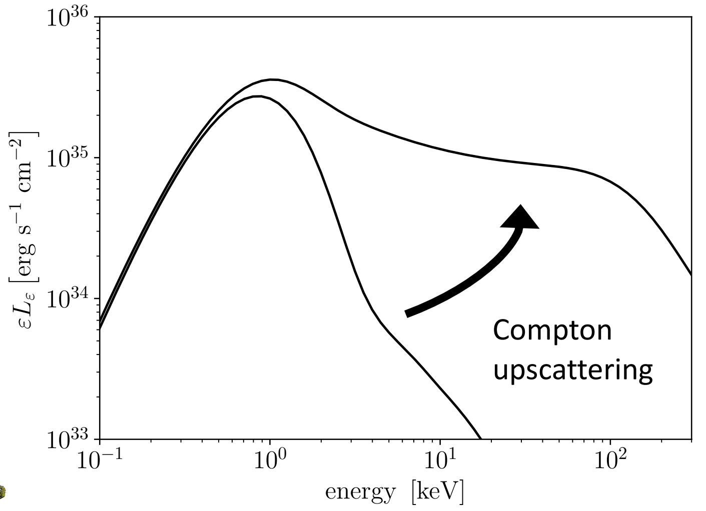

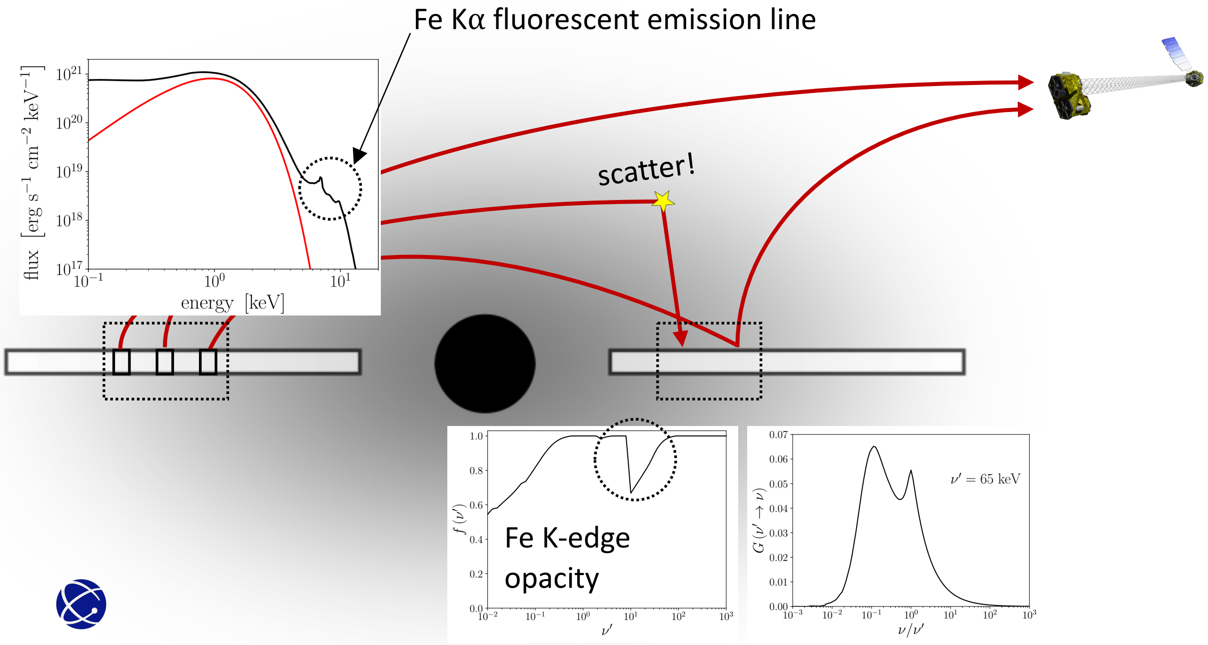

X-Ray Postprocessing – Corona + Disk

We still need a self-consistent treatment for:

- The seed photon spectrum (not simply a blackbody).
- How to transform a photon packet striking the disk surface.

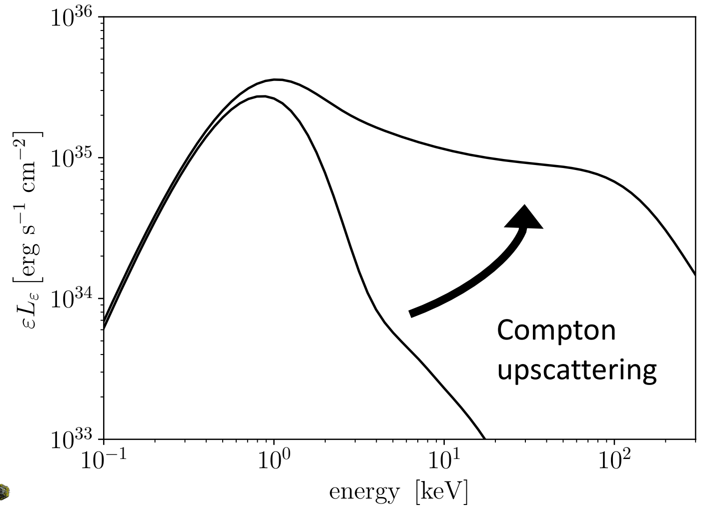

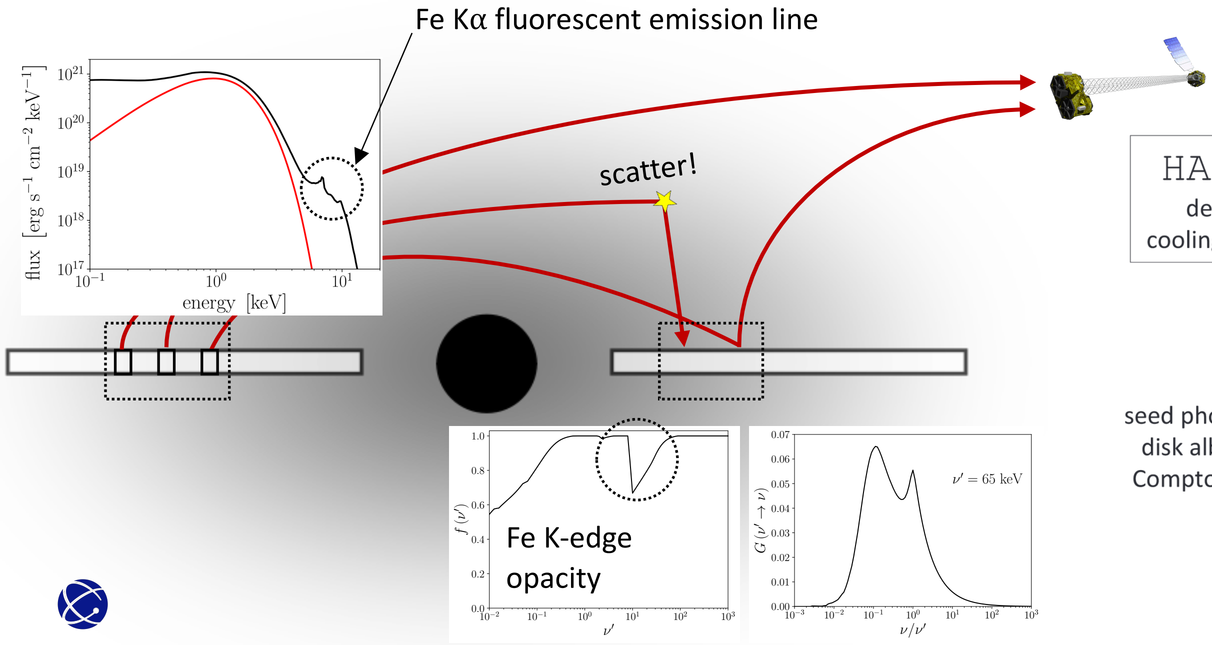

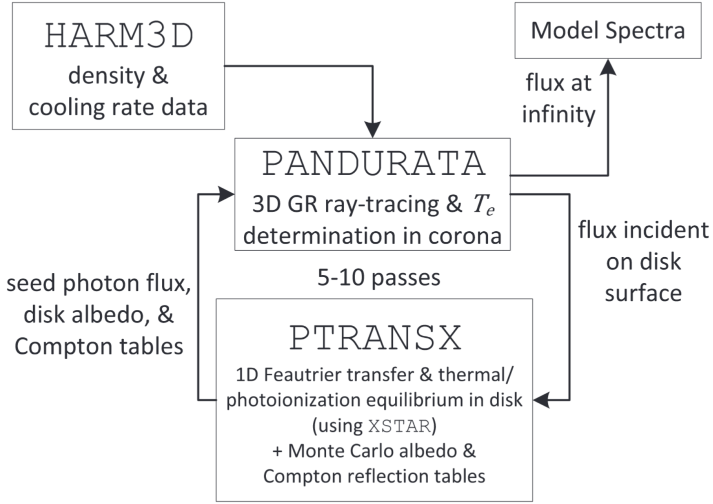

X-Ray Postprocessing – Corona + Disk

We still need a self-consistent treatment for:

The seed photon spectrum (not simply a blackbody).

How to transform a photon packet striking the disk surface.

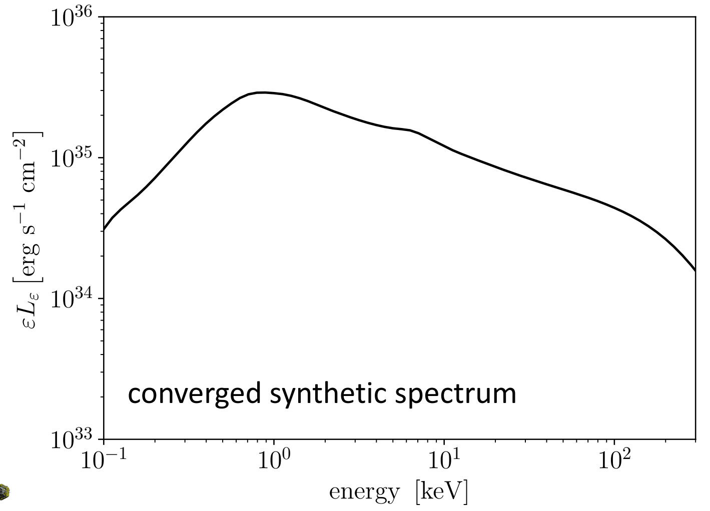

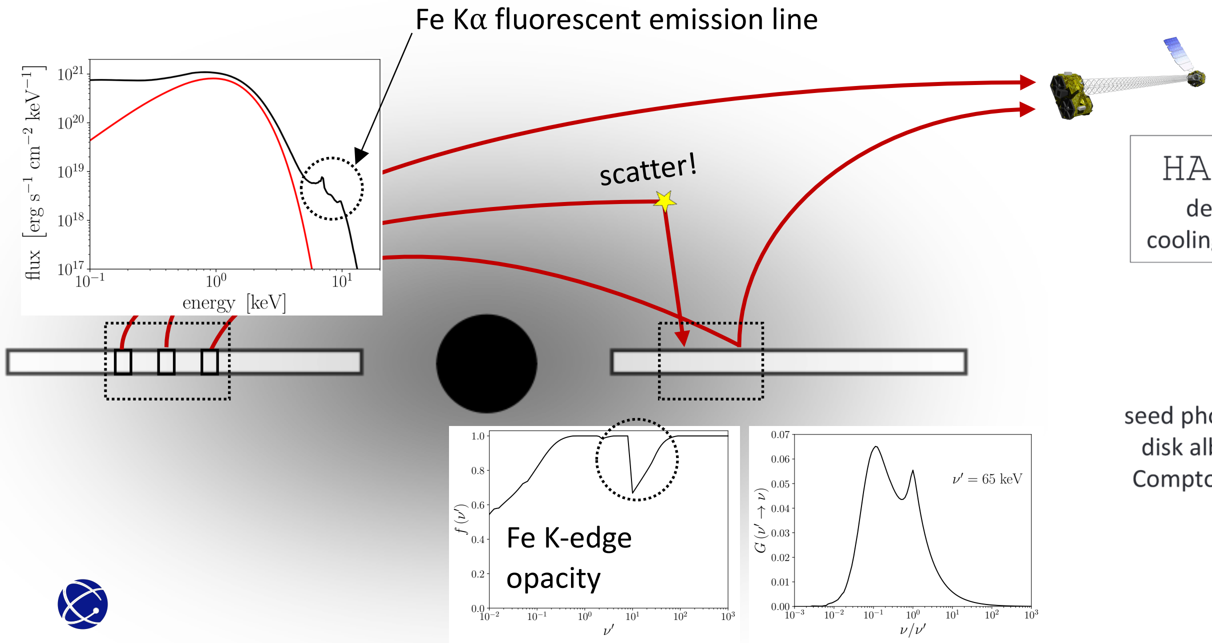

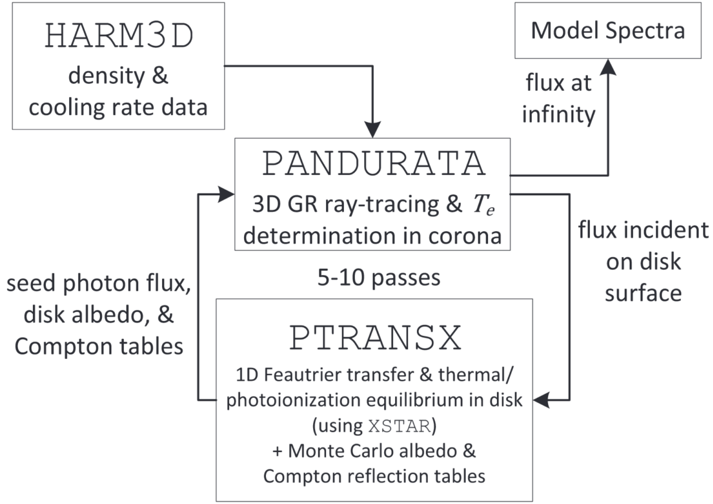

X-Ray Postprocessing – Corona + Disk

We still need a self-consistent treatment for:

The seed photon spectrum (not simply a blackbody).

How to transform a photon packet striking the disk surface.

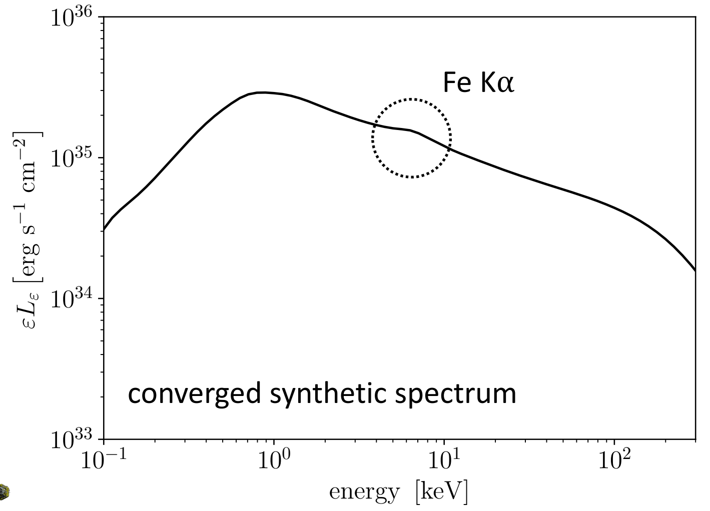

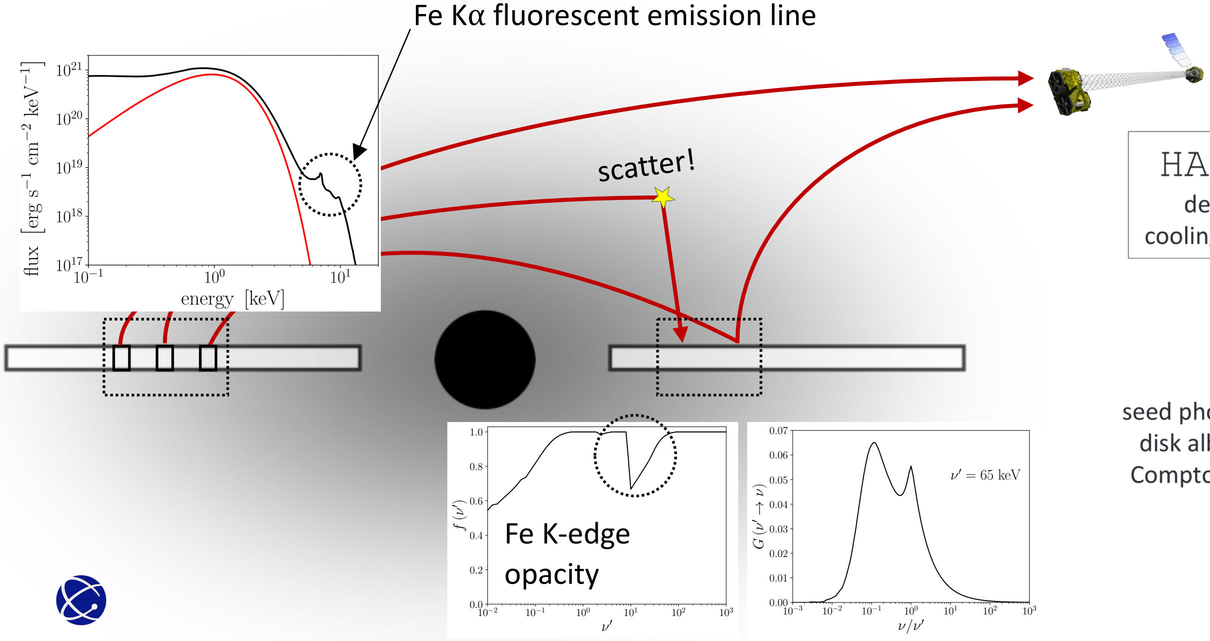

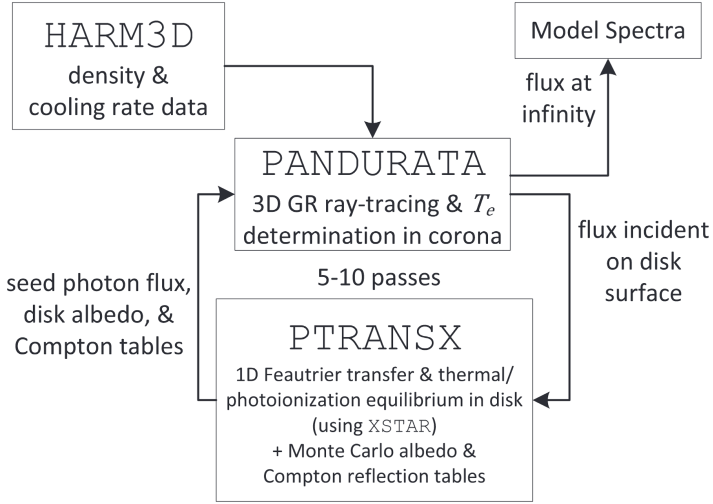

Generated X-ray spectra specifying only a *small number* of physically-meaningful parameters.

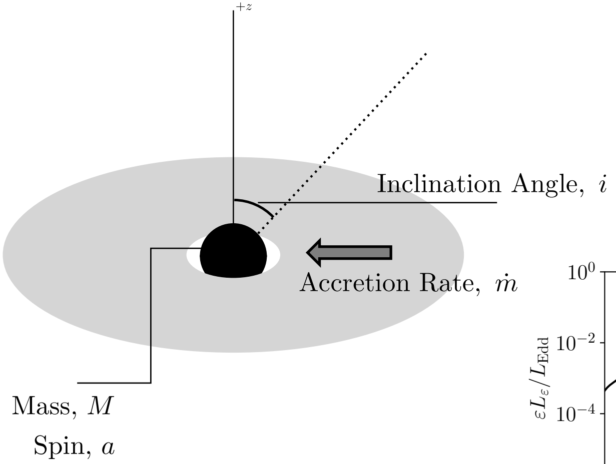

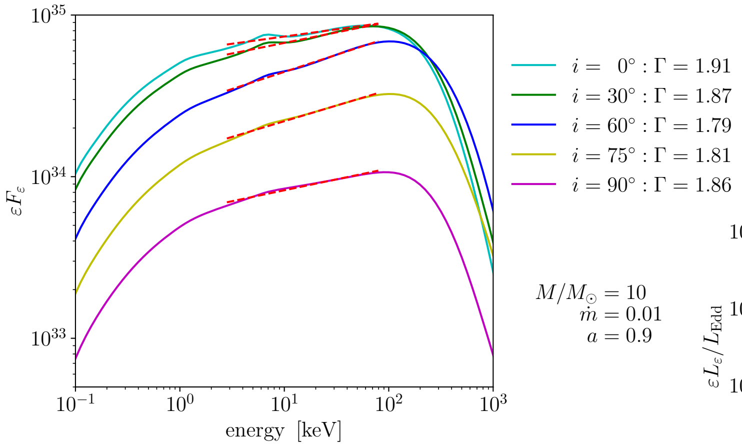

$$F_\nu/\nu \propto \nu^{-\Gamma}$$

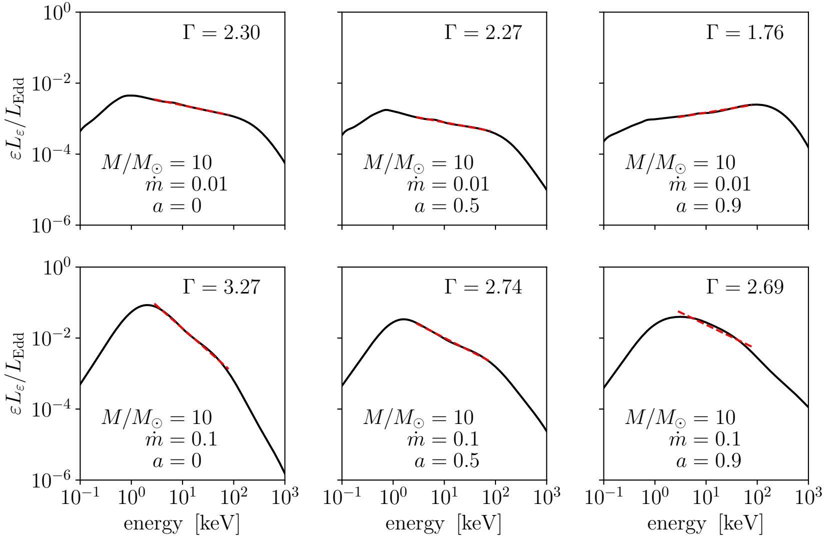

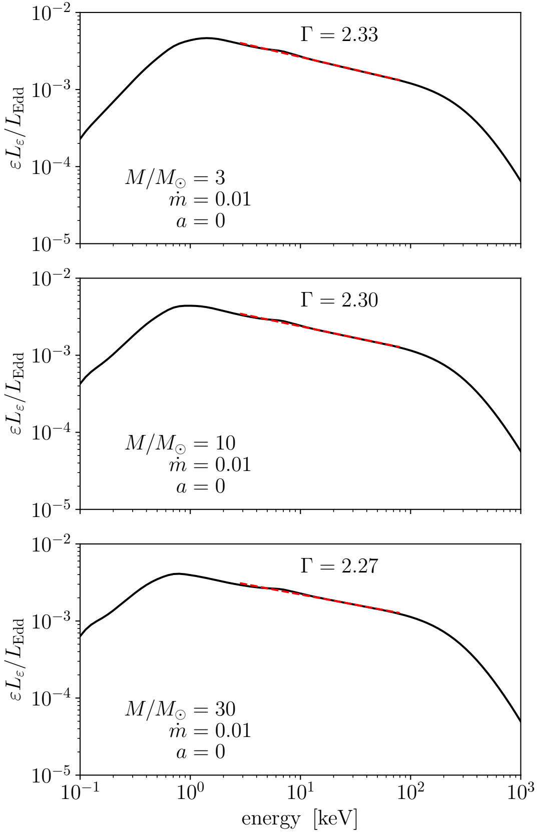

Often useful to look at spectrum divided by power-law fit.

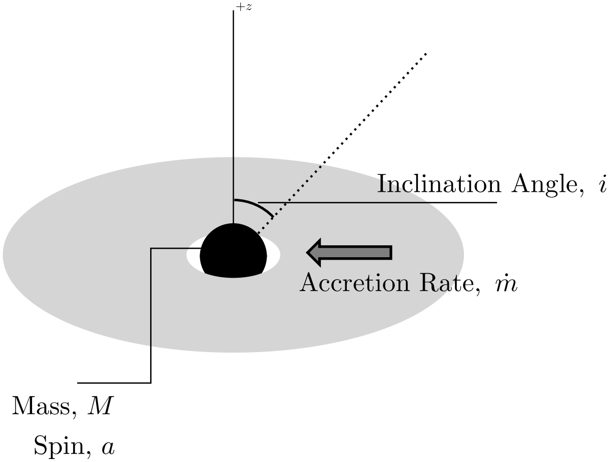

Fe Kα fluorescent emission line

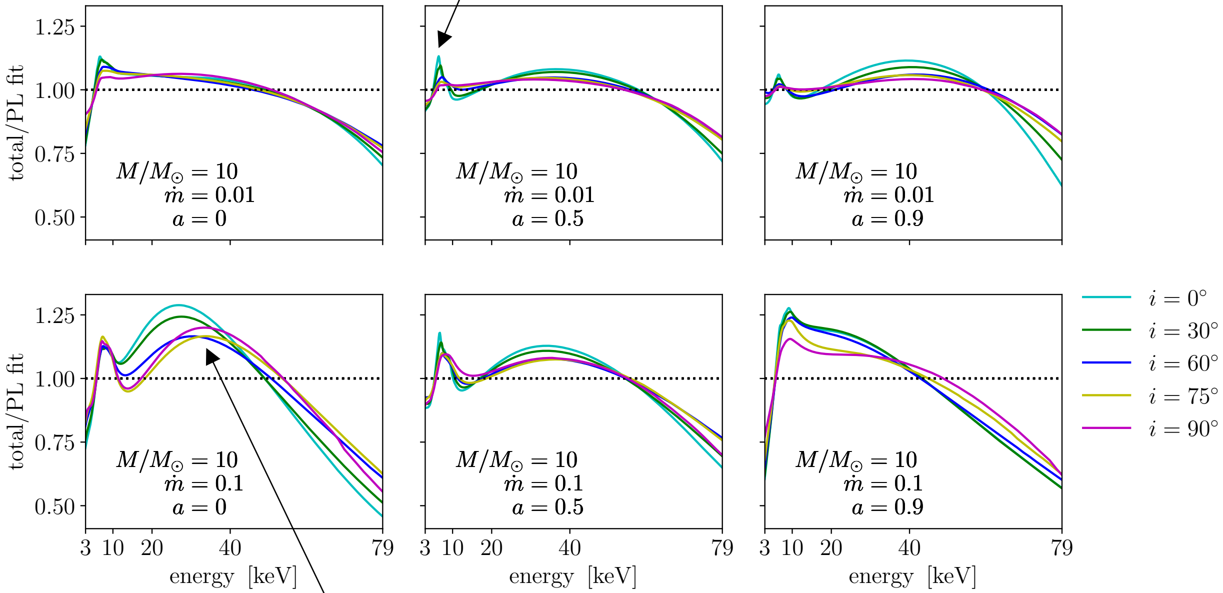

Compton "hump": high energy photons downscattering from disk interaction

Just the Fe Kα line flux (continuum-subtracted):

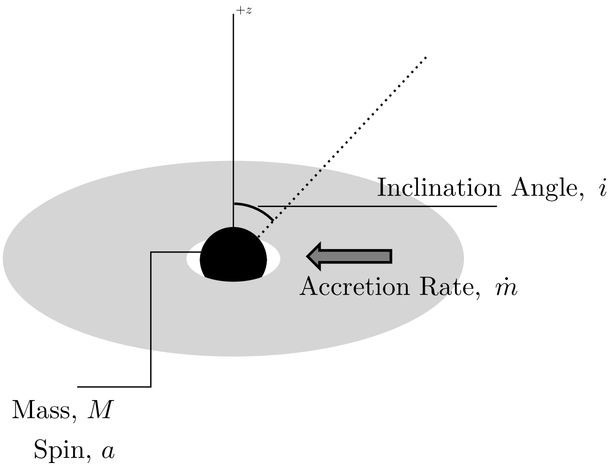

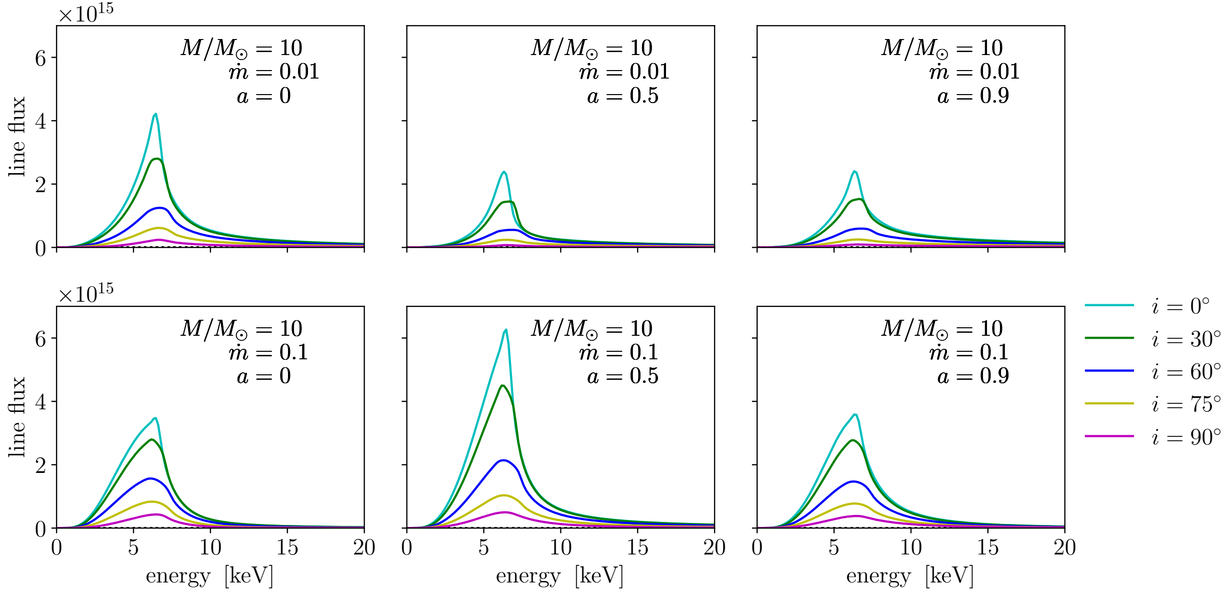

Our cutting edge:

Try to achieve reasonably good fits to real X-ray data.

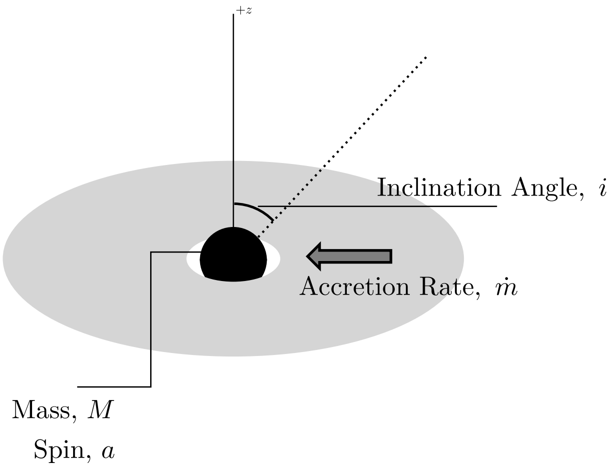

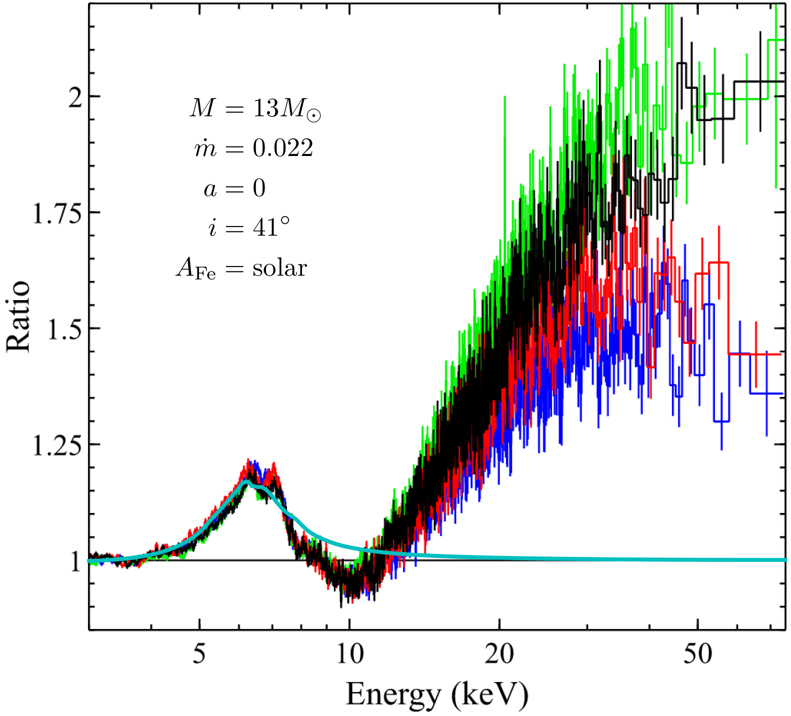

Fe Kα line profile of Cyg X-1
(Walton et al. 2016).

Simulation-Derived X-Ray Spectra Highlights:

- We get strong Kα lines with *only* solar abundances.
- Thermal peaks in the right spot, power-laws with expected slopes, roll-overs at high energy.

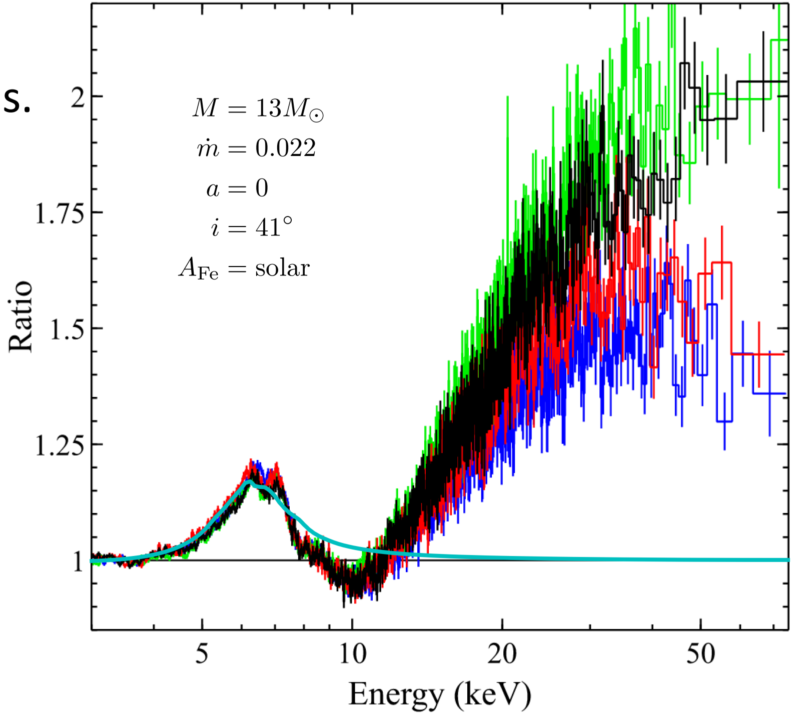

Fe Kα line profile of Cyg X-1 overlaid with our model (Walton et al. 2016).

Simulation-Derived X-Ray Spectra Highlights *and Challenges*:

- We get strong Kα lines with *only* solar abundances.
- Thermal peaks in the right spot, power-laws with expected slopes, roll-overs at high energy.

- We do not get Compton humps *as strong* as are typically observed – could be reflection by cold, distant gas (not in our model)?
- Right now, each synthetic spectrum is fabulously expensive to compute compared to more traditional methods.
- Need to connect with seasoned observers to make more progress fitting real data.

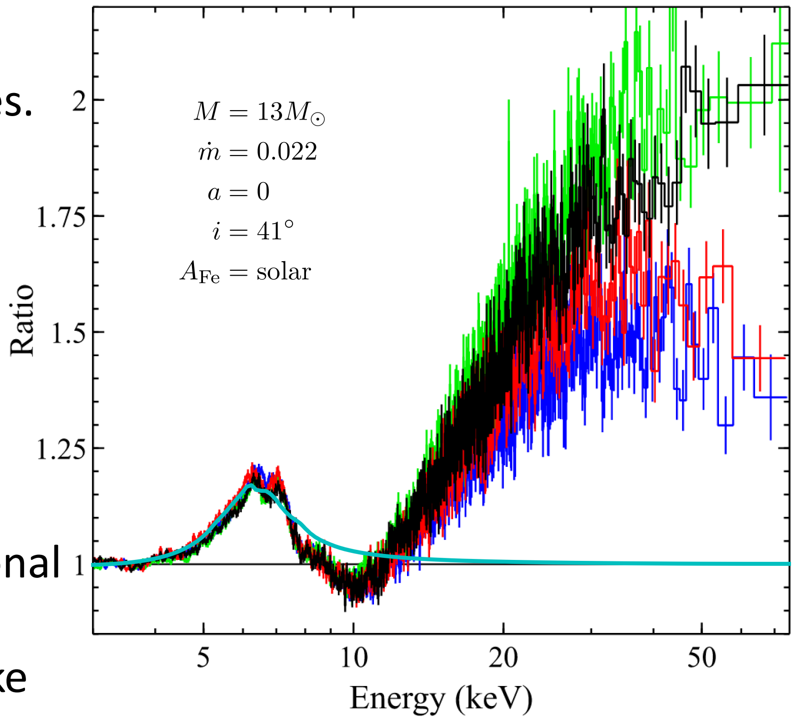

Fe Kα line profile of Cyg X-1 overlaid with our model (Walton et al. 2016).

Changing gears…

Operator Split Method for Compton Scattering in Monte Carlo Transport:

- In optically thin regimes where Compton scattering events are rare (e.g., the evacuated jet cone of a black hole simulation), *explicit* treatment of Compton scattering can lead to unacceptably variable temperature evolution.

- Example:
  One zone model with only Compton.
  Initially monochromatic radiation field equilibrates with thermal electron gas.

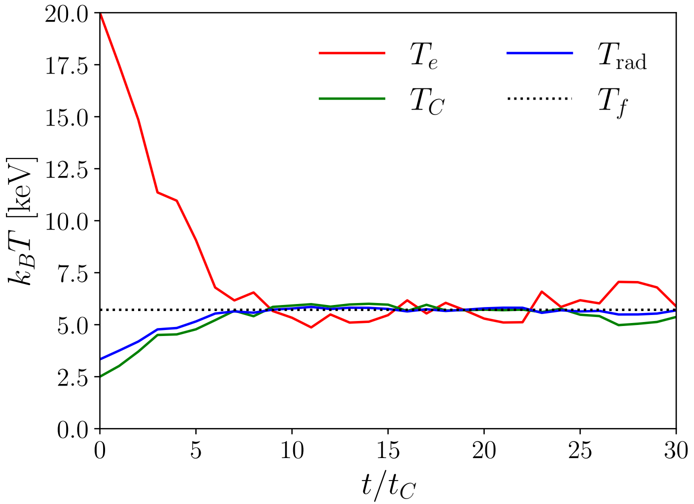

Operator Split Method for Compton Scattering in Monte Carlo Transport:

- In optically thin regimes where Compton scattering events are rare (e.g., the evacuated jet cone of a black hole simulation), *explicit* treatment of Compton scattering can lead to unacceptably variable temperature evolution.

- Example:
  One zone model with only Compton.
  Initially monochromatic radiation field equilibrates with thermal electron gas.

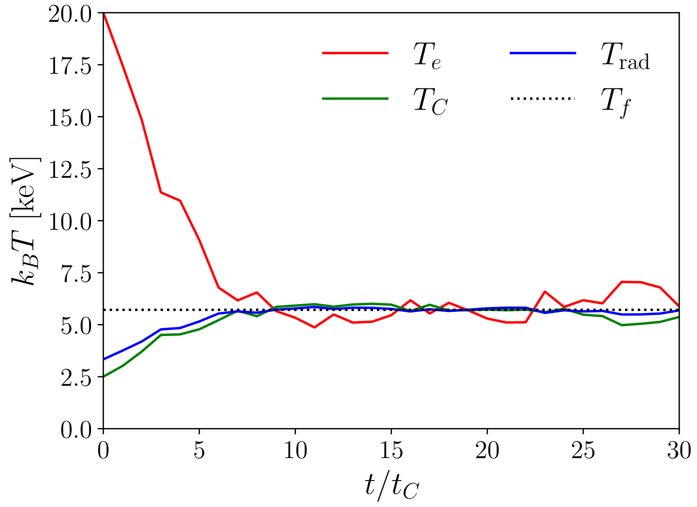

- Increasing starting particle count most reliable method to improve statistics, but not always feasible.

Operator Split Method for Compton Scattering in Monte Carlo Transport:

- In optically thin regimes where Compton scattering events are rare (e.g., the evacuated jet cone of a black hole simulation), *explicit* treatment of Compton scattering can lead to unacceptably variable temperature evolution.

- Example:
  One zone model with only Compton.
  Initially monochromatic radiation field equilibrates with thermal electron gas.

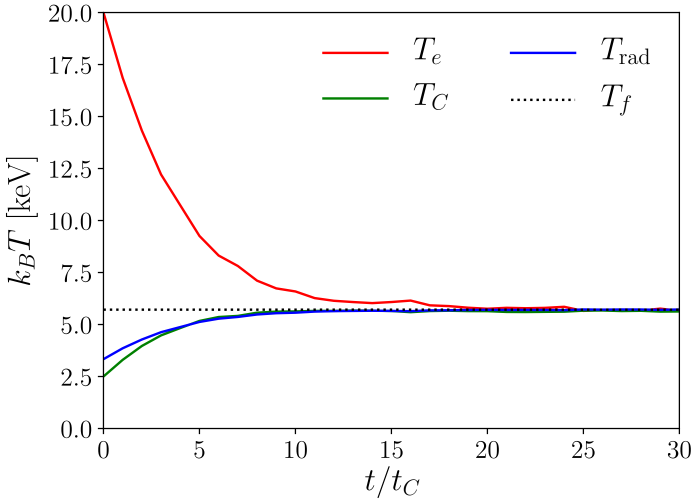

- Increasing starting particle count most reliable method to improve statistics, but not always feasible.

Operator Split Method for Compton Scattering in Monte Carlo Transport:

- Instead: Track the "scattered-out" energy-weight of each particle over every flight in each cell:

$$\Delta w_i = w_{i,0}\left\{1 - \exp\left[-n_e \sigma\left(\nu_i, T_e\right) d_i\right]\right\}$$

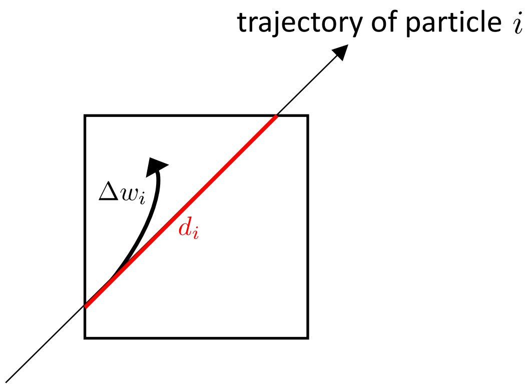

Operator Split Method for Compton Scattering in Monte Carlo Transport:

- Instead: Track the "scattered-out" energy-weight of each particle over every flight in each cell:

$$\Delta w_i = w_{i,0}\left\{1 - \exp\left[-n_e \sigma\left(\nu_i, T_e\right) d_i\right]\right\}$$

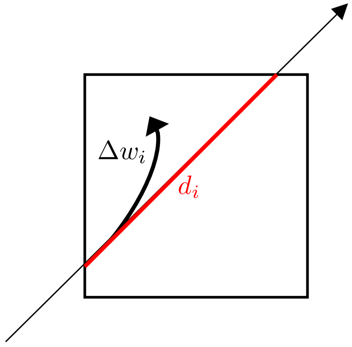

- Re-emit new particles at the end of the time step, one per group. For the j^{th} group, emit particle with energy-weight and frequency $w_j, \langle n_j \rangle$ according to:

$$N_j = \int_{\nu_j^l}^{\nu_j^u} n(\nu) d\nu = \sum_i \frac{\Delta w_i}{\nu_i} \int_{\nu_j^l}^{\nu_j^u} R\left(\nu_i \to \nu, 1, T_e\right) d\nu$$

$$\langle \nu_j \rangle = \frac{\int_{\nu_j^l}^{\nu_j^u} \nu n(\nu) d\nu}{\int_{\nu_j^l}^{\nu_j^u} n(\nu) d\nu} = \frac{1}{N_j} \sum_i \frac{\Delta w_i}{\nu_i} \int_{\nu_j^l}^{\nu_j^u} \nu R\left(\nu_i \to \nu, 1, T_e\right) d\nu$$

$$w_j = N_j \langle \nu_j \rangle$$

Operator Split Method for Compton Scattering in Monte Carlo Transport:

- Instead: Track the "scattered-out" energy-weight of each particle over every flight in each cell:

$$\Delta w_i = w_{i,0}\left\{1 - \exp\left[-n_e \sigma\left(\nu_i, T_e\right) d_i\right]\right\}$$

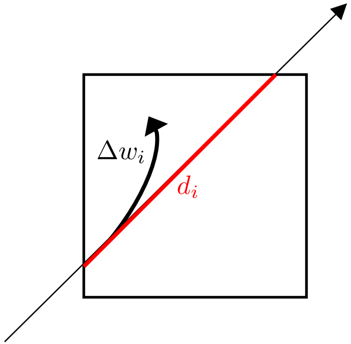

- Re-emit new particles at the end of the time step, one per group. For the j^th group, emit particle with energy-weight and frequency $w_j, \langle n_j \rangle$ according to:

$$N_j = \int_{\nu_j^l}^{\nu_j^u} n(\nu) d\nu = \sum_i \frac{\Delta w_i}{\nu_i} \int_{\nu_j^l}^{\nu_j^u} R\left(\nu_i \to \nu, 1, T_e\right) d\nu$$

$$\langle \nu_j \rangle = \frac{\int_{\nu_j^l}^{\nu_j^u} \nu n(\nu) d\nu}{\int_{\nu_j^l}^{\nu_j^u} n(\nu) d\nu} = \frac{1}{N_j} \sum_i \frac{\Delta w_i}{\nu_i} \int_{\nu_j^l}^{\nu_j^u} \nu R\left(\nu_i \to \nu, 1, T_e\right) d\nu$$

$$w_j = N_j \langle \nu_j \rangle$$

That is:
new particle has frequency equal to the *mean frequency* of all photons scattered to group j, and represents the *number* of photons scattered to group j

Operator Split Method for Compton Scattering in Monte Carlo Transport:

- Instead: Track the "scattered-out" energy-weight of each particle over every flight in each cell:

$$\Delta w_i = w_{i,0}\left\{1 - \exp\left[-n_e \sigma\left(\nu_i, T_e\right) d_i\right]\right\}$$

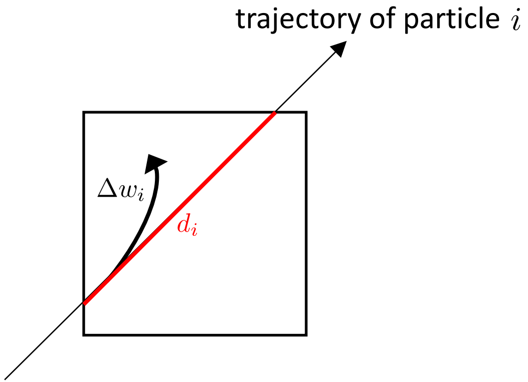

- Re-emit new particles at the end of the time step, one per group. For the j^th group, emit particle with energy-weight and frequency $w_j, \langle n_j \rangle$ according to:

$$N_j = \int_{\nu_j^l}^{\nu_j^u} n(\nu) d\nu = \sum_i \frac{\Delta w_i}{\nu_i} \int_{\nu_j^l}^{\nu_j^u} R\left(\nu_i \to \nu, 1, T_e\right) d\nu$$

$$\langle \nu_j \rangle = \frac{\int_{\nu_j^l}^{\nu_j^u} \nu n(\nu) d\nu}{\int_{\nu_j^l}^{\nu_j^u} n(\nu) d\nu} = \frac{1}{N_j} \sum_i \frac{\Delta w_i}{\nu_i} \int_{\nu_j^l}^{\nu_j^u} \nu R\left(\nu_i \to \nu, 1, T_e\right) d\nu$$

$$w_j = N_j \langle \nu_j \rangle$$

Manifestly conserves photon number.

But does require integrals over the *single-scatter redistribution function*.

Operator Split Method for Compton Scattering in Monte Carlo Transport:

explicit Compton

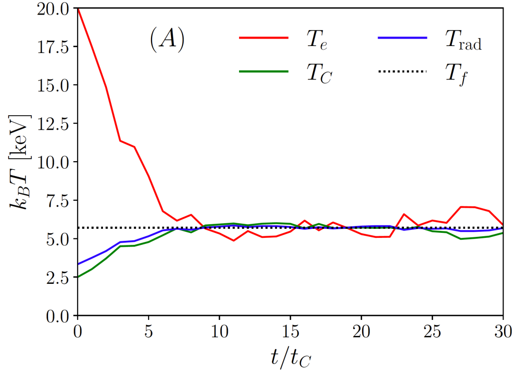

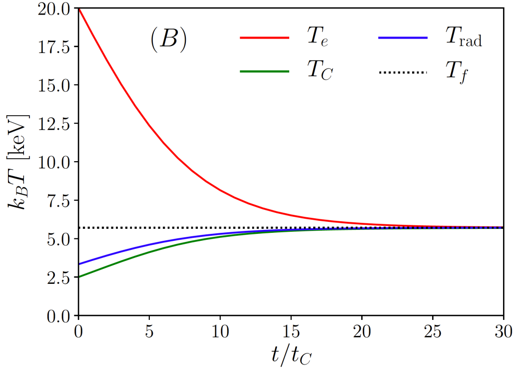

operator spit method

Temperature evolution is smoother (and energy-conserving); also correctly reproduces the no-induced-scattering distribution (Wien).

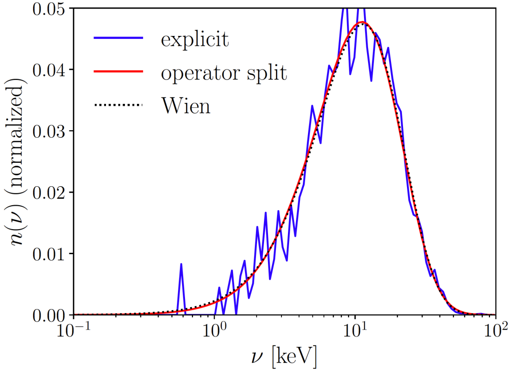

Operator Split Method for Compton Scattering in Monte Carlo Transport:

- In the nonrelativistic limit $\nu,\ k_B T_e \ll m_e c^2$
  a Gaussian approximation to the single-scatter kernel allows analytic evaluation of previous integrals:

$$R\left(\nu_i \rightarrow \nu'\right) = \frac{1}{\sigma_i \sqrt{\pi}} \exp\left[-\left(\nu' - \mu_i\right)^2 / \sigma_i^2\right]$$

$$\mu_i = \nu_i \left(1 + 4\Theta_e - \epsilon_i\right),$$

$$\sigma_i = \nu_i \sqrt{2\Theta_e + \frac{2}{5}\epsilon_i^2},$$

Operator Split Method for Compton Scattering in Monte Carlo Transport:

- In the nonrelativistic limit $\nu,\ k_B T_e \ll m_e c^2$
  a Gaussian approximation to the single-scatter kernel allows analytic evaluation of previous integrals:

$$N_j = \sum_i \frac{\Delta w_i}{\nu_i}\left[\mathrm{erf}\left(x_{ij}^u\right) - \mathrm{erf}\left(x_{ij}^l\right)\right]$$

$$R\left(\nu_i \to \nu'\right) = \frac{1}{\sigma_i\sqrt{\pi}}\exp\left[-\left(\nu' - \mu_i\right)^2/\sigma_i^2\right]$$

$$\langle\nu_j\rangle = \frac{1}{N_j}\sum_i \frac{\Delta w_i}{\nu_i}\frac{\sigma_i}{2\sqrt{\pi}}\left\{\exp\left[-\left(x_{ij}^l\right)^2\right] - \exp\left[-\left(x_{ij}^u\right)^2\right] + \mu_i\left[\mathrm{erf}\left(x_{ij}^u\right) - \mathrm{erf}\left(x_{ij}^l\right)\right]\right\}$$

$$\mu_i = \nu_i\left(1 + 4\Theta_e - \epsilon_i\right),$$

$$\sigma_i = \nu_i\sqrt{2\Theta_e + \frac{2}{5}\epsilon_i^2},$$

$$x_{ij}^u = \frac{\nu_j^u - \mu_i}{\sigma_i},\quad x_{ij}^l = \frac{\nu_j^l - \mu_i}{\sigma_i}$$

Operator Split Method for Compton Scattering in Monte Carlo Transport:

- In the nonrelativistic limit $\nu,\ k_B T_e \ll m_e c^2$
  a Gaussian approximation to the single-scatter kernel allows analytic evaluation of previous integrals:

$$N_j = \sum_i \frac{\Delta w_i}{\nu_i}\left[\mathrm{erf}\left(x_{ij}^u\right) - \mathrm{erf}\left(x_{ij}^l\right)\right]$$

$$R\left(\nu_i \to \nu'\right) = \frac{1}{\sigma_i\sqrt{\pi}}\exp\left[-\left(\nu' - \mu_i\right)^2/\sigma_i^2\right]$$

$$\langle \nu_j \rangle = \frac{1}{N_j}\sum_i \frac{\Delta w_i}{\nu_i}\frac{\sigma_i}{2\sqrt{\pi}}\left\{\exp\left[-\left(x_{ij}^l\right)^2\right] - \exp\left[-\left(x_{ij}^u\right)^2\right] + \mu_i\left[\mathrm{erf}\left(x_{ij}^u\right) - \mathrm{erf}\left(x_{ij}^l\right)\right]\right\}$$

$$\mu_i = \nu_i\left(1 + 4\Theta_e - \epsilon_i\right),$$

$$\sigma_i = \nu_i\sqrt{2\Theta_e + \frac{2}{5}\epsilon_i^2},$$

$$x_{ij}^u = \frac{\nu_j^u - \mu_i}{\sigma_i},\quad x_{ij}^l = \frac{\nu_j^l - \mu_i}{\sigma_i}$$

In relativistic limit `compy` works – and integral values can be tabulated in advance – but still requires table-lookup.

Operator Split Method for Compton Scattering in Monte Carlo Transport:

- Limitation: If the time step is long or comparable to the mean free time between scatters, this method will *under-calculate* the Compton heating/cooling rates.

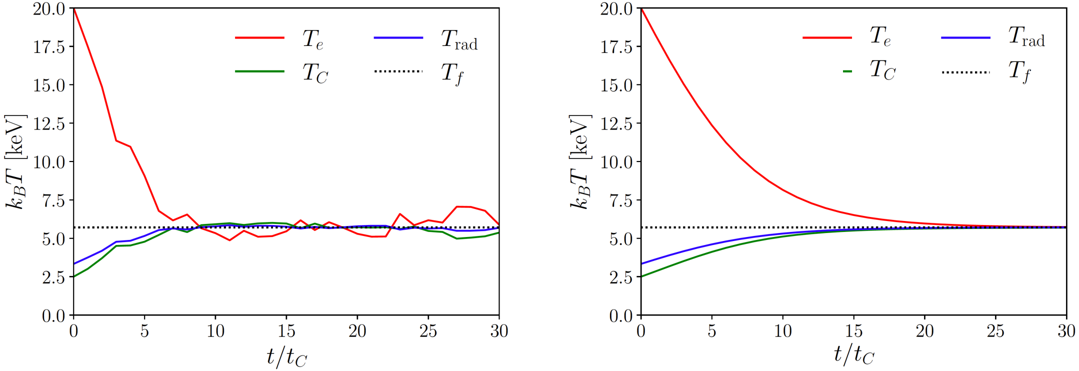

Time step equal to the mean free time between scatters.
Result: operator split run equilibrates too slowly.

Operator Split Method for Compton Scattering in Monte Carlo Transport:

- One solution is to *subcycle*:

$\Delta t = \chi t_C$ (t_C = mean time between scatters)

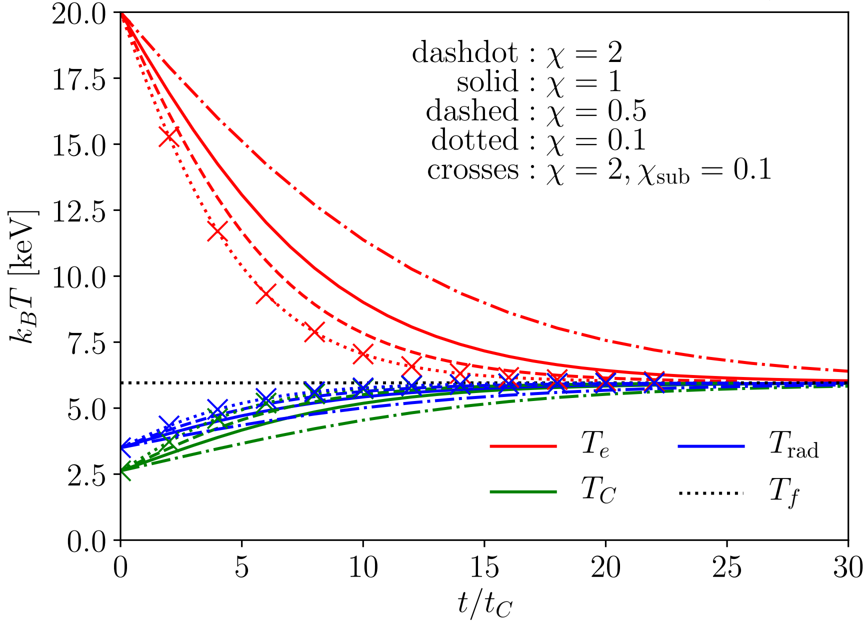

Simply run the whole procedure many times per "global" time step, emitting appropriately-averaged particles at the very end.

Operator Split Method for Compton Scattering in Monte Carlo Transport:

- A more elegant solution is to use the *multiscatter* redistribution function instead.

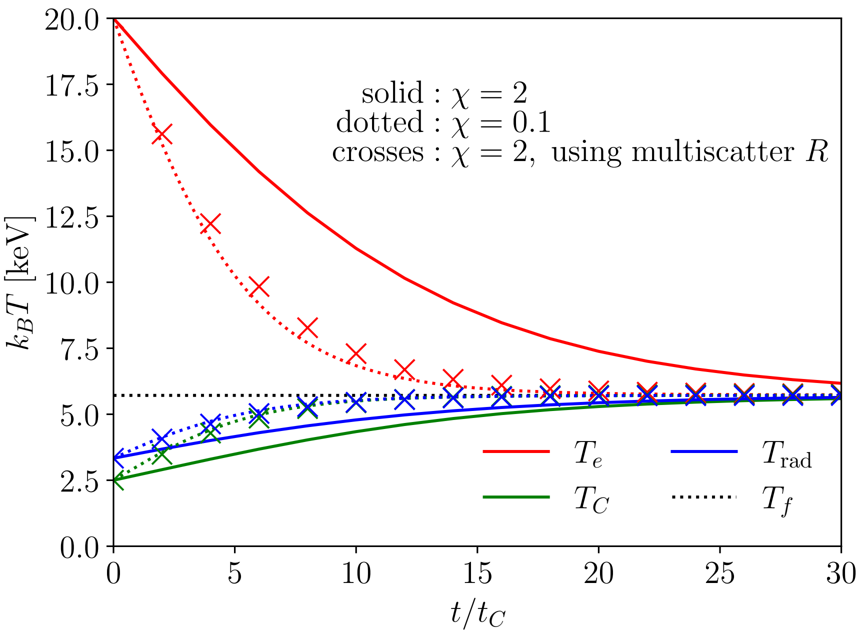

$$R\left(\nu' \to \nu, \Delta t/t_C, T_e\right) = \sum_{k=1}^{\infty} p\left(k, \Delta t/t_C\right) R\left(\nu' \to \nu, k, T_e\right)$$

$$p\left(k, \Delta t/t_C\right) = \frac{1}{k!}\left(\Delta t/t_C\right)^k \frac{\exp\left(-\Delta t/t_C\right)}{1 - \exp\left(-\Delta t/t_C\right)}$$

Sum over *k*-scatter redistribution functions to make a time-interval-dependent redistribution function.

No known multiscatter generalization of the Gaussian approximation technique – but tabulation of integral quantities in advance still possible.

Operator Split Method for Compton Scattering in Monte Carlo Transport:

- Highlights:
  - Much smoother temperature evolution.
  - Conserves photon number and energy.
  - In nonrelativistic, short time step limit, we have an inexpensive analytic formula.
  - Potentially expensive table-lookup, but much can be tabulated in advance.
  - Works just as well at relativistic temperatures – any rejection sampling inefficiency is wrapped up in the table construction in `compy`.

Operator Split Method for Compton Scattering in Monte Carlo Transport:

- Highlights:
  - Much smoother temperature evolution.
  - Conserves photon number and energy.
  - In nonrelativistic, short time step limit, we have an inexpensive analytic formula.
  - Potentially expensive table-lookup, but much can be tabulated in advance.
  - Works just as well at relativistic temperatures – any rejection sampling inefficiency is wrapped up in the table construction in `compy`.

- Precautions:
  - Analogous to absorption/re-emission, and likewise introduces "teleportation error."
  - Increases particle count every time step (but in a predictable way); standard population control techniques should handle this.

BACKUP SLIDES

General Relativistic Magnetohydrodynamics (GRMHD)

$$\frac{1}{\sqrt{-g}}\partial_\mu\left(\sqrt{-g}\rho u^\mu\right) = 0$$ conservation of mass

density

four-velocity

General Relativistic Magnetohydrodynamics (GRMHD)

$$\frac{1}{\sqrt{-g}}\partial_\mu\left(\sqrt{-g}\rho u^\mu\right) = 0$$ conservation of mass

density

four-velocity

(properties of the metric – they don't evolve in a static spacetime)

General Relativistic Magnetohydrodynamics (GRMHD)

$$\frac{1}{\sqrt{-g}}\partial_\mu\left(\sqrt{-g}\rho u^\mu\right)=0$$ conservation of mass

$$\partial_t\left(\sqrt{-g}T^t{}_\nu\right)=-\partial_i\left(\sqrt{-g}T^i{}_\nu\right)+\sqrt{-g}T^\kappa{}_\lambda\Gamma^\lambda{}_{\nu\kappa}$$ conservation of energy-momentum

stress-energy tensor

General Relativistic Magnetohydrodynamics (GRMHD)

$$\frac{1}{\sqrt{-g}}\partial_\mu\left(\sqrt{-g}\rho u^\mu\right) = 0$$ conservation of mass

$$\partial_t\left(\sqrt{-g}T^t{}_\nu\right) = -\partial_i\left(\sqrt{-g}T^i{}_\nu\right) + \sqrt{-g}T^\kappa{}_\lambda\Gamma^\lambda{}_{\nu\kappa}$$ conservation of energy-momentum

(properties of the metric – they don't evolve in a static spacetime)

stress-energy tensor

General Relativistic Magnetohydrodynamics (GRMHD)

$$\frac{1}{\sqrt{-g}}\partial_\mu\left(\sqrt{-g}\rho u^\mu\right) = 0$$ conservation of mass

$$\partial_t\left(\sqrt{-g}T^t{}_\nu\right) = -\partial_i\left(\sqrt{-g}T^i{}_\nu\right) + \sqrt{-g}T^\kappa{}_\lambda\Gamma^\lambda{}_{\nu\kappa}$$

conservation of energy-momentum (4 equations):
ν = 1 time and 3 space coordinates

stress-energy tensor

General Relativistic Magnetohydrodynamics (GRMHD)

$$\frac{1}{\sqrt{-g}}\partial_\mu \left(\sqrt{-g}\rho u^\mu\right) = 0$$ conservation of mass

$$\partial_t \left(\sqrt{-g}T^t{}_\nu\right) = -\partial_i \left(\sqrt{-g}T^i{}_\nu\right) + \sqrt{-g}T^\kappa{}_\lambda \Gamma^\lambda{}_{\nu\kappa}$$ conservation of energy-momentum (4 equations)

$$T^{\mu\nu}_{\mathrm{MHD}} = \left(\rho + u + p + b^2\right) u^\mu u^\nu + \left(p + \frac{b^2}{2}\right) g^{\mu\nu} - b^\mu b^\nu$$ ideal MHD tensor (zero fluid rest frame E field)

internal energy

fluid pressure

magnetic pressure

magnetic field 4-vector

General Relativistic Magnetohydrodynamics (GRMHD)

$$\frac{1}{\sqrt{-g}}\partial_\mu\left(\sqrt{-g}\rho u^\mu\right) = 0$$ conservation of mass

$$\partial_t\left(\sqrt{-g}T^t{}_\nu\right) = -\partial_i\left(\sqrt{-g}T^i{}_\nu\right) + \sqrt{-g}T^\kappa{}_\lambda\Gamma^\lambda{}_{\nu\kappa}$$ conservation of energy-momentum (4 equations)

$$T^{\mu\nu}_{\mathrm{MHD}} = \left(\rho + u + p + b^2\right)u^\mu u^\nu + \left(p + \frac{b^2}{2}\right)g^{\mu\nu} - b^\mu b^\nu$$ <u>ideal</u> MHD tensor (zero fluid rest frame E field)

$$\partial_t\left(\sqrt{-g}B^i\right) = \partial_j\left[\sqrt{-g}\left(b^j u^i - b^i u^j\right)\right]$$ <u>ideal</u> MHD induction equation (Faraday's law + Ohm's law)

magnetic field 3-vector

General Relativistic Magnetohydrodynamics (GRMHD)

$$\frac{1}{\sqrt{-g}}\partial_\mu\left(\sqrt{-g}\rho u^\mu\right)=0$$ conservation of mass

$$\partial_t\left(\sqrt{-g}T^t{}_\nu\right)=-\partial_i\left(\sqrt{-g}T^i{}_\nu\right)+\sqrt{-g}T^\kappa{}_\lambda\Gamma^\lambda{}_{\nu\kappa}$$ conservation of energy-momentum (4 equations)

$$T^{\mu\nu}_{\mathrm{MHD}}=\left(\rho+u+p+b^2\right)u^\mu u^\nu+\left(p+\frac{b^2}{2}\right)g^{\mu\nu}-b^\mu b^\nu$$ ideal MHD tensor (zero fluid rest frame E field)

$$\partial_t\left(\sqrt{-g}B^i\right)=\partial_j\left[\sqrt{-g}\left(b^j u^i-b^i u^j\right)\right]$$ ideal MHD induction equation (Faraday's law + Ohm's law)

$$\frac{1}{\sqrt{-g}}\partial_i\left(\sqrt{-g}B^i\right)=0$$ no magnetic monopoles constraint

General Relativistic Magnetohydrodynamics (GRMHD)

$$\frac{1}{\sqrt{-g}}\partial_\mu\left(\sqrt{-g}\rho u^\mu\right) = 0$$ conservation of mass

$$\partial_t\left(\sqrt{-g}T^t{}_\nu\right) = -\partial_i\left(\sqrt{-g}T^i{}_\nu\right) + \sqrt{-g}T^\kappa{}_\lambda\Gamma^\lambda{}_{\nu\kappa}$$ conservation of energy-momentum (4 equations)

$$T^{\mu\nu}_{\mathrm{MHD}} = \left(\rho + u + p + b^2\right)u^\mu u^\nu + \left(p + \frac{b^2}{2}\right)g^{\mu\nu} - b^\mu b^\nu$$ <u>ideal</u> MHD tensor (zero fluid rest frame E field)

$$\partial_t\left(\sqrt{-g}B^i\right) = \partial_j\left[\sqrt{-g}\left(b^j u^i - b^i u^j\right)\right]$$ <u>ideal</u> MHD induction equation (Faraday's law + Ohm's law)

$$\frac{1}{\sqrt{-g}}\partial_i\left(\sqrt{-g}B^i\right) = 0$$ no magnetic monopoles constraint

$$p = (\Gamma - 1)u$$ ideal gas equation of state (for closure)

adiabatic index

Optically thin thermal compton

courtesy of
Chris Done

- power law by multiple scattering of thermal electrons
- Number of photons dN/dE dE = E dN/dE dLog E = f (ε) dlog $\varepsilon \propto \varepsilon^{-\alpha}$
- For τ<1 scatter τ photons each time to energy $\varepsilon_{out}=(1+4\Theta+16\Theta^2)\varepsilon_{in}$
- index α=log(prob)/log(energy boost) ~ -log τ/log $(1+4\Theta+16\Theta^2)$

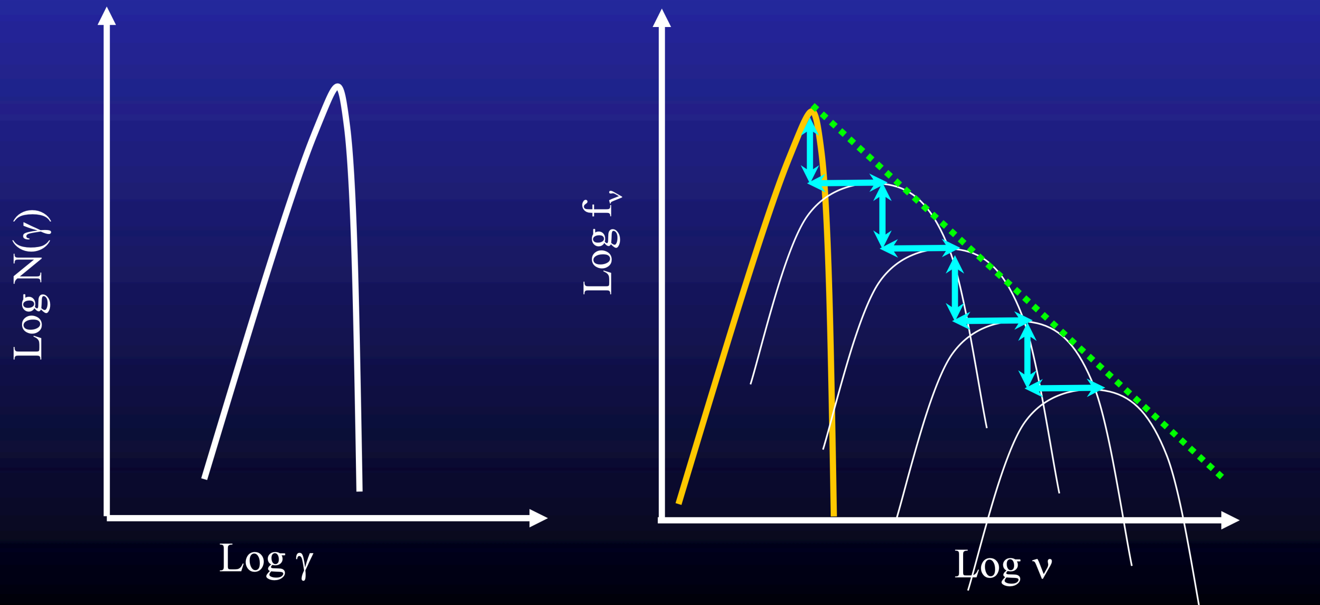

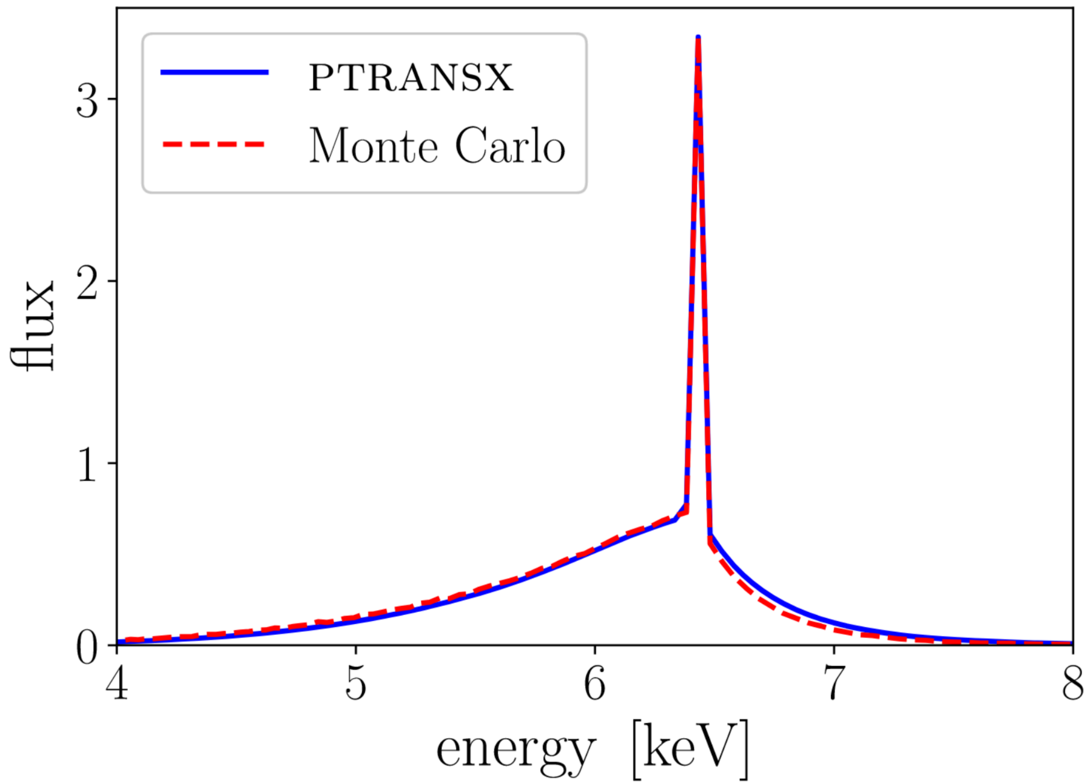
PTRANSX
Monte Carlo
flux
0
1
2
3
4
5
6
7
8
energy [keV]